Tomas Bata University in Zlín
Faculty of Applied Informatics

Dissertation work

MEASUREMENT SYSTEMS – CONNECTION BETWEEN SENSORS AND EMBEDDED SYSTEM

Tumenbayar Lkhagvatseren, M.Eng.

Supervisor: Assoc. Prof. Ing. František Hruška, Ph.D.

Tomas Bata University in Zlín
Faculty of Applied Informatics
Department of Electronics and Measurement

Zlín, 2011

Published by Tomas Bata University in Zlin, 2010

Title: Measurement Systems – connection between Sensors and Embedded System

Název: Měřicí Systémy – propojení mezi Senzory a Embedded Systémy

Key words: Sensor, Signal Condition, Communication Interface, Measurement System, Wireless communication, Path loss, Penetration loss, Smart suit

Klíčová slova: Senzor, Úprava Signálu, Komunikační Rozhraní Senzorů, Měřicí Systém, Bezdrátové sdìlování, Přenosová ztráta, Ztráta útlumem, Inteligentní oblek

The electronic version of the Doctoral Thesis Summary may be found at www.utb.cz.

Acknowledgement

First of all, I would like to express my deepest gratitude and appreciation to my supervisor Assoc. Prof. Ing. František Hruška, Ph.D for his continues support. He was always there to listen, to advice and guidance throughout my study. Even during his holiday he was responsible for his obligation. Once, my colleague told me, that "He does not know the word Holiday". Without his constant encouragement, vision, inspiration, I could not have completed this program. Thank you very much Dear, Assoc. Prof František Hruška, for being not only my supervisor but also for being very kind and patient in a professional way.

Besides my supervisor, I thank to Prof. Ing. Vladimír Vašek, CSc, for financial support, and research grant, to Assoc. Prof. RNDr. Vojtěch Křesálek, CSc. and Prof. Ing. Roman Prokop, CSc, for their academic suggestions, support as well as for an allowance of a fellowship, and to Ing. Stanislav Goňa, Ph.D. for his invaluable advice.

Last but not least, I thank to my parents for giving me life in the first place, for everything did for me and for my sisters, to my family shortly, I am fortunate being a part of you, and to my friends for their unfailing support.

The work was supported by the Ministry of Education, Youth and Sports of the Czech Republic under grant No. MSM 7088352101 and research project Modeling and Control of Natural and Synthetic Polymer Processing under grant No. MSM 7088352102.

ABSTRACT

Rapid growth in the sensors and sensor technology introduces a variety of products to the market. The increasing number of available sensor concepts and implementations demands more versatile sensor electronics and signal conditioning. Nowadays, signal conditioning for the available spectrum of sensors is becoming more and more challenging. In a meantime, there have been rapid advances in wireless technologies and an importance of a RF communication system is expanding day by day due to its advantages. With all the new implementation and wireless communications innovations, this work is devoted to illumination for a measurement system connection between sensors and embedded system. In this dissertation, we experiment with a measurement system consists of a classic sensor with modern System in Package system for a wireless communication. In addition, the thesis deals with the properties of propagation and penetration of the electromagnetic radiation in the range from 1 GHz to 8 GHz for the different power levels examined for a reliable communication system for sensors. Furthermore, the work reveals a test result of the penetration of the signal via a firemen garment for a further smart suite development.

RESUMÉ

Rychlý rozvoj senzorů a souvisejících technologií pomáhá k různorodosti produktů na trhu. Rostoucí počet dostupných senzorů, např. MEMS sensorů, jejich koncepty a implementace vyžaduje více studia elektroniky a úprav signálu. V nynější době zpracování signálů pro dostupné druhy senzorů se stále více rozšiřuje. Současně se rozšiřují aplikace bezdrátových systémů pro komunikaci. Tento rozvoj potřebuje poznat a objasnit mnoho problémů, V této práci se pracovalo s měřicím systémem se senzory a se systémem komunikace s elektromagnetickým zářením a studovaly se jejich vlastnosti. Cílem také bylo poznat vlastnosti šíření a průniků elektromagnetického záření v rozsahu od 1 GHz do 8 GHz pro různé hladiny výkonu pro spolehlivý bezdrátový systém komunikace. Specifická část práce uvádí výsledek testu absorpce signálu přes hasičský oděv pro využití u budoucích projektů souvisejících s inteligentními oděvy.

CONTENTS

LIST OF FIGURES

LIST OF TABLES

LIST OF SYMBOLS

Symbol	*Unit*	*Denotation*
$\Im$	A	Magnetomotive force
Φ	Wb	Magnetic flux
$\Re$	A/Wb	Reluctance
U	V	Voltage
I	A	Current
Z	Ω	Impedance
q	C	Charge
T	0C	Temperature
τ	-	Time constant
f	Hz	Frequency
R	Ω	Resistance
C	F	Capacitance
L	H	Inductance
H	A/m	Magnetic field
E	V/m	Electric field
ε_r	F/m	Relative permittivity
μ_r	H/m	Relative permeability
σ	S/m	Conductivity
λ	m	Wavelength
ω	rad/s	Angular frequency
P_t, P_r	mW, dBm	Transmitted and Received powers.
G_A	dBi	Antenna gain
U	%, dB	Uncertainty
F_W	-	Weighting or Coverage factor
F	N	Force
ε	dB	Error

LIST OF ABBREVIATIONS

ADC	Analogue to Digital Conversion
CMOS	Complementary Metal–Oxide–Semiconductor
CVC	Capacitance to Voltage Converter
DAQ	Data Acquisition
DC	Direct Current
DSP	Digital Signal Processor
FFTSA	Fast Fourier Transform based Spectrum Analyzer
FIR	Finite Impulse Response
GPIB	General Purpose Interface Bus
I2C	Inter-Integrated Circuit
IF	Intermediate Frequency
IIR	Infinite Impulse Response
LO	Local Oscillator
MCU	Micro Controller Unit
MEMS	Micro-Electro-Mechanical System
RF	Radio Frequency
SD	Standard Deviation
SiP	System in Package
SPI	Serial Peripheral Interface
SSA	Swept Spectrum Analyzer
T/R	Transmission/Reflection
USB	Universial Serial Bus
VSWR	Voltage Standing Wave Ratio
WLAN	Wireless Local Area Networks
WPAN	Wireless Personal Area Networks

1 INTRODUCTION

Looking wider – the importance of measurements has crucial significance for human civilization. From a beginning of our civilization people tried to understand and comprehend the surrounding world [97]. There are various explanations and definitions of the term "measurement" recommended by many sources. The International Organization for Standards Vocabulary proposes following definitions: Measurement is a process of experimentally obtaining information about the magnitude of a quantity. Measurement implies a measurement procedure based on a theoretical model. In practice measurement presupposes a calibrated measuring system, possibly subsequently verified. Metrology includes all theoretical and practical aspects of measurement, whichever the measurement uncertainty and field of application [40]. An expanded definition by [97] is given as: "The measurement is a cognitive process of gathering the information from the physical world. On this process a value of a quantity is determined (in defined time and conditions) by comparison it (with known uncertainty) with the standard value".

Recently, the field of measurement science has been significantly changed during last 30 years, due to the development of new internet technologies, micro and nano – technologies [76], informatics, microelectronics, and mechatronics [97].

Examples of intensive ongoing research and development areas include sensors, signal processing, data acquisition, data processing, and as well as a communication interface. For instance, the sensors are becoming more intelligent or smart, which strongly tend to contain a physical transducer, a network interface, a processor, and a memory core that can all be fabricated on a single die or chip, including Universal Serial Bus (USB), RS232, General Purpose Interface Bus (GPIB) or Ethernet [86]. Also, widespread of computer systems stimulated the development of measurement software, virtual instruments and intelligent data analysis methods by means of user friendly software which is enabling to design whole measurement system. The most popular software of such type is LabVIEW proposed by National Instruments (NILABVIEW).

At the same time, the explosive growth of mobile and wireless communications has radically changed and an evolution of wireless networking has also taken place during

this period [50]. Consequently, behaviors of electromagnetic radiation, in an indoor environment by means of propagation and penetration of the signal through engineering materials are becoming an important matter in a telecommunication system as well as in an application specific measurement system.

The nature of the thesis is stating that the analyses of electromagnetic radiation in indoor scenario, as well as a penetration through a certain building mediums are examined for a reliable communication system between the sensors and embedded systems.

The organization of the thesis as follows:

Chapter 2 gives the state of the art of a modern measurement system by means of a System in Package. Chapter 3 determines the goals of the dissertation work. Chapter 4 reviews the theoretical frame of the measurement system, including sensor, signal conditioning, and communication system for sensors. In that manner, demonstrates electromagnetic radiation, spectrum analyzer, apart from that an uncertainty evaluation of the measurement system. Chapter 5 reveals the experimental part concluding measurement model, setup, which are used in this work and results of the measurements. Chapter 6 concludes the limitations and objectives of the work and suggestions for the improvements.

2 STATE OF THE ART

At de fact, s measurement is an application oriented system. Recent developments in measurement technologies and practices—and user needs—are being discussed along the researchers from every point of view. The objectives of the measurement systems are:

- Process monitoring
- Process control
- Experimental purpose

Today's increasing demand for a wireless connectivity of electronic devices has driven toward an advanced technology which incorporates multiple components into a single package by means of System in Package (SiP).

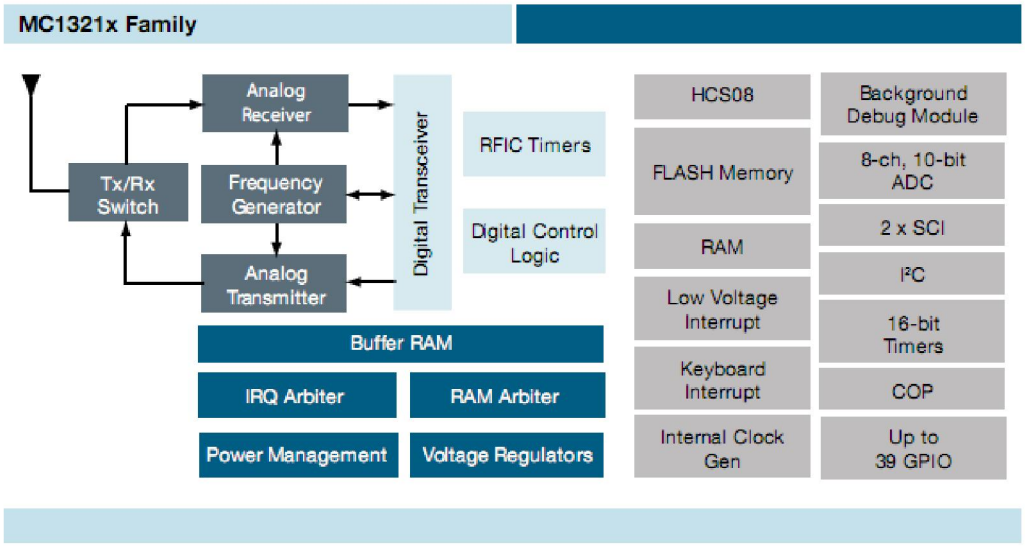

Fig. 1. Example of SiP (Freescale Semiconductor MC1321X) [24]

A development tendency of modern integrated circuit tends to comprise all units of the measurement system such as a signal conditioning circuit, digital signal processing, and communication interface for both analogue and digital interfaces. One of such technologies is given by Fig 1 as an example of SiP integration with the Zigbee compliant. The advantages of such an integrated system are low cost, high performance, low power consumption, and as well as reusable.

In a Measurement System Analysis, a critical first step that should precede any data-based decision making, including statistical analysis, correlation and regression analysis, as well as uncertainty analysis and design of experiments.

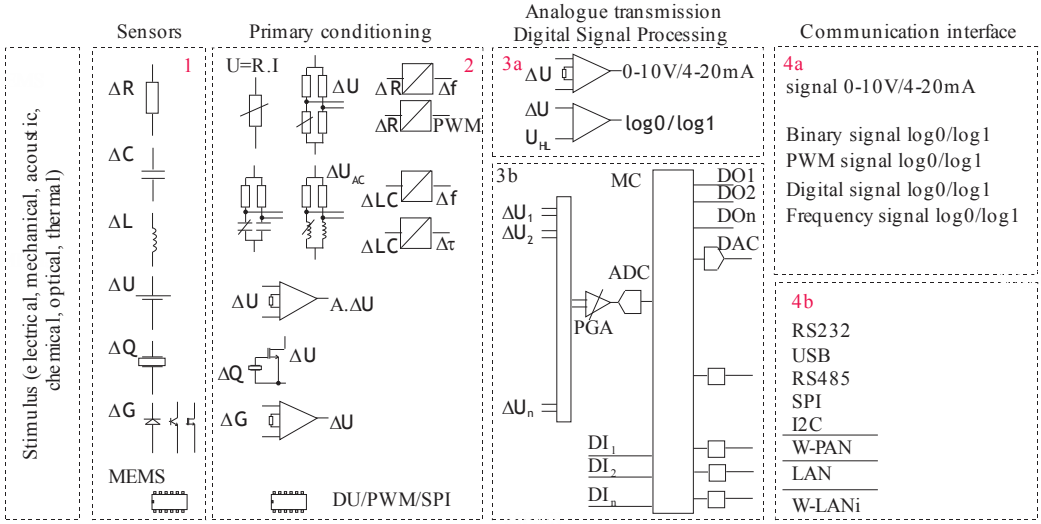

Fig. 2 Diagram of state of the art

The state-of-the-art has been investigated according to Fig 2, with a regard to existing classic sensor (1), primary analogue signal conditioning (2) and modern analogue signal transmission (3a) and digital signal processors (3b) and the communication system (analogue 4a, and digital 4b) between the constructed sensor and data acquisition system, in particular, including the uncertainty analysis of the system. Moreover, a propagation and penetration of the electromagnetic radiation have drawn special attention for the different signal levels to meet existing needs for modern communication system.

3 GOALS OF DISSERTATION WORK

In order to investigate a modern measurement system with the innovation of the new networks and wireless communication system, and the electromagnetic radiation in an indoor environment, the goals of the research work are:

1. Study the subfields of the sensors including: physical principles, theoretical base, signal conditioning, trends of a development
2. Setting a laboratory measurement system and testing the characteristics and functions of the experimental sensor.
3. Study the wireless communication systems for sensors and trends.
4. Measurement of propagation and penetration of a wireless signal communication.

4 THEORETICAL FRAME

4.1 Sensor

4.1.1 Introduction

A definition for a sensor can be found from various kinds of literature and from various aspects. A very broad definition is defined as a sensor is a device that receives and responds to a signal or stimulus [41]. The term stimulus is the quantity, property, or condition which is sensed and converted into the electrical signal. These quantities are electrical, mechanical, acoustic, chemical, optical, and thermal. There are six different kinds of signals: mechanical, thermal magnetic, electric, chemical, and radiation (corpuscular and electromagnetic, including light) [78].

Generally, sensors convert physical, chemical, geometrical, optical quantities into electrical signals. Today's modern sensors find their field of application in automobile engineering, house / industry automation, measurement, control, and others. Recently, application areas for sensor are extensively increasing due to a development of the technologies. These expanded areas include: military techniques, automobiles, aircraft, medical science, PCs, consumer electronics, home appliances as well as patient care techniques. In the middle of 1980s, the term smart sensor has coined. The intelligences required by such devices are Micro Controller Unit (MCU), Digital Signal Processor (DSP), and Application – Specific Integrated Circuit technologies. Also, the 1990s should be noticeable as the decade when a Micro – Electro – Mechanical System (MEMS) technology accelerated from the laboratory into a production system which means miniaturization of the system [79].

A development and an adaptation of the sensors are still under the consideration due to an advance of the technology and an improvement of the performance on demand of the consumers. For instance, researchers have been focused on MEMS, Chip Embedded Flexible Packaging technology, and Complementary Metal–Oxide–Semiconductor (CMOS) – MEMS integration [4, 54, and 55]. Simultaneously, a huge number of research

works are dealing with the adaptation of the sensors in order to achieve low cost, low power consumption, and with high accuracy sensors [5, 57, 69, 81, and 96].

4.1.2 Classification

Depending on the classification goal, different criteria may be selected [46]. However, some criterions are very common, for instance, with regard to a power supply modulating (or active) and self – generating (or passive) [41, 46, and 78], by output signal an analog and a digital, and for an operation mode deflection and null [78]. However, from the electronic engineer's point of view it is preferable to classify the sensors according to the variable electrical quantity, such as resistive, capacitive, and inductive. In spite of, the overall sensor classification can be drawn as shown below in Fig 3.

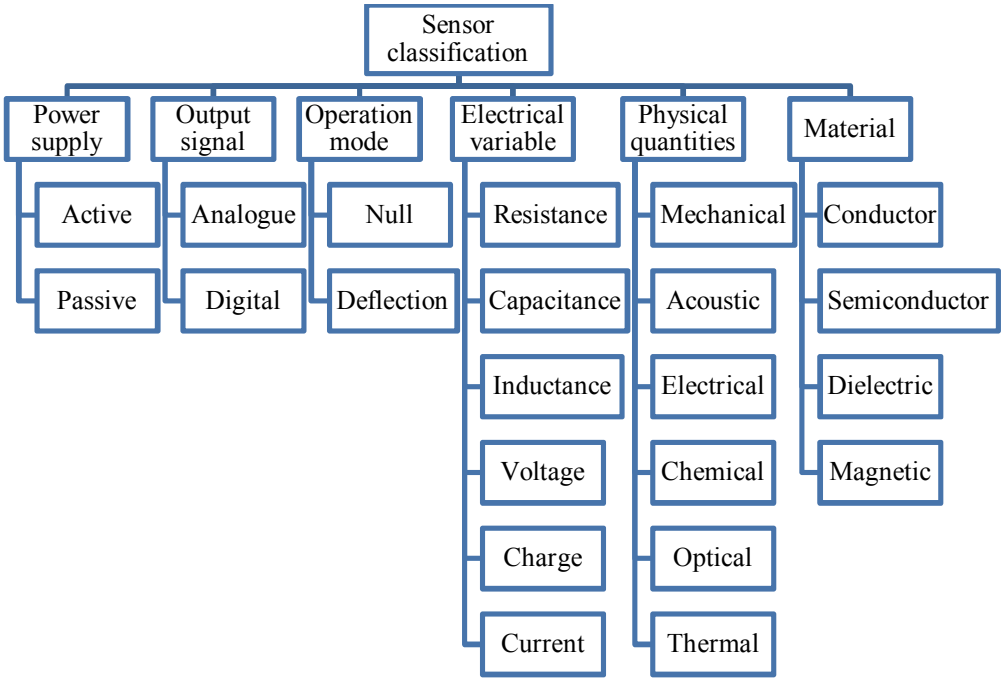

Fig. 3 Sensor classification scheme

4.1.3 Materials and Technology

Major changes in sensors come from new materials, new fabrication technique, or both. Therefore, materials and fabrication technology are playing a very important role in sensor science. From the material's chemical phenomena point of view the sensor material

can be divided into two classes: organic and inorganic [41]. The chemical and physical phenomena of the materials affect in the sensitivity, repeatability, electrical conductivity, thermal expansion and other specifications of the sensor.

Fig 4 shows the different materials used to sensor in 2006/2007 by: Sensors Polls and Surveys.

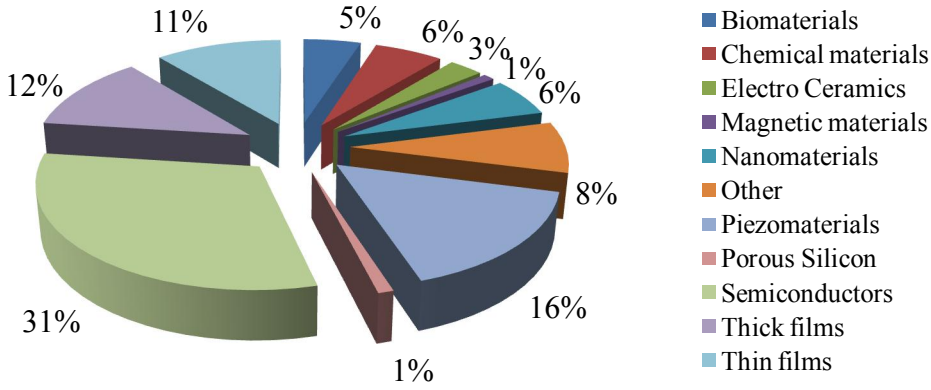

Fig. 4 Sensor materials and their usage [89]

However, depending on the application purpose and system a different composition of materials are available. For instance, different dielectric materials for wireless communication are given by [64]. Recently, nanocomposite materials are promising a great future for the sensor development, such as PPy–MWCNT nanocomposite and others [53]. Furthermore, as recorded by Ames Research Center, with the development of the nano technology the materials for the sensor are narrowing from a nanotube to a biomimetic material system.

The field of microsensors has grown rapidly during the past 20 years therefore; in this section semiconductor technology is considered. In the late 1980s, there has been the enormous effort to fabricate monolithic or integrated chips that can not only sense but also actuate, which means MEMS [28]. The importances of such devices are: compactness and sharply increased performances [42]. There are two main technologies for such sensor system as shown in Fig 5.

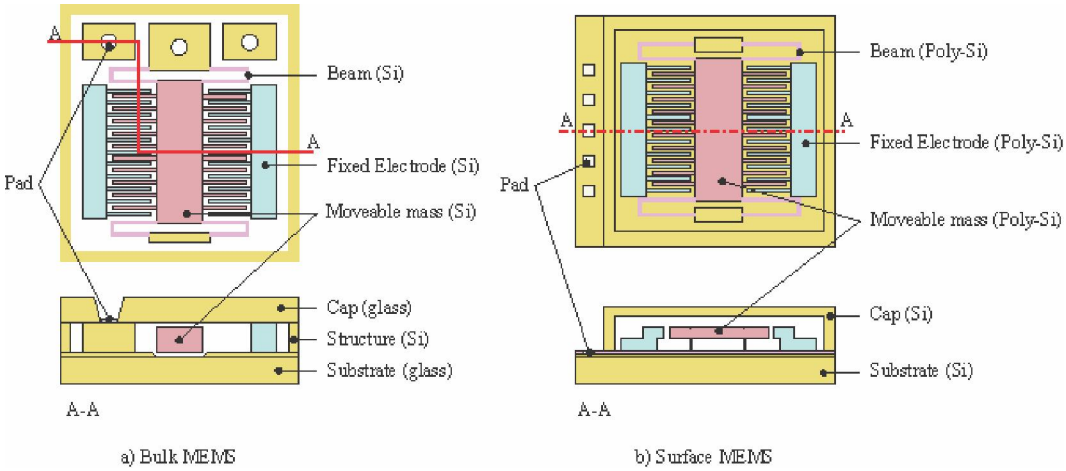

Fig. 5 Comparison of a) Bulk and b) Surface MEMS accelerometers [68]

Bulk Micromachining: is a process for making three – dimensional microstructures in which a masked silicon wafer is etched in an orientation – dependent etching solution [33]. Key parameters of this technology include: crystallographic orientation, etchant, etchant concentration, semiconductor starting material, temperature, and time [79]. The etch process employed in bulk micromachining comprise one or several of the following techniques [28]: Wet isotropic etching, Wet anisotropic etching, Plasma isotropic etching, Reactive ion etching, and Etch-stop techniques

Surface micromachining: allows smaller and more complex structures with the multiple layers to be fabricated on a substrate [79]. Three main technologies are: sacrificial layer, integrated circuit and wet anisotropic, and plasma etching. However, a special deposition process control is required to reduce stresses in the layers that can cause warping.

A combination of bulk and surface micromachining: a comparison of the two technologies, including their parameters such as mechanical, mass, capacitance, chip area, CMOS integration, size and cost can reveal their properties [18 and 27],. Therefore, a combination of above two technologies can eliminate a disadvantage and compensate the effects [51].

Other machining technologies: these technologies are being developed to overcome the limitations, extend the types of measurement and enhance the capabilities of former technologies. These are: Lithography, electroforming and molding process, Dry etching, Micromilling, and Laser micromaching

Recently, the nanotechnology promises a great opportunity not only for the sensor field but also for many current problems by means of smaller, lighter, faster and better performing materials, components and systems. Europe invested early with many programs in nanosciences starting during the mid- to late-1990s [12]. The ongoing advances in the sensor system, Nano Electro Mechanical System (NEMS) increasingly important [92].

4.1.4 Principle of sensing

A sensor is a converter of physical quantities into the electrical signals, and that requires one and more transformation techniques.

$$\begin{aligned} \Im &= \Phi\Re \\ U &= IZ \\ U &= q/C \\ U &= \frac{kT}{q}\ln\left(\frac{N_A N_D}{p_0 n_0}\right) \end{aligned} \tag{4.1.1}$$

Where: $\Im$ is the magnetomotive force (A), Φ is the magnetic flux (Wb), and $\Re$ is the reluctance (A/Wb), U -is the voltage (V), I is the current (A), Z is the impedance of the electrical elements (Ω). q is the charge (C), T is the temperature (^{0}C), k is Boltzmann constant, N_A, N_D are the concentrations of acceptor and donor atoms, $n_i^2 = p_0 n_0$ is the intrinsic carrier concentration.

All above transformation techniques are based on fundamental principles of circuits, which are Ohm's law in an electrical circuit and Hopkinson's law for magnetic circuit, electrostatic effect, and semiconductor junction, as stated by Equation (4.1.1).

Nevertheless, there are other sensing methods are also available such as sensors based of Metal Oxide Semiconductor Field Effect Transistor, CMOS image sensors, fiber optic sensors, ultrasonic sensors, and biosensors.

However, for the analyzing of an electrical network due to the range of the work a well-known Kirchhoff's current and voltage laws are useful, and equivalent mathematical model of the system units are given below [73, 82, 84, and 91]:

Table 1 Electrical elements and their equivalent equations

Element	Complex impedance	Network equivalent equation	
		Linear operator	Inverse operator
Resistive	R	$Ri(t)$	$\frac{1}{R}U(t)$
Capacitive	$-j\frac{1}{\omega C}$	$\frac{1}{C}\int_0^t idt$	$C\frac{dU}{dt}$
Inductive	$j\omega L$	$L\frac{di}{dt}$	$\frac{1}{L}\int_0^t U(t)$

Where: $\omega = 2\pi f$ - is the angular frequency (rad/s) $U(t)$ - is the voltage (V), and $i(t)$ - is the current (A).

Although, depending on the sensor type, the transformation techniques and connection of the network to the equation can vary from a simple Ohm's law to complex equation. Table 2 shows the main electrical sensors and their equations.

Table 2 Principle of electrical sensing

Sensor	Equation	Symbol description
		Resistive sensors
Potentiometer	$R = \frac{\rho l}{A}\alpha$	ρ is the resistivity, l is the length, A is the cross section α is the length fractional,
RTD	$R = R_0(1 + At + Bt^2 + Ct^3(t-100))$	R_0 - is the reference resistance, A , B and C are the constants (for metal sensors)
Thermistor	$R = R_0 e^{B\left(\frac{1}{T}-\frac{1}{T_0}\right)}$	R_0 is the reference resistance (25^0), T_0 is the corresponding temperature (K), B is the characteristic temperature of material.
Magnetoresistor	$R = R_{\min} + (R_{\max} - R_{\min})\left[1 - \left(\frac{H}{H_S}\right)^2\right]$	$R_{\max}$ and $R_{\min}$ are the maximum and minimum resistance, $H_S \geq H$ is the external magnetic field (for rotation 90^0).
LDR	$R = AE_v^{-\alpha}$	α and A are the manufacturing parameters depend on material.
Strain gauge	$R = R_0(1 + G\varepsilon)$	R_0 is the reference resistance, G is the gauge factor, ε is the applied strain.
		Capacitive sensors
Variable separation	$C = \frac{\varepsilon_0 \varepsilon_r S}{d + x}$	ε_0 and ε_r are the absolute and relative permittivity, S is the cross sectional area, d is the gap between electrodes, x is the displacement.
Variable area	$C = \frac{\varepsilon_0 \varepsilon_r}{d}(S - wx)$	w is the width of the plates, x is the area displacement.
1	2	3

1	2	3
Variable dielectric displacement	$C=\frac{\varepsilon_2 w}{d}[\varepsilon_2 l-(\varepsilon_2-\varepsilon_1)x]$	ε_2 and ε_1 are the permittivities of dielectric and air, l is the length of plate, x is the displacement.
Capacitive pressure	$\frac{\Delta C}{C}=\frac{(1-\nu^2)a^4}{16Edt^3}P$	ν is the Possion's ratio, a is the radius of diaphragm, E is the Young's modulus, t is the thickness of diaphragm.
Differential capacitive	$C_1=\frac{\varepsilon_0\varepsilon S}{d+x},\quad C_2=\frac{\varepsilon_0\varepsilon S}{d-x}$	C_1 and C_2 are the first and second capacitors of differential capacitor.
Capacitive level	$C=\frac{2\pi\varepsilon_0}{\log_e\left(\frac{b}{a}\right)}[l+(\varepsilon-1)h]$	l is the length of the cylinder capacitor, h is the height of liquid, b and a are the radius of outer and inner cylinder respectively.
	Inductive sensors	
Reluctance displacement	$L=\frac{n^2}{\Re_0+kd}=\frac{L_0}{1+\alpha d}$	n is the number of turns, $\Re_0$ is the reluctance at zero gap, $k=2/\mu_0\pi r^2$, d is the gap, L_0 is the inductance at zero gap, $\alpha=k/\Re_0$
Differential reluctance displacement	$L_1=\frac{L_0}{1+\alpha(a-x)},\quad L_2=\frac{L_0}{1+\alpha(a+x)}$	a is the core separation distance, x is the displacement
Eddy current	$\delta=\frac{1}{\sqrt{\pi f\mu\sigma}}$	δ is the standard depth of penetration, f is the frequency, μ is the permeability, σ is the conductivity,
LVDT	$S=\frac{2\pi f k_x}{\sqrt{R_1^2+(2\pi f L_1)^2}}$	R_1 is the resistance of primary winding L_1 is the inductance of primary winding, k_x is the variation of core (Note: when secondary winding is open), S is the sensitivity.
1	2	3

1	2	3
Flux – Gate	$U = NAB_e \frac{1-D}{[1+D(\mu_r-1)]^2}\frac{d\mu_r}{dt}$	D is the demagnetization factor, B_e is the external magnetic flux, N is the number of turn, A is the area of core.
		Electromagnetic sensors
Hall effect	$U = +(R_H / t)IB$	R_H is the Hall coefficient, B is the magnetic flux density, I is the slab current.
Tachometer	$e = k\omega n \sin(\omega t + \phi)$	n is the angular speed,
Linear velocity	$e = Bl\upsilon$	l is the conductor length, υ is the linear velocity.
Electromagnetic flowmeter	$e = kBD\upsilon$	k is the non dimensional constant, D is the electrode spacing.
		Active sensors
Thermocouples	$\Delta T = \sum_{n=0}^{N} a_n U^n$	a_n is the metall coefficient (0-5,13), U is the temocouple voltage (mV)
Piezoelectric	$E = -(gT)$ $Q = -(dF)$	E is the electric field (N/C), g is the voltage constant (V/με), T is the strain (με), Q is the charge (C), d is the charge constant (C/N), F is the applied force (N)
Pyroelectric	$U = pb\Delta T / \varepsilon$ $\Delta Q = pA_d \Delta T$	p is the pyroelectric coefficient (nC/cm^{2}K), b is the thickness (mm), ε is the dielectric constant, A_d is the area of incident radiation (cm^2)
Photovoltaic	$\phi = \frac{1}{\varepsilon}\int_{x1}^{x2} E dx$	ϕ is the internal potential (V)

4.1.5 Sensor characteristics

Behavior of the sensors influences on the characteristics of the whole measurement system. Therefore, it is important to describe its nature in a significant way by means of a sensor characteristic. The most common way is to describe their static and dynamic characteristics. Nevertheless, overall sensor characteristic includes the following concepts [77].

Transfer function	Dead band
Full – scale input	Resolution
Full – scale output	Special properties
Accuracy	Output impedance
Calibration	Excitation
Calibration error	Dynamic characteristic
Hysteresis	Environmental factor
Nonlinearity	Reliability
Saturation	Application characteristics
Repeatability	Uncertainty

It is impossible to reveal all the detailed characteristics of the sensors in this paper due to dependent of the sensor type and designs.

4.2 Signal conditioning

4.2.1 Introduction

Signal conditioning is one of the most important techniques in measurement and an automation system [72]. In order to obtain a useful signal, the signal conditioners are performing any of the following functions: conversion, level shifting, filtering, impedance matching, modulation, and demodulation. According to some literature [78], the signal conditioning and signal processing may be indistinct. The signal processing is performed for various purposes [97]:

Conditioning	Conversion
Acquisition	Recovery

Amplification	Harmonization
Separation	Modulation
Filtering	

Some of the signal processes can be performed digitally, but it is better to use a good quality analogue signal for a further digital processing.

4.2.2 Primary analogue signal conditioning

A primary conditioning is a conversion of output signal from the sensor, mainly into the function of voltage, frequency, and time. There are many reasons to choose processing of the analogue signals which are the output signals of most of the sensors are analogue, such kind of signals theoretically can take an infinite number of values. In spite of the fact that, the predominant principles by means of primary conditioning of resistance, inductance, and capacitive sensors into the function of voltage, time and frequency.

Electrical signal to voltage conversion

Voltage divider: commonly used to measure high value resistance and to create a reference voltage. The equation of the circuit in Fig 6a is given by:

$$U_{out} = \frac{Z_2}{Z_1 + Z_2} U_{in} \tag{4.2.1}$$

Wheatstone bridges: one of the most common techniques to used measure balance and deflection measurement for a very small resistance. The configuration of the bridge can vary as Quarter bridge, a Half bridge, and a Full bridge. The balance of the bridge (Fig 6b) is provided as:

$$Z_1 Z_3 = Z_2 Z_4 \tag{4.2.2}$$

In general form the voltage difference between both braches is:

$$U_{out} = U_S \left(\frac{Z_2}{Z_2 + Z_1} - \frac{Z_4}{Z_3 + Z_4} \right) \tag{4.2.3}$$

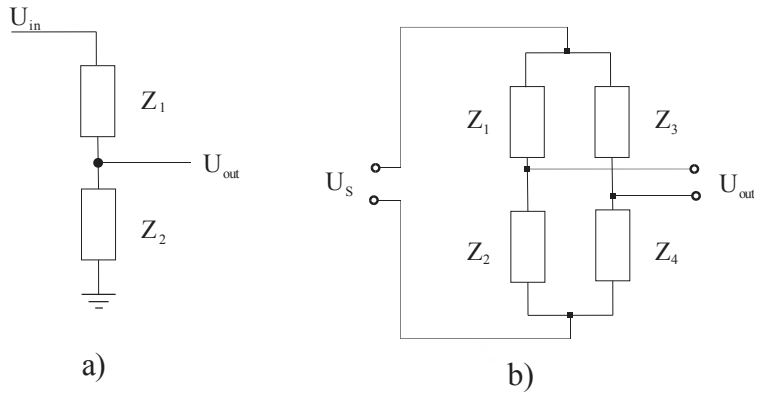

Fig. 6 Signal to voltage conversion scheme

Electrical signal to time conversion

Electrical signal to time conversion process is based on a time domain analysis of a system; by means of step response based methods are most commonly used for system identification. Especially, in process industries [85], as well as electrical and electronics engineering. A mathematical expression for the step response of the first order circuit is yields:

$$U_0 = U_S(1-e^{-t/\tau}) \quad \text{for} \quad t \geq 0 \tag{4.2.4}$$

Theoretically, the output voltage U_0 will take an infinite amount of time to settle its final value U_S, however, the standard method for describing a response of the circuit is the time constant of the system. In one time constant by means of $t = \tau$, the step response of the system reaches 63.2 percent of its final value.

$$U_0 = U_S(1-e^{-1}) = 0.632U_S \tag{4.2.5}$$

Fig 7 and Table 4 show normalized step response of the first order system, as well as its exponential components. As can be seen from the figure, how the elements of the circuit affects to the external influence as a function of the time.

Table 3 Characteristics of the first order system

Circuit	RC	RL
Scheme	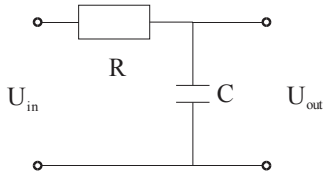	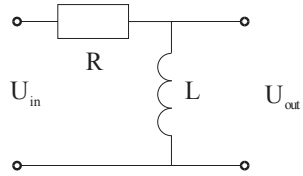
$\tau = \frac{1}{2\pi f_c}$	$\tau = RC$	$\tau = \frac{L}{R}$
f_{3dB}	$f_{3dB} = \frac{1}{2\pi\tau} = \frac{1}{2\pi RC}$	$f_{3dB} = \frac{1}{2\pi\tau} = \frac{R}{2\pi L}$
f_{6dB}	$f_{6dB} = \frac{\sqrt{3}}{2\pi\tau} = \frac{\sqrt{3}}{2\pi RC}$	$f_{6dB} = \frac{\sqrt{3}}{2\pi\tau} = \frac{\sqrt{3}R}{2\pi L}$

Where: τ - is the time constant (s), f_c - cutoff frequency (Hz), f_{3dB}, f_{6dB} - are the bandwidth frequencies (Hz).

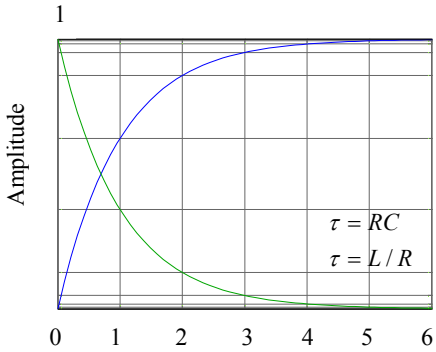

Fig. 7 Generalized Time constant for RC and RL circuit

Table 4 Exponential components of the RL and RC circuit

Time	$-t/\tau$	$y(0) = e^{-t/\tau}$	$y(t) = 1 - e^{-t/\tau}$
0	0.0	1.0000	0.0000
1τ	1.0	0.3679	0.6321
2τ	2.0	0.1353	0.8647
3τ	3.0	0.0498	0.9502
4τ	4.0	0.0183	0.9817
5τ	5.0	0.0067	0.9933
6τ	6.0	0.0025	0.9975

Another possible conversion is based on operational amplifier (op – amp) to time duration conversion. A simple linear resistance to time conversion circuit proposed by [49] consists of a bridge amplifier, an integrator and a comparator. The time interval of the circuit shown in Fig 8:

$$T = \frac{(1+\mu)^2 (R_2 R_x + R_1 R_3) C}{\mu R_1} \tag{4.2.6}$$

Where: $\mu = U_2 / U_1$

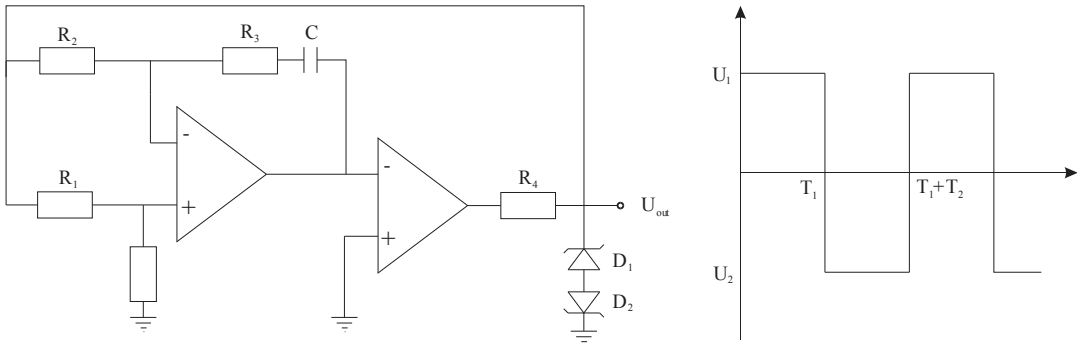

Fig. 8 Signal to time duration conversion

Electrical signal to frequency conversion

Voltage to frequency conversion circuits can yield an output frequency or period proportional to the measurand. An example of a frequency conversion from [78] which consists of differential integrator is given in Fig 9.

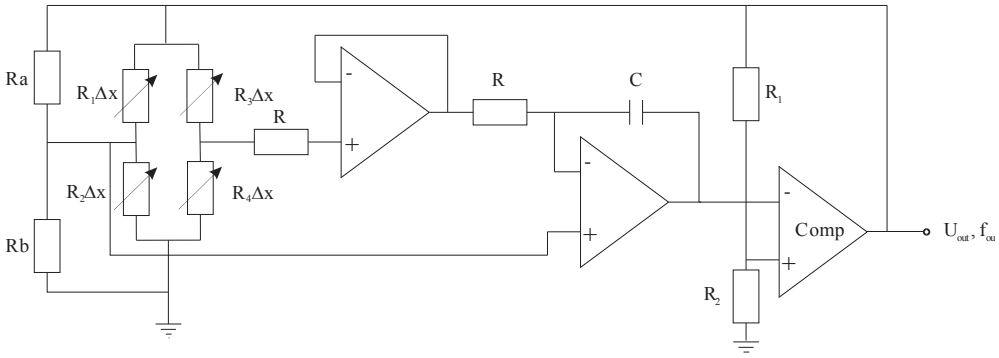

Fig. 9 Signal to Frequency conversion

When $t = T_1$:

$$T_1 = \left(U_0 - U_0' \right) \frac{R_2}{R_1 + R_2} \frac{RC}{x} U_0 \tag{4.2.7}$$

Where: U_0, U_0' are the high and low level voltage.

To switch the comparator back to U_0 at $t = T_2$ and

$$T_2 = \left(U_0 - U_0{}'\right)\frac{R_2}{R_1 + R_2}\frac{RC}{x}\left(\frac{1}{U_0} - \frac{1}{U_0{}'}\right) \tag{4.2.8}$$

The the frequency of the output signal which is proportional to the electrical signal is:

$$f_0 = \frac{x}{RC}\frac{R_1 + R_2}{R_2}\left(\frac{-U_0 U_0{}'}{\left(U_0 - U_0{}'\right)^2}\right) \tag{4.2.9}$$

Pulse Width Modulation (PWM) in signal conditioning

This circuit shown in Fig 10 delivers a rectangular signal with duty cycle varying between 0 and 100% in response to an input DC signal from [21]. The voltage at the inverting input swings between the two threshold levels, high and low. If we assume that $R_2 >> R_1$,then the voltage at noninverting input is always very close to $U_{IN}R_3C$ averages the signal at U_{OUT} ,and the DC voltage at inverting input is proportional to the duty cycle ofU_{OUT} .The closed feedback loop tends to equal inverting and noninverting inputs; therefore, the duty cycle at U_{OUT} is proportional to U_{IN} as follows:

$$DutyCycle = 100\frac{T_1}{T_1 + T_2} = 100\frac{U_{IN}}{U_{OH}} \tag{4.2.10}$$

An inverse relationship between duty cycle and U_{OH} can be useful in frequency conversion applications, so consider U_{OH} as an additional input. The output frequency follows the relationship:

$$f = \frac{\left(R_1 + R_2\right)\left(U_{OH}U_{IN} - U_{IN}{}^2\right)}{\left(R_3 C U_{OH}{}^2 R_1\right)} \tag{4.2.11}$$

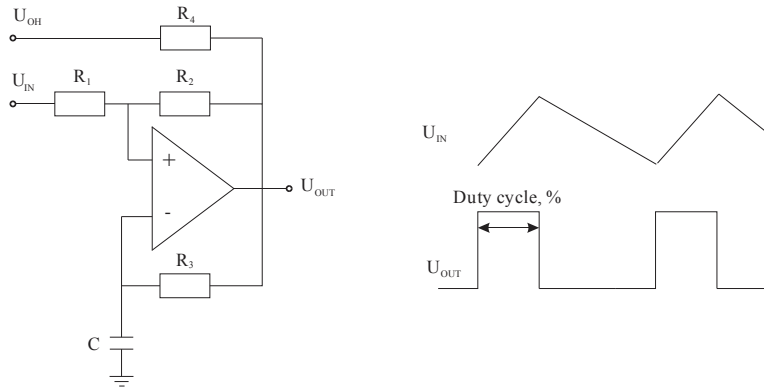

Fig. 10 Simple voltage controlled PWM

MOSFET transistors in analogue signal conditioning

One kind of field effect transistor, which are commonly used for amplifying, and converting the signals typically for charge variation sensors such as piezoelectric and pyroelectric sensors as a shown in Fig 11.

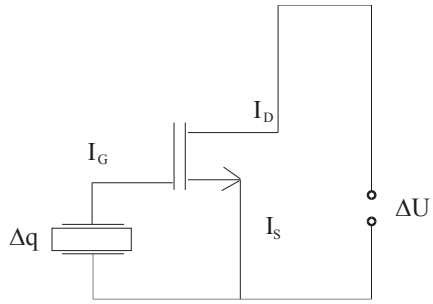

Fig. 11 MOSFET tansistor appication in signal conditioning

With the output voltage according to the law of electrostatic:

$$\Delta U \approx g \times R \partial q / \partial t \tag{4.2.12}$$

Where: g is the gain of transistor

Specific monolithic integration for capacitive sensors

Capacitive sensors suit monolithic integration, consequently has led to the development of the specific signal conditioners for capacitive sensors. For instance, [51,

and 52] capacitance measurement by charge integration and switched capacitances connected to the same voltage level in opposite clock cycles circuit is shown in Fig 12a.

During the charging phase, C_x charges and the output is zeroed. In contrast to, during the integration phase, the difference in charge between $C_x - C_r$ produces an output voltage:

$$U_0 = U\frac{C_x - C_r}{C} \tag{4.2.13}$$

Where: U is the amplitude of the clock signal.

Fig 12b depicts a specific capacitance to the voltage converter (CVC) which is proposed by [90]. The CVC operation can be divided into the two consecutive phases, namely, the sensing phase and reset phase. During the reset phase, S1 and S2 are closed, S3 and S4 are open. By releasing the charge periodically, this switching bias strategy suppresses the undesirable charge leakage to or from the sensing electrode and eliminates the bias voltage drift caused by charging. When reset phase is over, S1 and S2 are open before S3 and S4 are closed to avoid shorting between power rails. A function as a charge integrator and the output DC voltage is states:

$$U_0 = \frac{\Delta C}{C_1}\frac{U}{2} \tag{4.2.14}$$

One of the capacitance to frequency conversion method is the combination of CVC with voltage to frequency conversion.

The rest of the analogue signal conditioning such as an amplification circuits and voltage regulator can be seen in Section 5.1.2 in order to avoid duplicity.

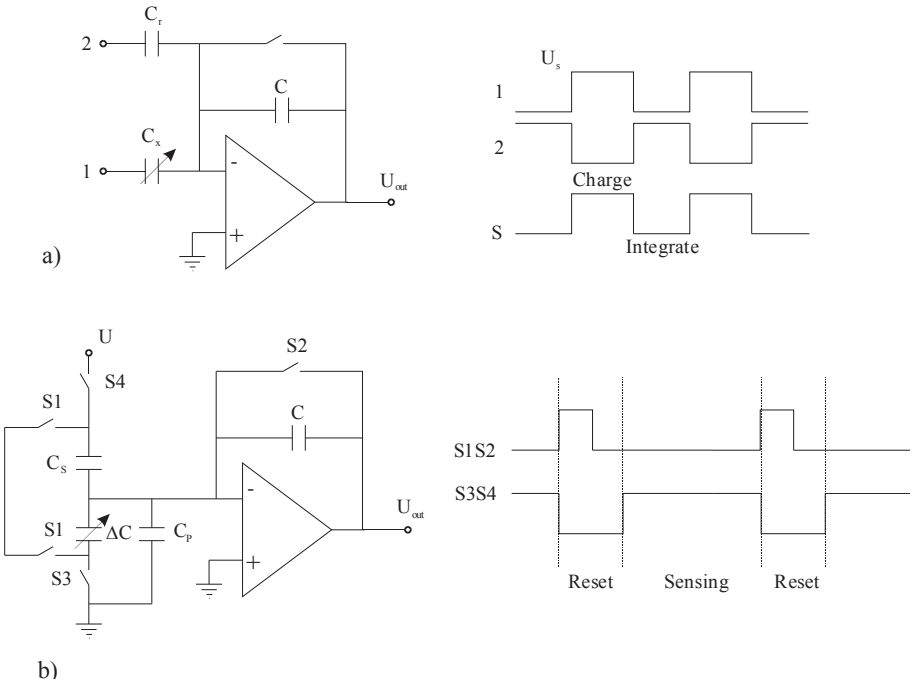

Fig. 12 Capacitance to time duration converters

4.2.3 Secondary signal conditioning

Analogue signal processing

Secondary analogue signal processing refers a circuit that translates the signal into the 4-20 mA analogue current and a 0 to 10 V analogue voltage output or directly into binary signals as logic 0/logic 1. The three main amplifiers are commonly used for this reason those are difference, operational and instrumentation amplifiers. Apart from that, a conversion directly into the logic values depending on a system requirement (Table 6). The generalized scheme is given by Fig 13.

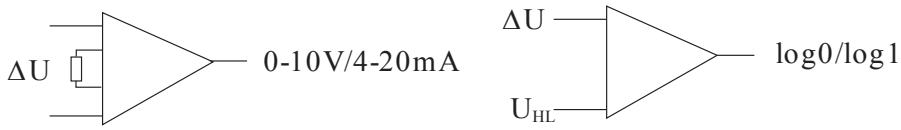

Fig. 13 Generalized analogue signal processing

Digital signal processing

DSP is an important field of study that has come about due to advances digital (computer) technology, consumer devices [99], as well as in a measurement and the analysis [14]. DSP is the post processing of the analogue signals at present executes by the microcontroller. A reason is obvious to processing signals digitally states that major advantage is consistency (by means of it is not sensitive to offset and drifts in electronic components). Second major advantage is very complex digital logic circuits can be packed onto a single chip, thus reducing the component count and a size and a reliability of the system [19]. Theoretically, behind the DSP a number of subfields lie, starting from a discrete time system to the most complex algorithm, but a typical DSP system is often realized in the following sequence: analogue to digital conversion (ADC), appropriate DSP, digital to analogue conversion.

Multiplexers

In digital circuit design, a multiplexer is a combination of logic gates resulting into circuits with two or more data inputs and one output. Main architectures are designed to 2-to1, 4-to-1, 8-to-1 and 16-to-1. The Boolean equations for 2-to1 and 4-to-1 are:

$$\begin{aligned} Z &= \left(A\overline{S}\right) + \left(BS\right) \\ F &= \left(A\overline{S_0}\,\overline{S_1}\right) + \left(B\overline{S_0}S_1\right) + \left(CS_0\overline{S_1}\right) + \left(DS_0S_1\right) \end{aligned} \tag{4.2.15}$$

Digital Filters

Anti-aliasing filters are always analog filters as they process the signal before it is sampled. In most cases, they are also low-pass filters [19], to remove the high frequency content which would otherwise be aliased down, ultimately to appear as a lower frequency signal contamination [75].

Besides, there are two main kinds of linear digital filter that operate in the time domain; the finite impulse response (FIR) and the infinite impulse response (IIR) filters variety. Only ever three operations that a processor uses to execute them: time shift, multiplication and addition.

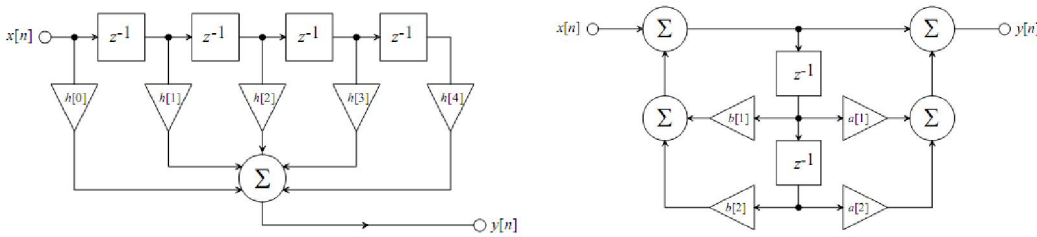

a) FIR *b) Typical IIR*

Fig. 14 Block scheme diagrams of digital filters

Filter selection and criteria are predicated on efficiency, phase linearity, a transition zone performance, and stability, ease of design and word length immunity. The following Table 5 compares the main properties of FIR and IIR filters.

Table 5 FIR versus IIR

Property/Filter type	***FIR***	***IIR***
Unconditional stability	Yes	No
Phase distortion	No	Yes
Design ease	Easy	Difficult
Arbitrary response	Easy	Difficult
Computational load	High	Low
Word length immunity	Good	Poor
Analogue equivalent	No	Yes
Real time operation	Yes	Yes

Depending on the architecture (Harvard, Super Harvard, and Von Neumann [93]) DSP can vary for the different sequences of internal components.

Programmable gain amplifier (PGA)

PGA is an electronic amplifier and enabling a new level of signal-conditioning performance in the sensor interface applications and data acquisition systems, targeting the industrial and instrumentation markets. On the other hand, PGA is performing the circuits

requiring nonstandard gains, which mean the gains not easily achievable, the circuits requiring low cost. An example of PGA can be seen in Fig 15.

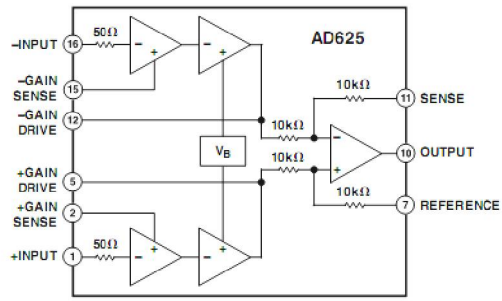

Fig. 15 Functional block diagram of PGA from [3]

Several semiconductor manufacturers produce a range of DSP chips with different capabilities. Most of the DSP chips are single processor devices. There exist chips that integrate multiple DSP processors on the same chip such as the Texas Instruments TMS320C8x, and Analog devices DSP-SHARC. Others combine a DSP processor with a microcontroller such as the Motorola DSP568xx, and Freescale DSP56XXX [3, 23, 70, and 95]. Due to capability of the work we have just considered on the main points of DSP further detailed information can be found, for instance, logic system, gates and their theory in [98], and more theoretical background and their Matlab examples can be found from [99].

4.3 Communication system for sensors

4.3.1 Introduction

A communication system organizes not only the transferring of the pure data from secondary signal processing, but also sending the messages, commands, instructions and synchronization signals analogically (or digitally). A data to be transmitted in the communication system can take a one of the following forms in Fig 16.

The four main challenges to the ground sensor communications system are Operational Suitability (Does the system fulfill the functional requirements for a data transport of the sensor data?), Robust Performance (a reliable and a robust performance in

the face of a range of physical and electromagnetic environments and threats), Battery Life (a energy efficiency), and Affordability (a low acquisition and a support cost, a long useful life) [8].

a) Simplex *b) Duplex* *c) Half-Duplex* *d) Full-Duplex*

Fig. 16 Data transmission connection

The four main challenges to the ground sensor communications system are Operational Suitability (Does the system fulfill the functional requirements for a data transport of the sensor data?), Robust Performance (a reliable and a robust performance in the face of a range of physical and electromagnetic environments and threats), Battery Life (a energy efficiency), and Affordability (a low acquisition and a support cost, a long useful life) [8].

The most of the communication systems are standardized and such standardized systems are called an *interface*. The *interface bus* is a connection of the subsystem that transfers the data between computer components [97]. The information or data to be communicated can exist in either of two forms, whether through air or wire: analogue and digital.

The process of altering one signal by means of another is known as modulation; an original information is called the baseband signal, and the signal modulated by the baseband signal is termed the carrier (because it “carries” the information) [44]. Such modulation techniques are: amplitude, frequency, and phase, quadrature amplitude modulation for analogue signals, and frequency shift, amplitude shift, phase shift keying, pulse position modulation for digital signals.

4.3.2 Analogue communication system

The most data collected by the sensors are continues and those signals provide main two advantages: a less attenuation than those digital signals over the same distance, and can be multiplexed to increase a bandwidth. In industry, the collection of equipment is known as a measurement loop or a loop. Those loops can be divided into the three groups such as a two, three, and four wire loop [15].

On the other hand, the analogue signals can be divided as the voltage signals (voltage loop Fig 17b) and the current signals (current loop Fig 17a). The current signals are standardized into two ranges: these are 4 to 20 mA, and 10 to 50mA, nowadays the latter range has been dropped [100]. Sometimes it is enough to amplify the signal to a level acceptable by the most of ADC, for example, ±5V or ±10V [97]. The advantage of such signal is that it is independent of the changes of the resistance of connections (for example caused by the change of the temperature). Under such assumption the data transmission at distances up to 2 km is possible by current loop [97].

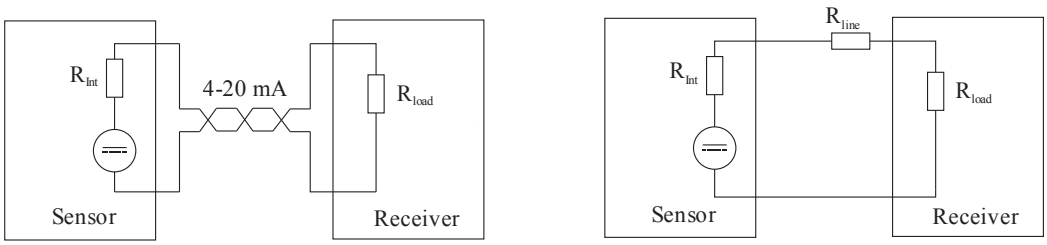

a) Current loop *b) Voltage loop*

Fig. 17 Typical analogue measurement loops

Logic level

Two logical states of the signal are usually represented by two different voltages a high and a low, but current is used in some logic families. When the signal is below from a threshold, the logic is "low, (L)" when above "high, (H)". Intermediate levels are undefined and the behavior of the connected circuits is highly implementation-specific. Table 6 compares the most common logic levels. However, that level varies widely from one system to another.

Table 6 Common logic levels

Technology	L voltage (V)	H voltage (V)	Specification
DTL	< 2.7	$8.2 \div 15$	In voltage
CMOS	$0 \div U_{DD} / 2$	$U_{DD} / 2 \div U_{DD}$	U_{DD} is the supply voltage
TTL	$0 \div 0.8$	$2 \div U_{CC}$	$U_{CC} = 5 \pm 10\%$
ECL	$U_{EE} \div (-1.4)$	$-1.2 \div 0$	$U_{EE} = -5.2$

4.3.3 Digital communication system

The data represented by the digital bits can be transferred through a serial interface or through a parallel interface. The advantages of digital communication systems are numerous, such as reliable, easy for signaling, multiplexing, encryption, and compression and others.

Serial interface: is the process of sending the data one bit at a time, sequentially, over a communication channel or an interface bus. The most common serial interface busses are: Serial Peripheral Interface (SPI) (Fig18a), Inter Integrated Circuit (I2C) (Fig18b), UNI/O (Fig18c), 1-Wire (Fig18d), RS485 (Fig18e) and USB (Fig18f) [38 and 65].

Moreover, the data in the serial communication system can be transferred as an asynchronous (or SCI, transmission of data without the use of an external clock signal) and a synchronous (SPI).

Parallel interface: is a method of sending a data or the signals simultaneously over the several channels contraversing to Serial interface. Examples of parallel interfaces for computers are: Industry Standard Architecture, AT Attachment, Small Computer System Interface, Peripheral Component Interconnect, and others. However, for laboratory instrumentation a bus IEEE-488 was created by HP-IB, or commonly called GPIB.

GPIB: is a 24 pin, double sided, 8 bits, and electrically parallel bus. The standard allows up to 15 devices to share a single physical bus of up to 20 meters total cable length with the maximum data rate of 1 Mb/s.

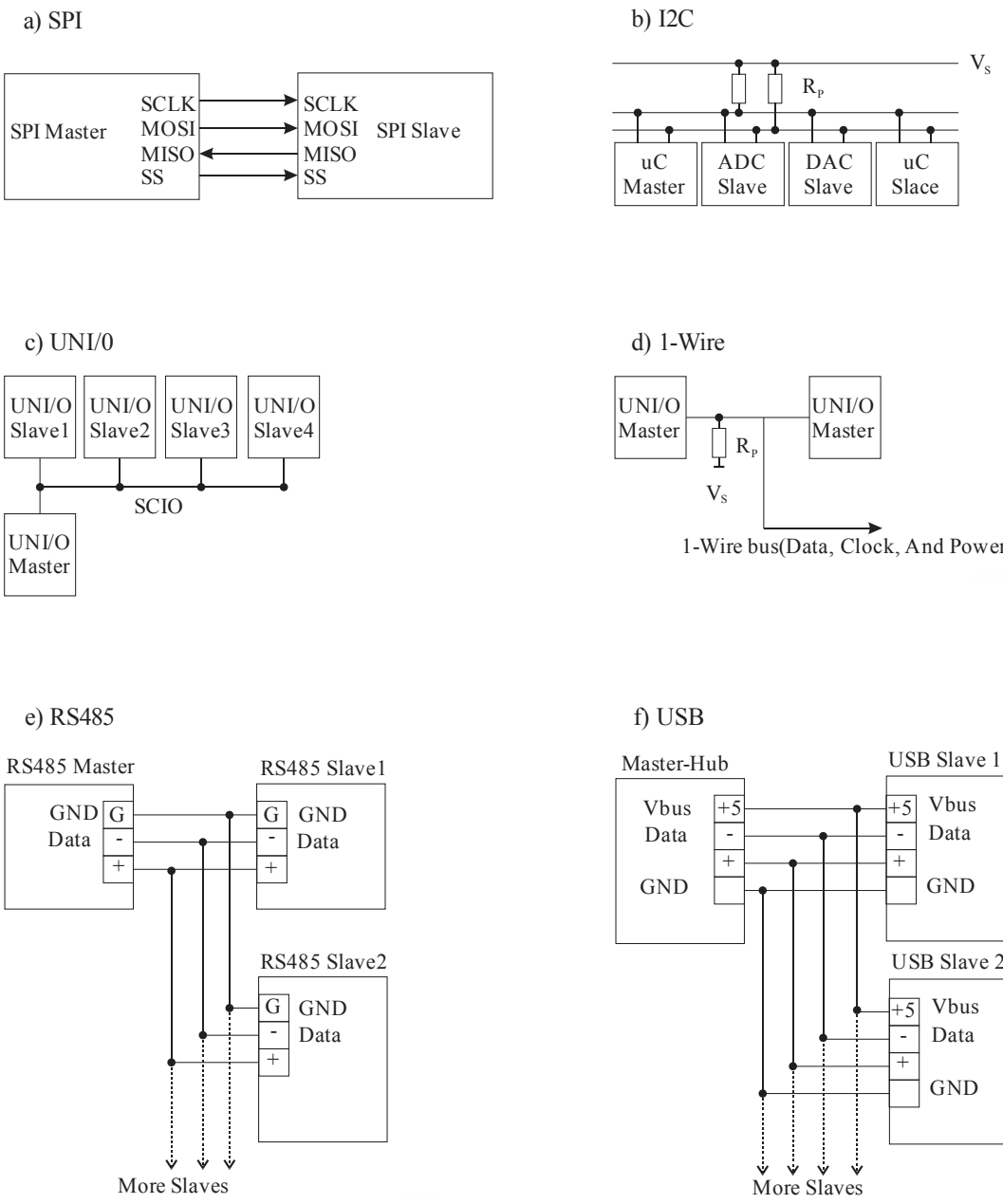

Fig. 18 Serial communication busses

In spite of that, the communication system with their specification for the sensor data transmission can be found from Table 7.

Table 7 Sensor data communication systems

Signal and Standards	Specifications
Voltage signal (V)	0-10 (max 200m, R>2700Ω)
Current signal (mA)	4-20 (max 2000m, R<750Ω)
Wired PAN	
RS485	MP, M/S, 1+254 units, <2MB/s, <1200m, R=120Ω, various protocols (Profibus, CAN, M-Bus, etc.)
RS232	Duplex, <15m, <19kb/s,
USB	Plug&Play, <5m, 1.0 (<12Mb/s), 2.0 (480Mb/s), 3.0 (<5Gb/s)
FireWire	Serial bus for high speed transmission, Video, HDD, DVD, IEEE 1394a (400Mb/s), IEEE 1394b (800Mb/s) , IEEE 1394c (3200Mb/s)
HART	Parallel analogue signal transmission, 100 KHz modulation
WPAN	
IEEE 802.15.1	Bluetooth, 720 kb/s, ver.1 <10m ver.3 <400 m
IEEE 802.15.4	ZigBee, <250 kb/s, <100m
Wired LAN	
IEEE 802.3	Ethernet 10 Base, 100 Base, 1000 Base
WLAN	
IEEE 802.11	TCP/IP protocol based Wi-Fi, VER: a (5GHz,54Mb/s), b (2,4GHz, 11Mb/s), g (2,4GHz ,54Mb/s), n (2,4/5GHz, 600Mb/s), y (3,7GHz ,54Mb/s), ac (2,4/5GHz, 1000Mb/s)

4.4 Fundamental of electromagnetic waves

4.4.1 Introduction

Wireless communication system is becoming a more omnipresent in daily lives ranging from a mobile communication system to local and personal area networks [6, 30, 58, and 67]. Furthermore, a short – range indoor wireless communication system is playing a more important role with the emergence of a portable system as well as a prime significant demand is to reduce the number of wires needed to be connected [88]. Above

all, it avoids obstacles such as crossing objects owned by others but also in industry, there was a large dream of generations of designers for wireless connections among sensors fixed on rotating parts of machines and control systems however, there are many problems in a realization of wireless communication in industrial applications [104]. The essence of Maxwell's equations is that a time-varying electric field produces a magnetic field, and the time-varying magnetic field produces an electric field. The time-varying magnetic field can be generated by an accelerated charge [43].

The interactions between a macroscopic material and the electromagnetic fields can be generally described by Maxwell's equations [11]:

$$\begin{aligned} &\nabla \times D = \rho \\ &\nabla \times B = 0 \\ &\nabla \times H = \partial D / \partial t + J \\ &\nabla \times E = -\partial B / \partial t \end{aligned} \tag{4.4.1}$$

With the following constitutive relations:

$$\begin{aligned} &D = \varepsilon E = (\varepsilon' - j\varepsilon'')E \\ &B = \mu H = (\mu' - j\mu'')H \\ &J = \sigma E \end{aligned} \tag{4.4.2}$$

Where: H and E are the respectively, magnetic and electric field strength vector. B is the magnetic flux density vector, D is the electric displacement vector, J is the current density vector, ρ is the charge density, $\varepsilon = (\varepsilon' - j\varepsilon'')$ and $\mu = (\mu' - j\mu'')$ are the complex permittivity and permeability of the material, and σ is the conductivity of the material.

Equations (4.4.1) to (4.4.2) indicate that the responses of the electromagnetic material to electromagnetic fields are determined essentially by three constitutive parameters, namely permittivity ε, permeability μ, and conductivity σ.

For low conductivity materials: the propagation of electromagnetic waves in a medium is determined by the characteristic wave impedance η of the medium and the wave velocity υ in the medium complies:

$$\eta = \sqrt{\frac{\mu}{\varepsilon}}$$
$$\upsilon = \frac{1}{\sqrt{\mu\varepsilon}} \tag{4.4.3}$$

Where: $\eta = \sqrt{\mu_0 / \varepsilon_0} = 376.7\,(\Omega)$, free space impedance, and $\upsilon = c = 1/\sqrt{\mu\varepsilon} = 2.998 \times 10^8$ (m/s) wave velocity in free space.

Sometimes, it is more convenient to use a complex propagation coefficient γ to describe the propagation of electromagnetic waves in the medium for low and high conductivity materials:

$$\gamma = \alpha + j\beta = j\omega\sqrt{\mu\varepsilon} = j\frac{\omega}{c}\sqrt{\mu_r\varepsilon_r} = j\frac{\omega}{c}n \tag{4.4.4}$$

$$\gamma = \alpha + j\beta = j\omega\sqrt{\mu\varepsilon}\sqrt{\frac{\sigma}{j\omega\varepsilon}} = (1+j)\sqrt{\frac{\omega\mu\sigma}{2}} \tag{4.4.5}$$

Where: n is the complex index of refraction, ω is the angular frequency, α is the attenuation coefficient, $\beta = 2\pi/\lambda$ is the phase change coefficient, and λ is the operating wavelength in the medium.

A skin depth of the high conductivity material is:

$$\delta_x = \frac{1}{\alpha} = \sqrt{\frac{2}{\omega\mu\sigma}} \tag{4.4.6}$$

Because of the skin effect behavior of high conductivity materials at microwave frequencies are mainly determined by their surface impedance Z_S:

$$Z_s = R_s + jX_s = \frac{E_t}{H_t} = (1+j)\sqrt{\frac{\omega\mu}{2\sigma}} \tag{4.4.7}$$

Where: $R_s = X_s = \sqrt{\frac{\omega\mu}{2\sigma}}$ are the surface resistance and reactance respectively.

Most wireless systems must propagate signals through the nonideal environments. Modes of radio wave propagation are given by Fig 19 particularly, the characteristics of waves depend upon a path and a frequency of transmission [43, and74].

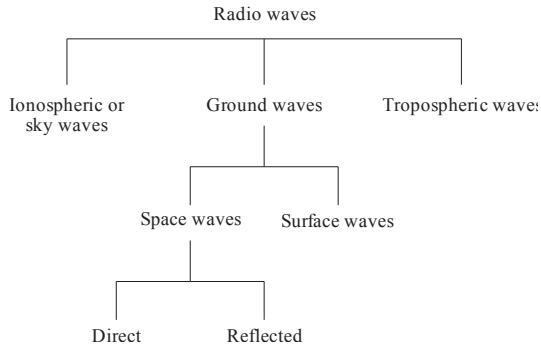

Fig. 19 Electromagnetic radiation propagation

There are a variety of phenomena that occur when an electromagnetic wave is incident. These phenomena are: Reflection, Scattering, Diffraction, Refraction, Absorption, and Depolarization [20, and 87]. Path loss is the main constituent of propagation and is a measure of the average radio wave attenuation experienced by the propagated signal when it reaches the receiver, after having navigated through a path of several wavelengths. Path loss is given by [104]:

$$PL_{dB} = 10 \log \frac{P_r}{P_t} \tag{4.4.8}$$

Where: P_t and P_r are the respectively transmitted and received powers.

A number of research workers are dealing with RF (Radio Frequency) signal propagation and penetration due to a development of the communication system. Many measurements for both single-floor and multiple-floor propagation have been made in the interest of determining the statistical properties of the propagation. Especially, a penetration measurement which is based on the electromagnetic theory has drawn much attention of many researchers [7, 10, 31, 101, and 102].

4.4.2 RF Propagation models

The goal of propagation modeling is often to determine the probability of satisfactory performance of a communication system or other system that is dependent upon electromagnetic wave propagation. Generally, it is a good idea to employ two or more independent models if they are available and use the results as bounds on the expected performance. There are number of indoor propagation models are available as mentioned before. Apparently, there are a number of the propagation model exist. The most famous or well – known model is Friis transformation equation is states that [43, and 48]:

$$\begin{aligned} P_r &= 10\log_{10} P_t + 10\log_{10} G_t + 10\log_{10} G_r + \\ &+ 147.558 - 20\log_{10} f - 20\log_{10} d \end{aligned} \tag{4.4.9}$$

Where: P_t and P_r are the apparently transmitted and received powers respectively. G_t and G_r are the correspondingly transmitting and receiving antennas gains, d is the distance (m), f is the specified operating frequency (MHz).

In spite of the mentioned models, there are several site – specific models proposed by different resources, which are shown below.

The *ITU site-general* model for path loss prediction in an indoor propagation environment is follows [87]:

$$L_{total} = 20\log_{10} f + N\log_{10} d + Lf(n) - 28 \tag{4.4.10}$$

Where: N is the distance power decay index, f is the frequency (MHz), d is the distance (m) $(d > 1)$, $Lf(n)$ is the floor penetration loss factor and n is the number of floors between the transmitter and the receiver.

The *log – distance* path loss model is another site general model and it yields [80]:

$$L_{total} = PL(d_0) + N\log_{10}(d/d_0) + X_s \tag{4.4.11}$$

Where: $PL(d_0)$ is the path loss at the reference distance, usually taken as (theoretical) free-space loss at 1m, $N/10$ is the path loss distance exponent X_s is a Gaussian random variable with zero mean and standard deviation of σ dB.

For frequencies between 800 MHz and 1.9 GHz, COST 231 reports the following values for the path loss exponent [16]:

Table 8 Exponent function for different environment

Environment	Exponent	Propagation mechanism
Corridors	1.4-1.9	Wave guidance
Large open room	2	Free space loss
Furnished room	3	Free space loss+multipath
Densely furnished room	4	Non-Los, diffraction, scattering
Different floors	5	Loss of floor (wall)

The *COST231-Hata* Model is designed for a frequency range from 1.5 to 2 GHz and is given by [9]:

$$L_{total} = 46.3 + 39.9\log f - 13.82\log h_{te} - ah_{re} + \\ + (44.9 - 6.55\log h_{te})\log d + C_m \tag{4.4.12}$$

Where: f is the frequency (MHz), d is the link distance (m), h_{te} is the transmitter height (m), h_{re} is the receiver height (m), and C_m is the 0 dB for soft and suburban areas, 3 dB for dense urban areas.

The path loss model referred in [1], the *ECC-33* model is defined as:

$$PL = A_{f_s} + A_{bm} - G_b - G_r \tag{4.4.13}$$

Where: A_{f_s}, A_{bm}, G_b and G_r are the free space attenuation, and individually defined as:

$$
\begin{aligned}
A_{f_s} &= 92.4 + 20\log_{10} d + 20\log_{10} f \\
A_{bm} &= 20.41 + 9.83\log_{10} d + 7.894\log_{10} f + 9.56[\log_{10} f]^2 \\
G_b &= \log_{10}(h_b / 200)\{13.958 + 5.8[\log_{10} d]^2\} \\
G_r &= [42.57 + 13.7\log_{10} f][\log_{10} h_r - 0.585]
\end{aligned}
\tag{4.4.14}
$$

Where: f is the frequency (GHz), d is the distance between two antennas (km), h_b is the transmitting antenna height (m), and h_r is the receiver antenna height (m).

As noted by [1], the predictions produced by the ECC-33 model do not lie on straight lines when plotted against distance having a log scale.

Table 9 contrasts former propagation models.

Table 9 Comparison of propagation models

Model	Environment	Application specification	Consideration
ITU	Indoor (including penetration)	900 MHz-5.2 GHZ, Floor penetration 1 to 3	Dependent on the distance power loss coefficient and floor loss penetration factor
Log-Distance	Indoor or densely populated area	Fading is taken into account(by Gaussian random variable)	Dependent on a path loss at the reference distance (1km or 1 mile)
COST231-Hata	Urban, suburban, dense urban areas	1.5÷2 GHz, up to 20 km	Requires: the base station antenna is higher than all adjacent rooftops.
ECC-33	Suburban	More suit to fixed wireless system	Dependent on the empirical constants

4.4.3 RF Penetration

In recent years, there has been an increasing interest in using free space techniques [29] for the measurement of electromagnetic properties of materials and for estimating plasma parameters of magneto active plasma. The advantages of the free space method are: inhomogeneous (unwanted higher order modes), nondestructive and contactless.

Fig 19 compares two methods, which are Transmission/Reflection (T/R) and spread spectrum transmission system used for Non Line of Sight research [101].

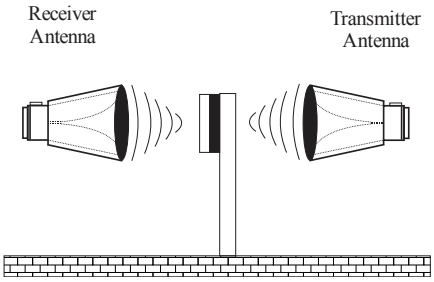

a) T/R method

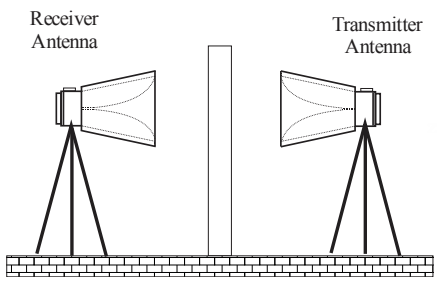

b) Schematic of Non Line of Sight Research

Fig. 20 Free space measurement method

As can be seen in Fig 20a, the T/R method requires a spot focusing lens. However, in the case of wireless sensor signal penetration which is totally impossible. In contrast to, the method is shown Fig: 20b has not used the lens, if when the antennas are not totally separated then the diffraction and reflection would occur.

According to [102], the transmission coefficient into the wall is:

$$T_{\uparrow} = \frac{2}{1+\sqrt{\varepsilon_r}} \tag{4.4.15}$$

and the transmission coefficient out of the wall is given by:

$$T_{\downarrow} = \frac{2\sqrt{\varepsilon_r}}{1+\sqrt{\varepsilon_r}} \tag{4.4.16}$$

Therefore, the loss power due to transmission (not attenuation inside the wall) is:

$$L = 20\log_{10}\left|T_{\uparrow}T_{\downarrow}\right| = 20\log_{10}\frac{4\sqrt{\varepsilon_r}}{\left(1+\sqrt{\varepsilon_r}\right)^2} \tag{4.4.17}$$

The multiple layered structure, According to transmission line theory, the overall reflection coefficient (expressed in dB) for multilayer absorber at the air-absorber interface can be expressed as [59] (Fig 21 left hand side):

$$R = 20\log\left|\left(Z_i - 1\right)/\left(Z_i + 1\right)\right| \tag{4.4.18}$$

Where: Z_i is the normalized impedance of i th layer.

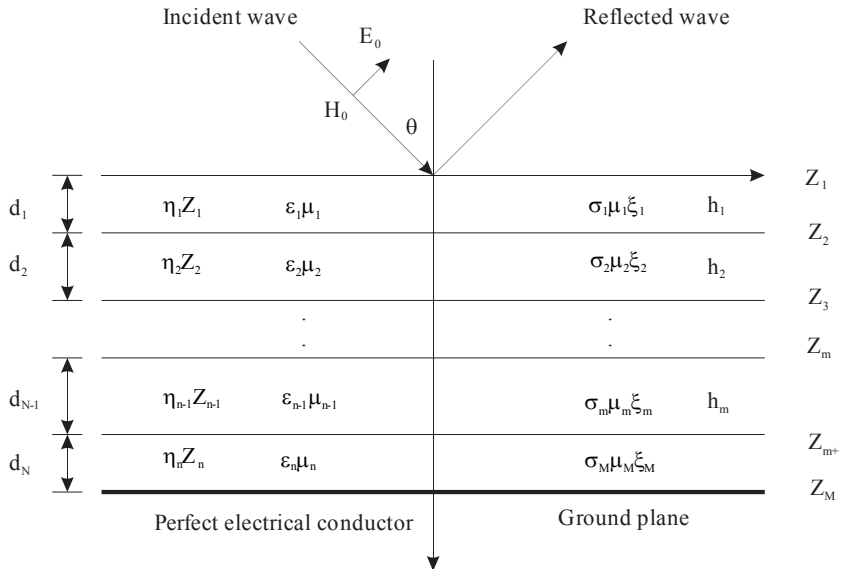

Fig. 21 Model of multilayer absorber

Another approach proposed by [47] as a numerical technique called Powell method, to design radar absorbing materials (Fig 21 right hand side). According to author's formulation: The wave impedance Z can be calculated by a recurrence formula given by:

$$Z_1 = K_1\left[\frac{Z_2 + K_1 \tanh(U_1 h_1)}{K_1 + Z_2 \tanh(U_1 h_1)}\right]$$

$$Z_2 = K_2\left[\frac{Z_3 + K_2 \tanh(U_2 h_2)}{K_2 + Z_3 \tanh(U_2 h_2)}\right] \qquad (4.4.19)$$

etc

$$Z_{m-1} = K_{m-1}\left[\frac{Z_m + K_{m-1} \tanh(U_{m-1} h_{m-1})}{K_{m-1} + Z_m \tanh(U_{m-1} h_{m-1})}\right]$$

Where: K_m is the wave impedance of the layer *m,* given by:

$$K_m = \frac{U_m}{\sigma_m + j\omega\varepsilon_m} \qquad (4.4.20)$$

Where: $\omega = 2\pi f$ is the radian frequency. U_m is the propagation constant and:

$$U_m = \sqrt{L^2 + \gamma_m^2} \qquad (4.4.21)$$

With the

$$L = j\gamma_0 \sin\theta$$
$$\gamma_m^2 = -\mu_m \varepsilon_m \omega^2 + j\sigma_m \mu_m \omega \tag{4.4.22}$$

Now, we know the impedance, at the interface between the free-space incidence regions. And the first layer, we can calculate the reflection coefficient of the layered media. It is given by:

$$R_0 = \frac{K_0 - Z_1}{K_0 + Z_1} \tag{4.4.23}$$

Where: $K_0 = 377\cos\theta$ is the wave impedance of the incidence region, for an angle of incidence.

In addition, as noted by this method to design the radar absorption material for both polarizations, the parallel and the perpendicular are the similar.

It can be concluded that a former model is an only function of the relative permittivity, and the test was performed under the 0 dBm reference value. In contrast to the second numerical method is a both functions of the permittivity, the permeability, and the conductivity.

4.5 Spectrum analyzer, uncertainty evaluation, modeling and simulation

4.5.1 Introduction

A French mathematician and physicist, named Jean Baptiste Joseph Fourier, who lived from 1768 to 1830 also started to look at how signals are seen in another format, in the frequency domain where signals are viewed as a function of their frequency rather than time. He discovered that any waveform seen in the time domain, there is an equivalent representation in the frequency domain as depicted by Fig 22 [35].

The main objective of spectrum analyzer or frequency domain analysis is better for determining the harmonic content of a signal. The specialized application of the spectrum

analyzer involves the monitoring of radio frequency (RF) interface, electromagnetic interference, and electromagnetic compatibility.

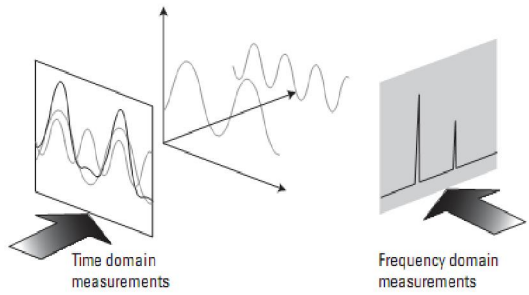

Fig. 22 Time and frequency domain

There are two main types of the analyzer [36, 37, and 63]: Swept spectrum analyzer (SSA): based on the superheterodyne principle, and most widely used type. Fast Fourier transform based spectrum analyzer (FFTSA): use FFT, converting the signals into digital format and analysis digitally. Both SSA and FFTSA technologies have their own advantages. The more commonly used technology is the SSA as it the type used in general-purpose analyzers enabling these analyzers to operate up to millimeter wave frequencies. However, the SSA is only capable of detecting continuous signals, and they are not able to capture any phase information. FFTSA technology is able to capture a sample very quickly and then analyze it. As a result an FFTSA can capture short lived or one-shot phenomena. They are also able to capture phase information. However, the disadvantage of the FFTSA is that its frequency range is limited by the sampling rate of the ADC.

Nothing is perfect in the world, at least in the sense of a thing everything has two sides, a positive (or a disadvantage) and a negative (an advantage). In a same manner, the error for any particular error source is unknown and unknowable, its limits, at a given confidence, must be estimated. This estimate is called the uncertainty. It is important to be able to estimate the overall uncertainty, in particular, the test setup and measurement equipment uncertainty.

Generally, modeling and simulation is a discipline for developing a level of understanding and solving a particular problem of the interaction of the parts of a system, and of the system as a whole.

4.5.2 Superheterodyne principle for SSA

A simplified block diagram of the superheterodyne SSA analyzer is given by Fig 23.

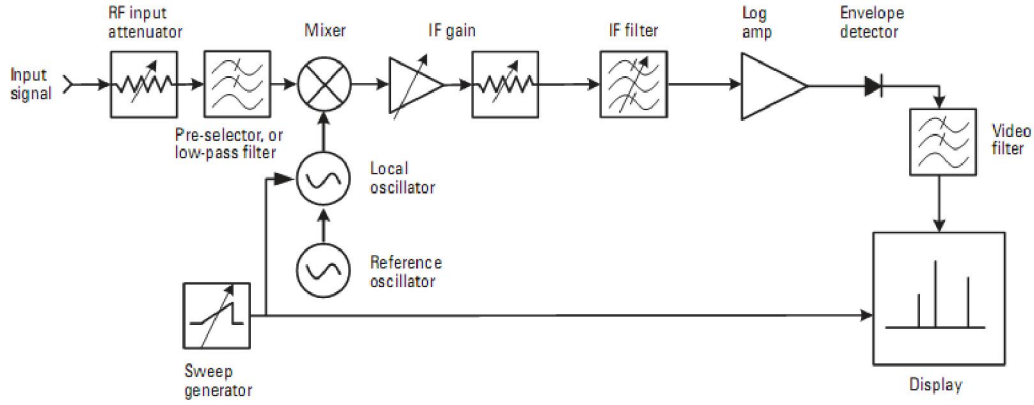

Fig. 23 Block diagram of a classic superheterodyne SSA

A signal flow of the analyzer is following: input signal passes through an attenuator, then through a low-pass filter to a mixer, where it mixes with a signal from the local oscillator (LO). Because the mixer is a non-linear device, its output includes not only the two original signals, but also their harmonics and the sums and differences of the original frequencies and their harmonics. If any of the mixed signals fall within the passband of the intermediate-frequency (IF) filter. It is essentially rectified by the envelope detector, digitized, and displayed. A ramp generator creates the horizontal movement across the display from left to right. The ramp also tunes the LO so that its frequency change is in proportion to the ramp voltage. The signal to be wanted to examine is either above or below the LO frequency by the IF, then the sign of the equation can be either minus or plus. The general form of tuning or mixing equation is:

$$f_{sig} = nf_{LO} \pm f_{IF} \tag{4.5.1}$$

Where: f_{sig} is the signal frequency, f_{LO} is the local LO, and f_{IF} is the IF frequency, and n is the number of the LO.

For a detection of the small signal, a filter skirt is used to determine how far down the filter skirt is at a given offset, the following equation is useful:

$$H(\Delta f) = -10N \log_{10}\left[\left(\frac{\Delta f}{f_0}\right)^2 + 1\right] \tag{4.5.2}$$

Where: $H(\Delta f)$ is the filter skirt rejection (dB), N is the number of filter poles, and Δf is the frequency offset from the center (Hz). f_0 is the offset frequency (Hz) and given by:

$$f_0 = \frac{RBW}{2\sqrt{2^{1/N} - 1}} \tag{4.5.3}$$

The resolution affects sweep time, which determines a time of the measurement. IF filters are band-limited circuits that require finite times to charge and discharge. In case of the mixing products stay in the passband of the IF filter, the following relationship holds:

$$T = \frac{RBW}{Span / ST} = \frac{(RBW)(ST)}{Span} \tag{4.5.4}$$

Where: T is the time in passband, RBW is the resolution bandwidth, ST is the sweep time.

On the other hand, the rise time of a filter is inversely proportional to its bandwidth, with the constant proportionality k :

$$RT = \frac{k}{RBW} \tag{4.5.5}$$

Then if we resolve the sweep time from above equations we have:

$$\frac{k}{RBW} = \frac{(RBW)(ST)}{Span} \quad \text{or} \quad ST = \frac{k(Span)}{RBW^2} \quad \text{or} \quad ST = \frac{k(Span)}{(RBW)(VBW)} \tag{4.5.6}$$

For the detection of the value several different detector modes that dramatically effect how the signal to be displayed. For the optimum analysis, one of the following detectors can be chosen: Sample, Maximum peak, Minimum peak, Normal, Average, Root mean square, and Quasi peak. Some of those detectors are well understood, while some of

them are more complex than that others and detailed study can be found from [2]. Other important parameters of the spectrum analyzer include accuracy, sensitivity, and noise. Modern spectrum analyzer producers provide detailed characteristics of such parameters for instance Agilent Technologies.

4.5.3 Uncertainty evaluation

There are two classification systems are used in uncertainty evaluation. The two classification utilized are the ISO and the engineering classification [45].

There are two types of uncertainty types for both groups. In the former case, Type A, data for the calculation of the standard deviation (arises from random effects), while Type B (arises from systematic effects) based on scientific judgment (previous measurement data, equipment specifications, calibration, and others).

According to ISO classification method which we will use, the expanded uncertainty of the system can be expressed by the following relationship:

$$U_{R,ISO} = \pm t_{95}\left[(U_A)^2 + (U_B)^2\right]^{1/2} \tag{4.5.7}$$

Where: $\pm t_{95}$ students t for degrees of freedom.

Alternative confidences are permissible such as 99% or 99.7% however, for uncertainty analysis 95% is recommended, other confidence is possible to obtain by choosing the appropriate Student's t [94].

When the result of a measurement is presented, the expanded uncertainty of the data can inform us a fitness of a result, on the other hand, a parameter associated with the result of a measurement that characterizes the dispersion of the data that might be expected.

Type A: standard uncertainty is usually expressed as the standard deviation (or error) of the mean value of a set of independent measurements using the same instruments. For normal distribution:

$$U_A \cong s\left(\bar{q}\right) = \frac{s(q_i)}{\sqrt{n}} \tag{4.5.8}$$

Where: $s(\bar{q})$ is the standard deviation (or standard error) of the mean value of a distribution of data, $s(q_i)$ is the standard deviation of values of q , and n is the number of measurement (or number of values of q).

Type B: the four most distributions are used, which are normal, rectangular, triangular, and u shaped distributions. For the calculation analysis:

$$U_B = a \times F_W \tag{4.5.9}$$

Where: a is the manufacturer-specified tolerance or error, and F_W is the weighting factor. For normal distribution: $F_W = 2$, for rectangular distribution: $F_W = 1/\sqrt{3}$, for triangular distribution: $F_W = 1/\sqrt{6}$, and for u-shaped distribution: $F_W = 1/\sqrt{2}$.

However, when the data which is provided by manufacturer as a tolerance or error is unsymmetrical; the further analysis should be required.

4.5.4 Modeling and Simulation

Conceptually, the investigation of complex systems using mathematical models and simulation may include the following steps where: Problem identification (problem identification that is to be solved), System analysis (formulation of part of the system which is relevant to the problem), Modeling (development of a model of the system), Simulation (application of the model to the problem solution), and Validation (application into a real system).

Nowadays, Matlab/Simulink provides a possibility of multidomain simulation, model based design for dynamic and embedded systems, including set of block libraries. Moreover, computer simulation software COMSOL, CST, and ANSYS are promising a great opportunity not only for RF modeling, including optimum radiation frequency, antenna impedance, and radiation pattern but also for the sensors such as MEMS sensors, Hall, Piezoelectric, Accelerometers and others. The abilities of these products are not limited by the above mentioned examples.

5 EXPERIMENTAL PART

Introductory

In order to fulfill the goals of the work the experimental part is divided into the three sections. In section 5.1, the sensor, analogue and digital signal processing is analyzed. Next section 5.2 investigates a propagation of the electromagnetic signal in the different indoor environments. The penetration of the signal trough some construction medium is studied in a section 5.3.

5.1 Measurement of force in two axes

5.1.1 Introduction

Sensors based on the variation of the electric resistance of a device are very common. The resistive sensors are used to solve many measurement problems [78]. They are usually used for force, mass, pressure, torque, acceleration and deformation electric measurements. Therefore, strain gauge sensor is chosen as an example from the field of sensors to study and experiment.

Dependence of resistance to deformation and temperature can be expressed as:

$$R = R_{0,t} + R_{0,25}\left[C_1\left(\varepsilon + \left(\alpha_m - \alpha_{Si}\right)\left(t - 25\right)\right) + C_2\left(\varepsilon + \left(\alpha_m - \alpha_{Si}\right)\left(t - 25\right)\right)^2\right] \quad (5.1.1)$$

Where: $R_{0,t}$ is the resistance to temperature (Ω), $R_{0,25}$ is the resistance of free gauge at 25^0C (Ω), C_1 and C_2 are the constants, ε is the strain (m/m), α_m and α_{Si} are the coefficients of thermal expansion of material and silicon respectively ($1/^0$C).

In this section, we examine the principle of two channels wireless force measurement with the solution of, analogue, and digital signal conditioning circuits, as well as a RF communication interface.

5.1.2 Experimental model

In order to conduct the measurement process, the experimental model is constructed as shown in Fig 24. As revealed by figure, that the model consists of two main parts a sender (strain gauge bridge circuit, analogue signal conditioning, security circuit, DSP, and antenna), and receiver (antenna, DSP, and USB connection to Data Acquisition (DAQ)).

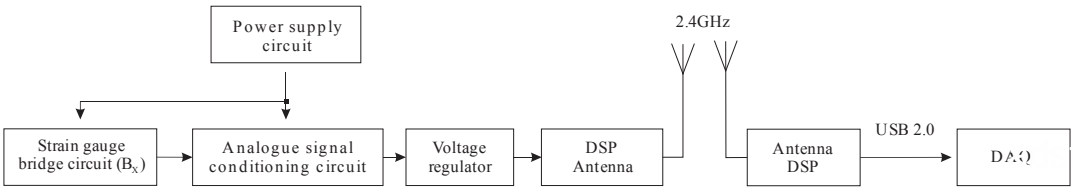

Fig. 24 Block diagram of experimental model

A. Strain gauge bridge sensor

The semiconductor strain gauges have a very considerable and accurate change of the electrical resistance with applied mechanical strain. In our case, the sensor is attached on the two different deformation units as displayed below.

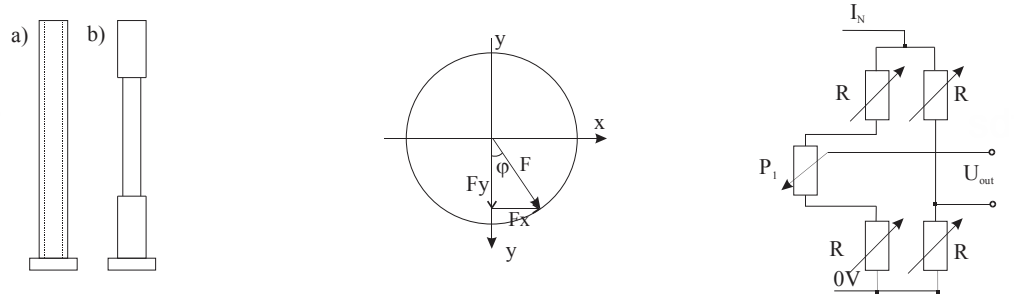

a) Deformation units *b) Acting forces* *b) Electrical scheme*

Fig. 25 Block diagram of experimental model

The acting forces on the deformation units (Fig 25) have following relations:

$$F^2 = F_x^2 + F_y^2$$
$$tg\varphi = F_y / F_x \qquad (5.1.2)$$

The applied forces were executed by a force – spring system and calculated by Hooke's law:

$$F = -kx \tag{5.1.3}$$

Where: x is the stretched distance (m), and k is the spring constant (in our case for X: -930.4 for Y: -881.7) (N/m).

The output signal depends on the applied mechanical stress but also on the supply current. The special stabilized power supply circuit designed with adjustable shunt regulator TL431C and NPN small signal transistor BC547. The zero adjustment of the bridge or the difference voltage is executed via a potentiometer P_1 and has the following relationship:

$$U_{out} = 0 = I_{N,a}(R_1 - \alpha P_1) - I_{N,b}(R_3) \tag{5.1.4}$$

Where: $I_{N,a}$ and $I_{N,b}$ - are the parts current, α - is the fractional coefficient of the potentiometer.

B. Analogue signal conditioning

The primary outputs from the sensors were in the range from 0.1 to 1 mV with respect to the applied force. In this case, the amplification of the signal is obligatory for further signal processing. According to some literature [78, and 97] chopper and differential amplifiers are recommended for the very small DC signals. However, in simplicity of the techniques, it would be of interest to certainly distinguish between the operational, differential, and instrumentation amplifiers [34].

Fig 26 shows tested amplifiers as the analogue signal conditioning. As described in Fig 26a, the main problem of the circuit is very different input impedance for inverting and non – inverting inputs as known. In case of study the op – amp of OP1177, R_2 was 22KΩ and R_1 was 8.2KΩ. The amplification is defined in below equation:

$$U_{out} = (U_{inp} + -U_{inp-})R_2 / R_1 \tag{5.1.5}$$

The instrumentation amplifier is the IC with differential amplifier, which is attractive due to its low cost general simplicity of the circuit in Fig 26b. In case of study, AD 620AN instrumentation amplifier is used for $G = 100$, and is evaluated to the following mathematical expression:

$$U_{out} = G(U_{inp+} - U_{inp-}) \tag{5.1.6}$$

Where: G is the amplification factor and can be adjusted by a single resistor R_g according to:

$$G = \frac{49400 + R_g}{R_g} \tag{5.1.7}$$

The goal of non – inverting connection as shown in Fig 26c is to achieve very high input impedance for both inputs. The bridge arms are loaded by the equal impedance. The op – amps TL071CN and TL082CP types were used in the circuit. The amplification factor is defined as:

$$U_{out} = \left[(U_a - U_b)\frac{R_2}{R_1} \pm U_{P1} \right] \frac{R_2 R_4}{R_1 R_3} \tag{5.1.8}$$

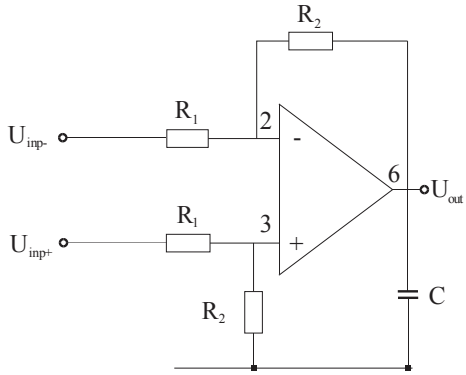

a) Difference amplifier

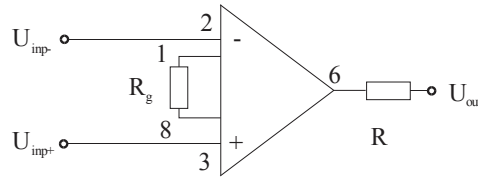

b) Instrumentation amplifier

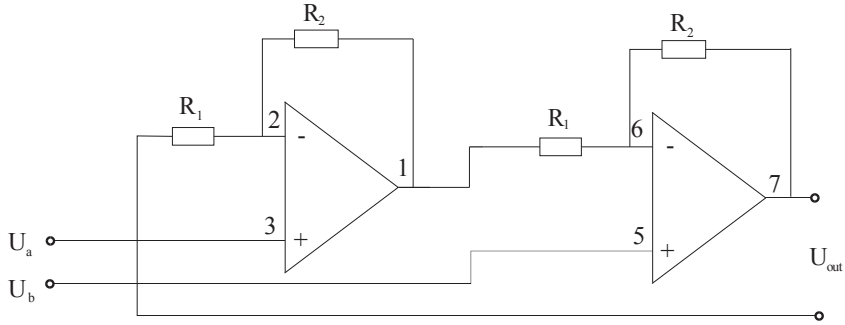

c) Noninverting operational amplifier

Fig. 26 Amplifiers for analogue signal conditioning

C. Voltage regulator

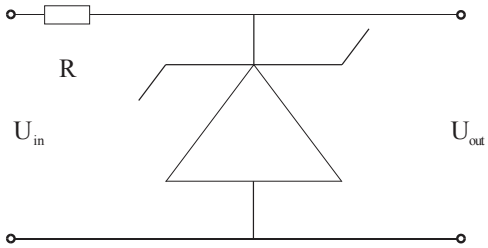

Fig. 27 Voltage regulator

One of the most common signal conditioners is the voltage regulator, which transforms a varying voltage into a constant voltage either for power supply or for referenced voltage applications. Voltage regulators are more usually considering an operation from a single source of unregulated DC voltage source.

For a simple Zener diode voltage regulator as shown in Fig 27, the relationship holds:

$$U_{out} = U_{in} - RI_Z \tag{5.1.9}$$

D. DSP and RF communication

The Freescale's ZSTAR3 wireless kit is used to DSP and as the communication system for the experimental model. The reasons are being that: the MC1321x family is Freescale's RF transceiver, which is an IEEE 802.15.4 standard compliant radio that operates a low power (1mW) in the 2.4 GHz range. For the same frequency band, the MC13191 is a short range, low power which contains a complete packet data modem which is compliant with the IEEE 802.15.4 Standard PHY (Physical) layer.

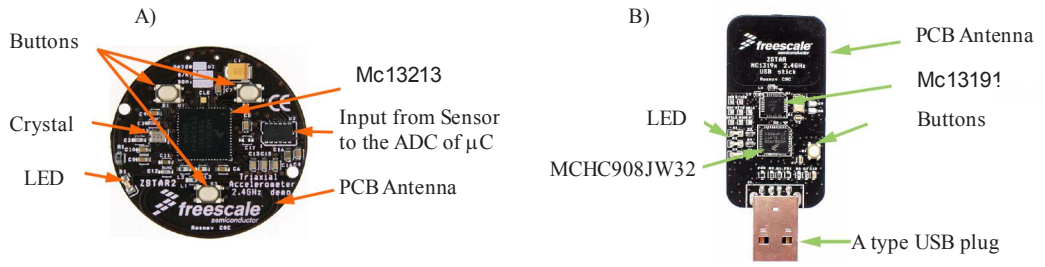

a) a Sender *b) a Receiver*

Fig. 28 ZSTAR3 kit from Freescale Semiconductor[22]

From the Fig 28a, in the sender, the original accelerometer sensor is removed. The outputs from primary signal conditioning circuits are connected through the voltage regulator to the ADC of the microcontroller. The main tasks of the Sensor Board are:

- Periodically wake – up from power saving mode
- Measure all three XY force values from the full bridge circuit
- Compose a data frame using simple The ZSTAR3 RF Protocol
- Use SMAC to send this data frame over the RF link
- Go to sleep

In contrast to there are two main tasks of the USB stick board or the receiver (Fig 28b):

- Receive the data from the MC13191 transceiver and store in the RAM buffer.
- Handle the USB module communication, decode and provide the data from the RAM buffer.

Fig 29 indicates a system level block diagram of the MC13213 MCU. RIN_M and RIN_P are the bi – directional negative and positive RF ports respectively, for the internal low noise amplifier and power amplifier. PAO_P and PAO_M are the positive and negative modem power amplifiers for RF outputs. As suggested by manufacturer those pins should be connected when internal T/R switch is used to the modem analog regulated supply output.

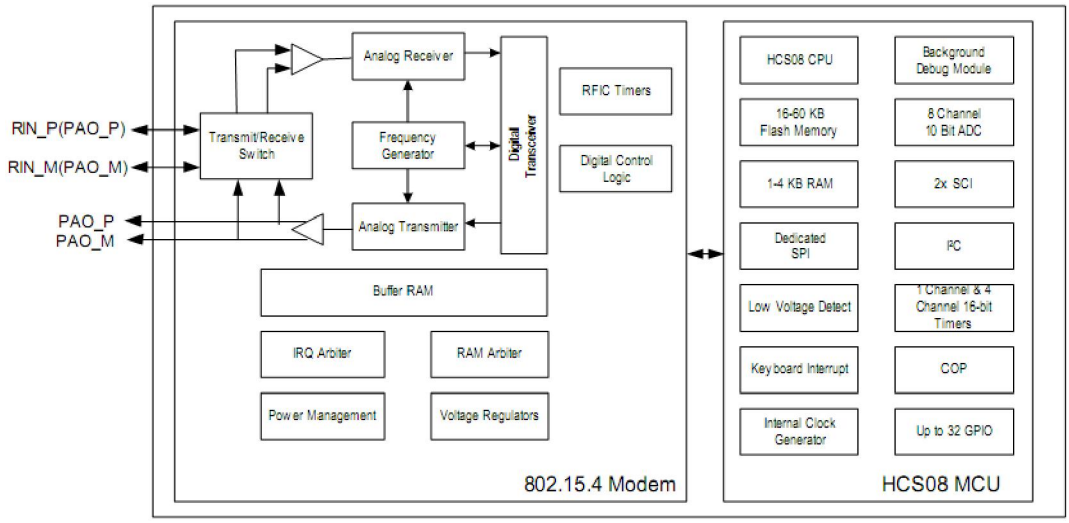

Fig. 29 MC13213 system level block diagram [26]

The basic system block diagram of the MC13191 MCU is provided by Fig 30 in an application. Interface with the transceiver is accomplished through a 4-wire SPI port and interrupt request line. The media access control, drivers, and network and application software (as required) reside on the host processor. The host can vary from a simple 8-bit device up to a sophisticated 64-bit processor depending on application requirements.

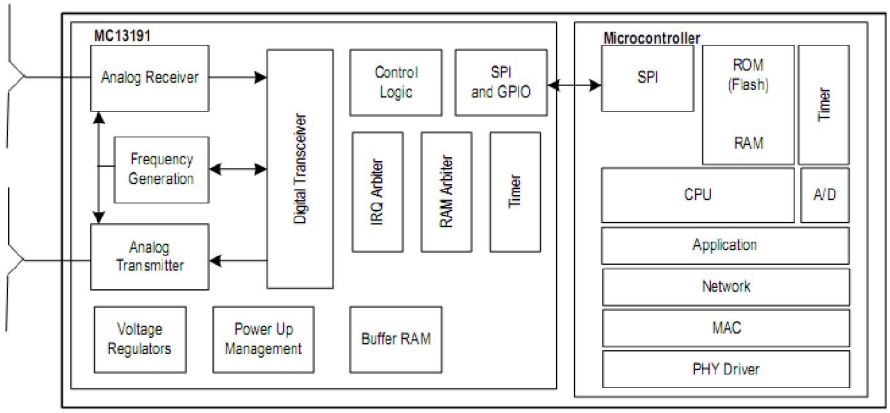

Fig. 30 MS13191 system level block diagram [25]

For the USB board operation MCHC908JW32 hardware modules are used: 32 kb flash, 1 kb Random Access Memory, 34 General Purpose Input Output, SPI, as well as USB 2.0.

The scheme for one transmission/sleep cycle is used for a typical data transfer:

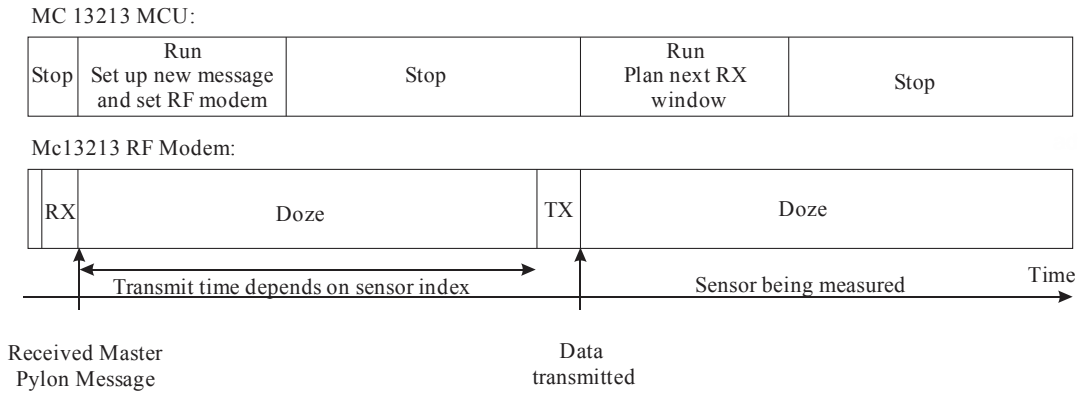

Fig. 31 Transmission sleep cycle at 30 Hz data rate [22]

As stated in Fig 31, MCU remain most of the time in Doze/Stop modes, by means of current consumption is very low: in operation mode 1.8 to 3.9 mA, in sleep mode less than 900 nA.

On the other hand, all data is transferred in so – called Zpacket, which is a simple time based protocol for an RF transfer of information between sensor boards and the USB receiver. The ZSTAR Zpacket is contained inside the MC1319x/MC1321x standard packet structure, which is consistent with the IEEE 802.15.4 Standard.

As has been demonstrated by Fig 32, the Zpacket format includes Network number, RX strength, Zcommand, and Zdata. MC 13213 packet structure contains Start of Frame Delimiter (SFD), Frame Length Indicator (FLI), and Frame Check Sequence (FCS).

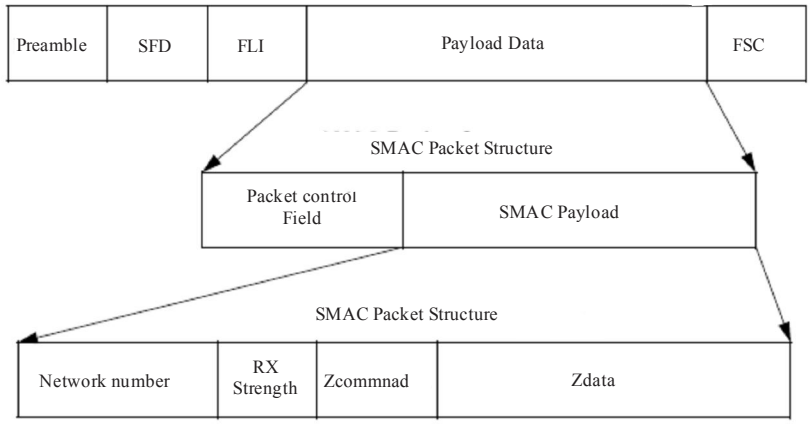

Fig. 32 Zpacket format for data transmission

The wireless communication with the sensors through the 2.4 GHz band, data rate of the sensor is 30, 60 or 120 Hz, and the sensor sensitivity is defined by the strain gauge bridge circuit.

E. Measurement procedure

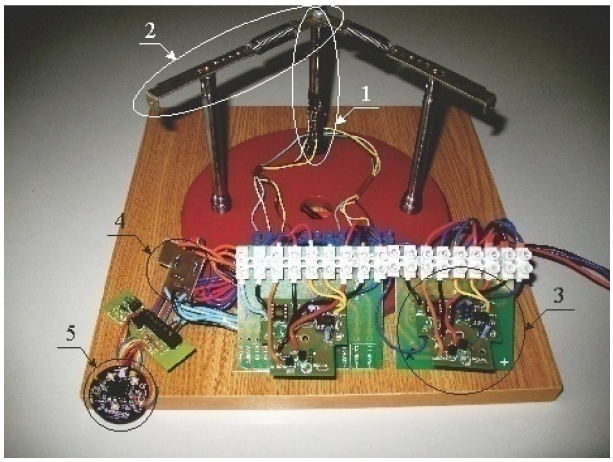

Fig. 33 Photograph of experimental model

As can be seen in Fig 33, the experimental model is consisting of strain gauge bridge circuit (1), force – spring system (2), power supply and analogue signal processing circuit (3), voltage regulator (4), and DSP and communication interface is used Zstar3 kit without sensor (5). The unit 5 was communicated via wirelessly with DAQ.

The deformation unit is loaded in two axes by the forces of F_x , F_y and contemporaneously varied 0 to 25N. The mechanical strain is measured for both directions by the semiconductor full strain gauge in the bridge circuit. Both output voltages U_x , U_y are amplified by amplifiers and regulated by Zener circuit finally connected to the MCU on the Zsrar3 kit. 2.4 GHz RF communication is established between the sensor and receiver board. The receiver board is connected to the DAQ by USB, and data are acquired at 30 Hz rate. In order for study cross sensitivity of two axes the measurement is repeated when the different amounts of forces were applied to the rest of the axis.

5.1.3 Result and Discussion

The previous study has revealed that, the instrumentation amplifier gives a more linear characteristic between the applied force and the output voltage, than those operational and differential amplifiers [34, and 61].

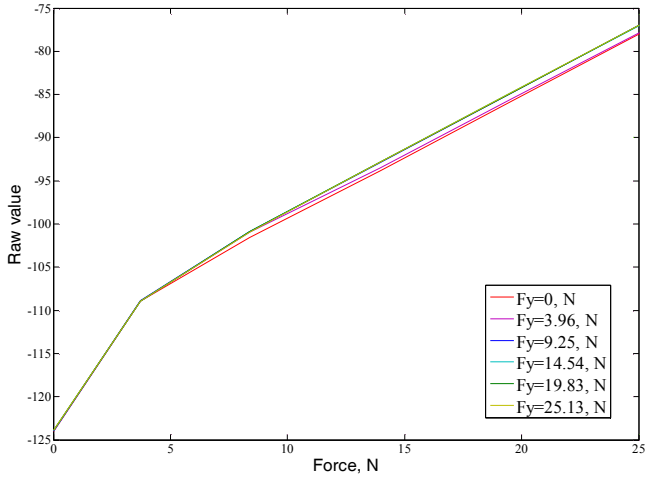

a) Relationship between F_x and X raw value

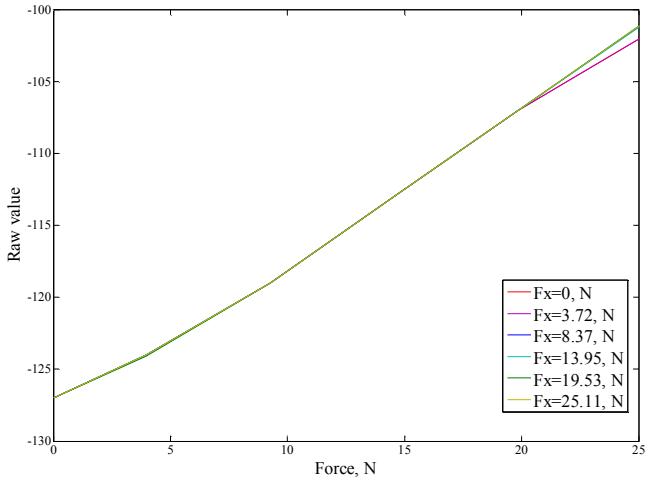

b) Relationship between F_y and Y raw value

Fig. 34 Measured data of wireless force measurement

The tendency of the differential amplifier was unstable, in contrast to the findings for operational amplifier were both unstable and too high for further application of the signals. The signal condition for very small change of resistance the instrumentation amplifier is suitable [34].

As depicted in the Fig 34, both measured results are merely linear. However, X – axis measurements tend to be more nonlinear than that Y axis in any case of cross channel of values. The applied forces were acquired as a raw value: which means basic data of the sensor in general text format over a virtual serial port. On the other hand, raw value is unprocessed data after wireless transmission.

Table 10 F_x dependence analysis

F_y ,N	Voltage (V)	Min	Max	Average	SD
0	0.044	-124.00	-123.90	-123.95	0.05
3.96	0.197	-108.93	-108.88	-108.91	0.01
9.25	0.276	-101.58	-100.91	-101.03	0.27
14.54	0.357	-93.86	-92.82	-93.14	0.44
19.83	0.438	-85.83	-84.81	-85.12	0.45
25.13	0.512	-77.81	-76.80	-77.14	0.49

Table 11 F_y dependence analysis

F_x ,N	Voltage (V)	Min	Max	Average	SD
0	0.001	-127.00	-127.00	-127.00	0.00
3.72	0.099	-124.08	-124.00	-124.02	0.03
8.37	0.160	-119.00	-119.00	-119.00	0.00
13.95	0.222	-113.00	-113.00	-113.00	0.00
19.53	0.282	-107.00	-107.00	-107.00	0.00
25.11	0.344	-101.91	-101.00	-101.31	0.46

A maximum cross sensitivity for X – axis is calculated to be -0.037 (raw/N), the same parameters are evaluated for Y – axis, which is lower that hat former one and found to be 0.13 (raw/N). The Tables 10 and 11 evaluates the measured results for the final parameter evaluation for the constructed experimental model as given by Table 12.

Then the summarized sensor model can be expressed with the following standard evaluation. Detailed statistical analysis can be found from appendix A.

Table 12: Model summery

F_x Model Summary				
Model	R	R Square	Adjusted R Square	Mean Error of the Estimate
F_x vs Raw value	0.981a	0.962	0.952	2.093
a. Predictors: (Constant), Raw value				
F_y Model Summary				
Model	R	R Square	Adjusted R Square	Mean Error of the Estimate
F_y vs Raw value	0.998a	0.997	0.996	0.624
a. Predictors: (Constant), Raw value				

As can be seen, Y axis model has more linear results than that rest of the axis case. The difference may can be eliminated by readjusting the sensor position. One of the principle benefits of the latest tendency is the strong suggestion that all the uncertainty contributions should be listed in a table along with their probability distribution.

Usually, but not often the uncertainty distribution is considered to be normally distributed when the uncertainty disturbance is combined. Estimating measurement uncertainty, the a-priori distribution would be applied to processes known to produce tightly clustered centrally located data; so it is called a-priori because the analyst needs prior knowledge of the process to which it is applied. According to Table 13, the latter calculation has clearly specified that the uncertainty value of 4.32% corresponds to the confidence level of 95%. However, it should be noted that the values are only known uncertainty provided by the manufacturer.

Table 13: Uncertainty budget of experimental measurement

Source	Accuracy	Type	Probability Distribution	Weighting factor	Uncertainty
SD error F_x	0.93	A	-	-	0.93
SD error F_y	0.27	A	-	-	0.27
Sensor					
Thermal drift	0.02	B	U shaped	1/sqrt(2)	0.01
Sensitivity	0.03	B	Normal	2	0.06
Hysteresis	0.05	B	U shaped	1/sqrt(2)	0.04
Stability	0.05	B	Normal	2	0.10
Power supply					
Accuracy	0.5	B	Normal	2	1.00
Temperature coefficient	0.02	B	U shaped	1/sqrt(2)	0.01
Multimeter	0.53	B	Normal	2	1.06
AD620an	0.3	B	Normal	2	0.60
DSP	1	B	Rectangular	1/sqrt(3)	0.57
95% confidence expanded uncertainty $t = 2.228$					***4.32***

5.2 Measurement of RF signal propagation

5.2.1 Introduction

Ubiquitous communication requires anytime, anywhere connectivity, leading to a spectrum crowded with users seeking reliable, high data rate communications in potentially dense geographies, especially in indoor environments. The amount of frequency spectrums available to Wireless Local Area Networks (WLAN) and Wireless Personal Area Networks (WPAN) is limited, with no relief in sight. As WLAN and WPAN rise in popularity, they will be required to carry increasingly larger amounts of data for multimedia and other services, while at the same time, overcrowding of these bands can lead to service degradation and undermine the goals of ubiquitous computing.

5.2.2 Site description

During the measurement of the propagation three kinds of laboratory rooms and some corridors are considered as the environments. Each room is equipped by different devices and equipments. Furthermore, the corridors are differed by its architecture from each other. Detailed descriptions of the sites are given below.

A. Laboratory room 306

This room is intended to study a classical sensor system and equipped by corresponding devices. Prevailing equipments are: power suppliers, multimeters, several personal computers, and the sensor units such as a strain gauge, capacitive sensors, Proportional Integral Derivative regulator and others. However, all the time during the measurement the laboratory devices were inactive. A floor plan of the room can be seen in ***Appendix B***.

B. Laboratory room 309

With compared to the former room this room does not comprise such sensor devices but, equipped by Laboratories of Integrated Automation, which are new modern laboratories accessible locally and remotely controllable by an internet. There are about 10 personal computers furnished in the room, floor plan of the room is in ***Appendix C***.

C. Industrial hall 107

This room is dedicated for production engineering students. Therefore, the laboratory room is a well equipped with production machines such as CNCs, drilling stations, laser cutter, as well as one robot. This room is expected to be industrial hall (Fig 35) or environment with a noise ***Appendix D***.

Fig. 35 Photograph of the Room 107

D. Corridors

The corridor has a U – shape. Each sleeve of the corridor is assumed to be a different environment due to its architecture. For instance, in a Corridor 1 there is a wireless router, a Corridor 2 is widest, and Corridor 3 leads to spectrum analyzer laboratory room. The floor plans of the corridors are given by ***Appendix E***.

5.2.3 Measurement setup

In study case, a SMR20 microwave signal generator and FSP spectrum analyzers are used. For the 2.4 GHz frequency measurement, the same condition applied with a later description. Photo of the measurement set is given by Fig 36.

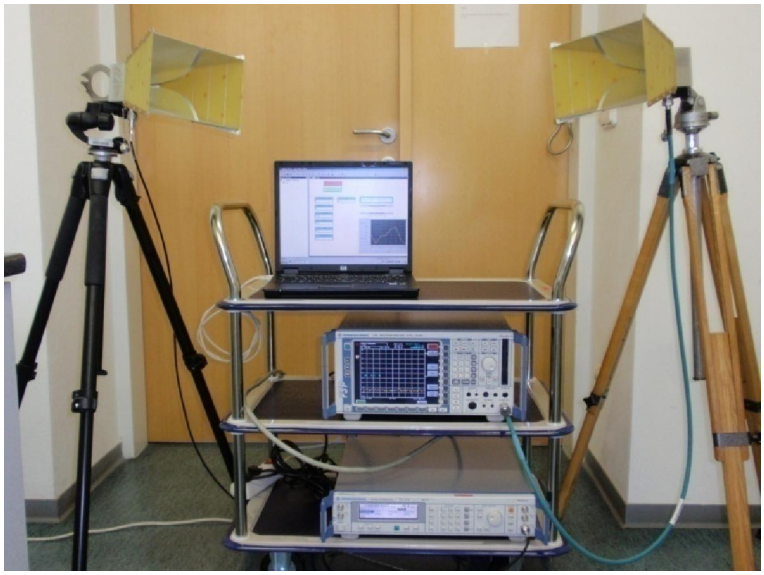

Fig. 36 Photograph of instruments

During the both propagation and penetration measurement, the frequency was increasing 1 GHz to 8 GHz with a step frequency of 1 MHz, for five different power levels, which are -10dBm, -20dBm, -30dBm, -40dBm, and -50dBm. In each indoor propagation scenario, the transmitter and receiver distances were 4m, 5.35m, and 7m. One measurement with the each setting of the parameter is repeated 10 times for a true statistical calculation.

The distances between transmitter and receiver were considered to be far – field measurement, according to Fraunhoffer region [43], which is:

$$d > \frac{2D^2}{\lambda} \tag{5.2.1}$$

Where: d is the far field distance (m), D is the maximum linear dimension of the antenna (m), and λ is the wavelength (m).

The following Table 14 shows the measurement constants and holds during both propagation and absorption measurement procedure; even so, the parameters are tunable.

Table 14: Measurement constants

Constants	Value	Unit
Step	100	MHz
Span	100	KHz
RBW	3000	-
Sweep Time	10	s

When considering indoor RF propagation, it is apparent in many cases propagation depends upon reflection, diffraction, scattering and fading by means of multipath, which individually can degrade and grade the signal. Fig 37 shows a general measurement setup for propagation measurement.

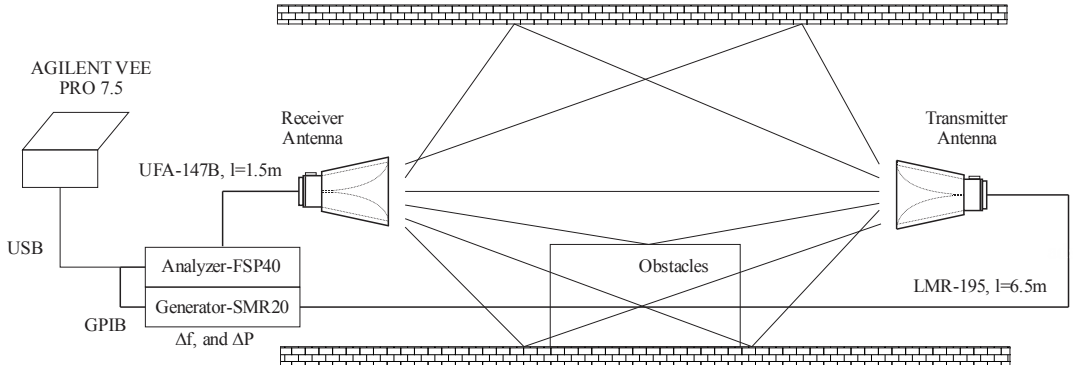

Fig. 37 Propagation measurement setup

The data are acquired in the computer by using a software Agilent VEE Pro version of 7.5. Illustrations of the source code and user application window are given by Fig 37 and Fig 38 [83].

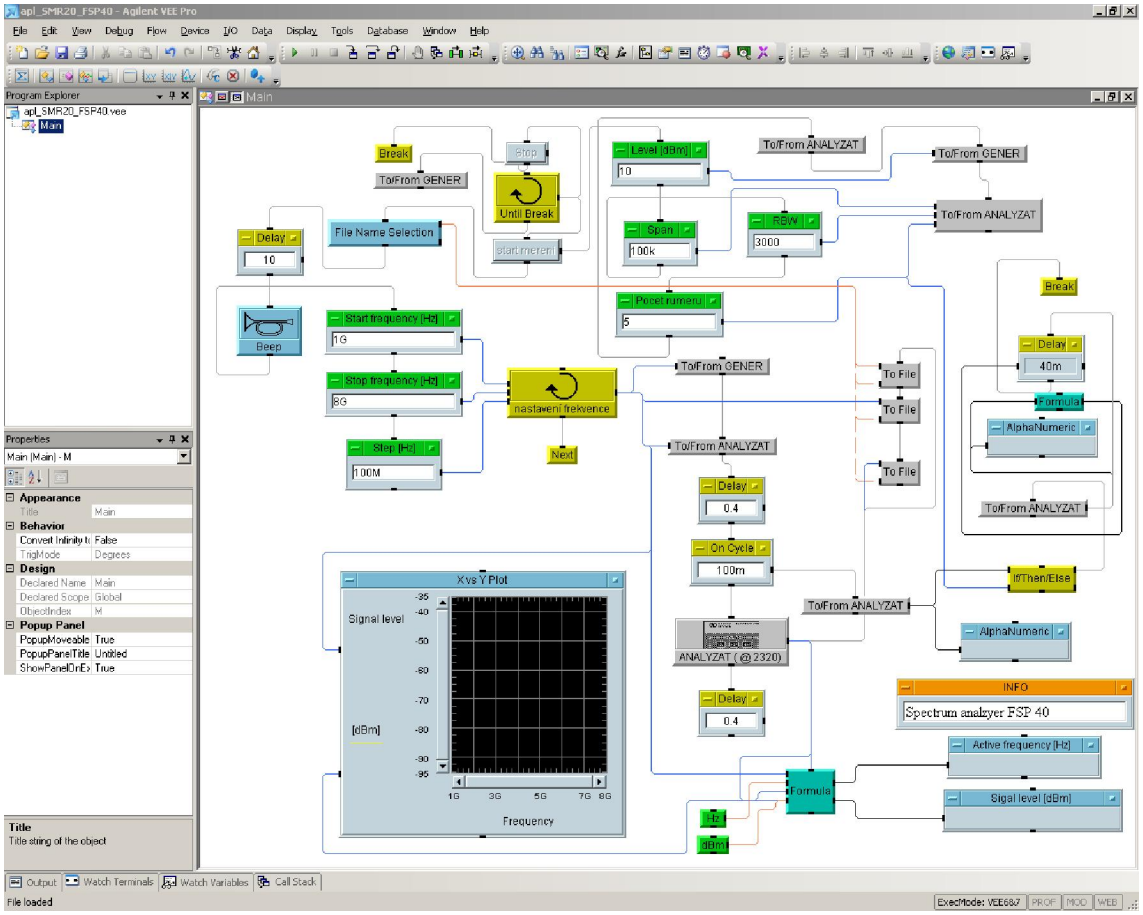

Fig. 38 Source code of software created in Agilent VEE Pro

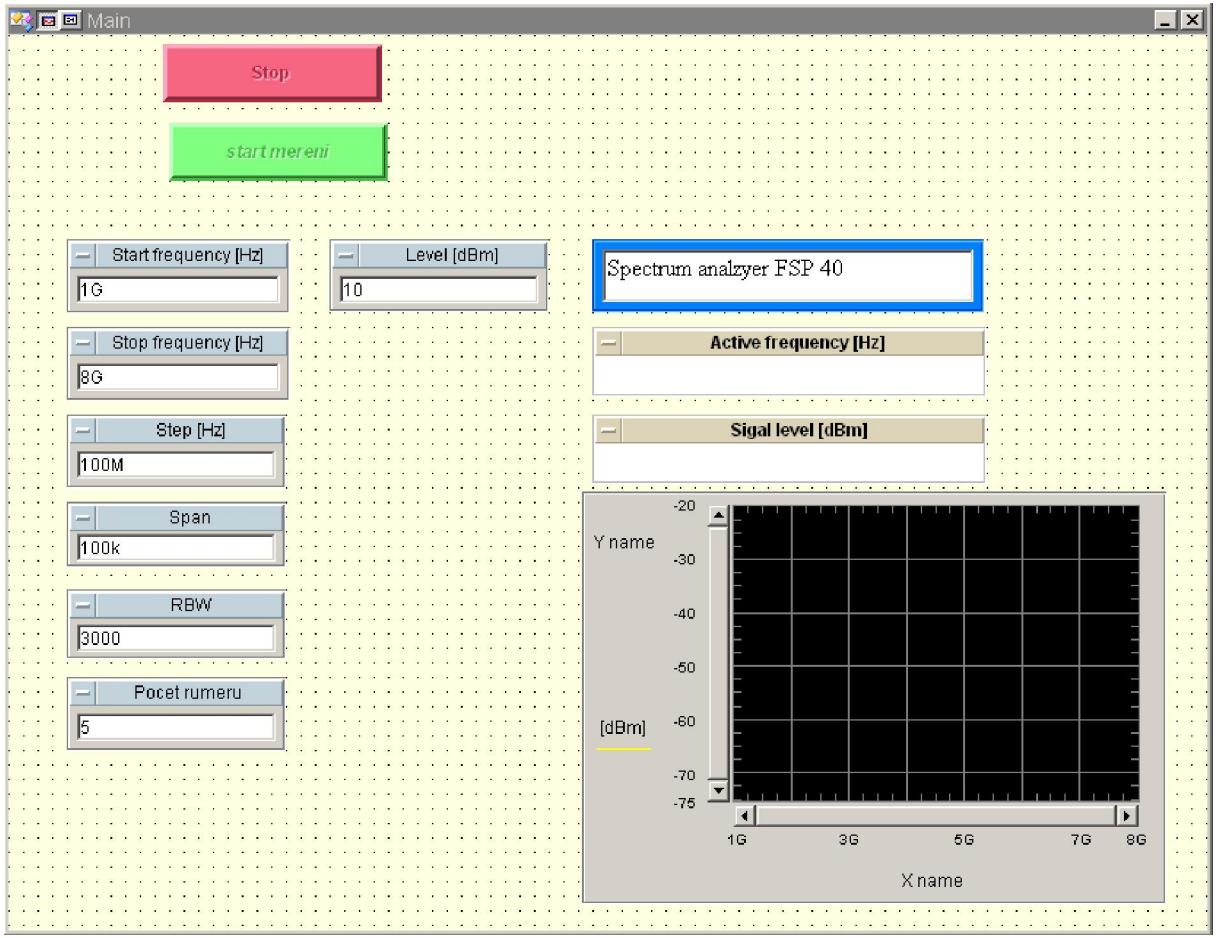

Fig. 39 Appearance of user application window

The actual received power with regard to the existing noise is assumed to be:

$$P_r = P_t - 2G_A - P_n \tag{5.2.2}$$

Where: P_r is the received power (dBm) P_t - is the transmitted (dBm), G_A is the gain of the antenna (dBi), P_n is the noise floor level (measured without generator) (dBm)

A measurement with the Zstar3 kit, a setup is accomplished with analyzer and receiver antenna. The analyzer was calibrated to measure adjacent channel power measurement configuration. Different types of detectors are used such as: RMS, MAXH, MINH, and Average detectors. The sender of the kit is located in the same distances as mentioned former. All the time of measurement the sensor was transmitting the signal to the receiver which is connected to the laptop in order to avoid from a sleep mode. In a same channel, the receiver and sender were communicating therefore, the signal of the receiver should be subtracted from the measured signal, which is:

$$P_r = P_t - G_A - P_{USB} - P_n \tag{5.2.3}$$

Where: P_{USB} - is the measured USB signal level (dBm).

A reference value of the kit is considered to be 0 dBm according to the Federal Communication Commission rule. Then the total path loss model is computed by using Equation (4.4.8) with regard to the transmitted power.

5.2.4 Result and Discussion

The Figures 40 to 42 depicts the path loss models for different corridor scenario. In general case, the path losses were increasing proportionally with regard to the distance between transmitter and receiver. The measurements in 7m distance, the path losses resulted in higher value respect to the all measurements. In contrast to, 4m and 5.35m cases, the path losses were fluctuating by several tens of dB. **Appendixes F** to **H** evaluates the mean path loss values for five different power levels in corridors. During the measurement in the corridor 1, the noticeable low path loss values are: for 7m range 1.4, 2.1, 2.8, 3.9, and 4.1 GHz and for 5.35m range 3.9, 5.3, and 6.5 GHz, for 4m range 1.7, 2.1, 3, 3.3, 4.1, 5, 6.2, and 7.3 GHz frequency bands resulted respectively.

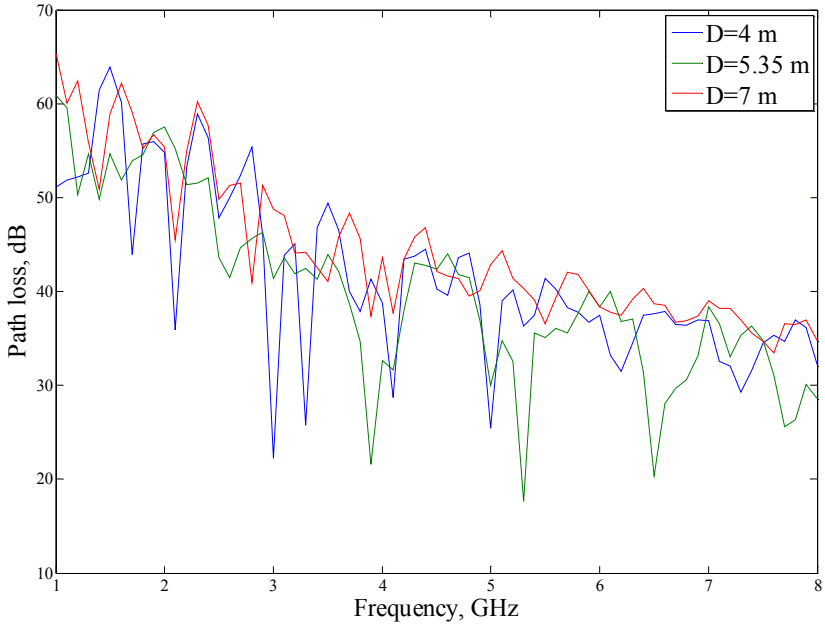

Fig. 40 Path loss measurement in corridor 1

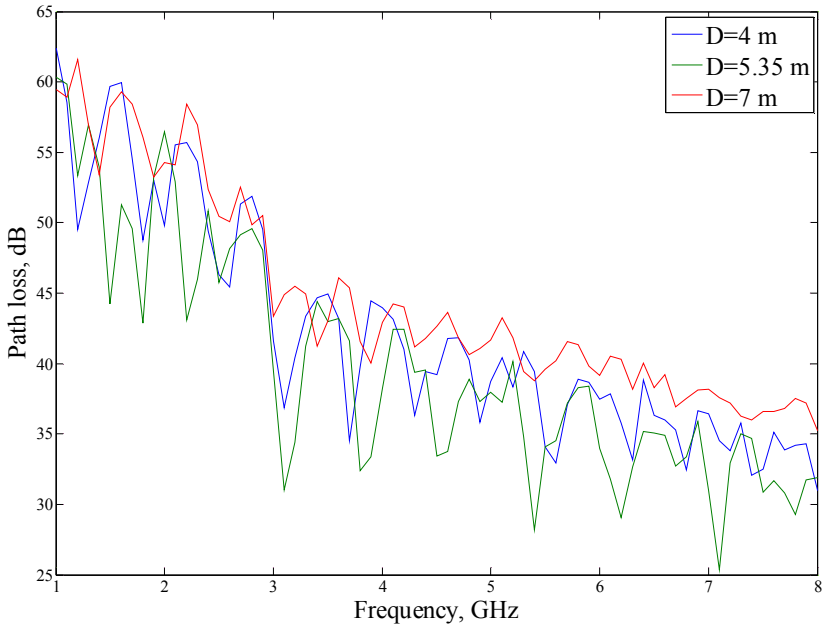

Fig. 41 Path loss measurement in corridor 2

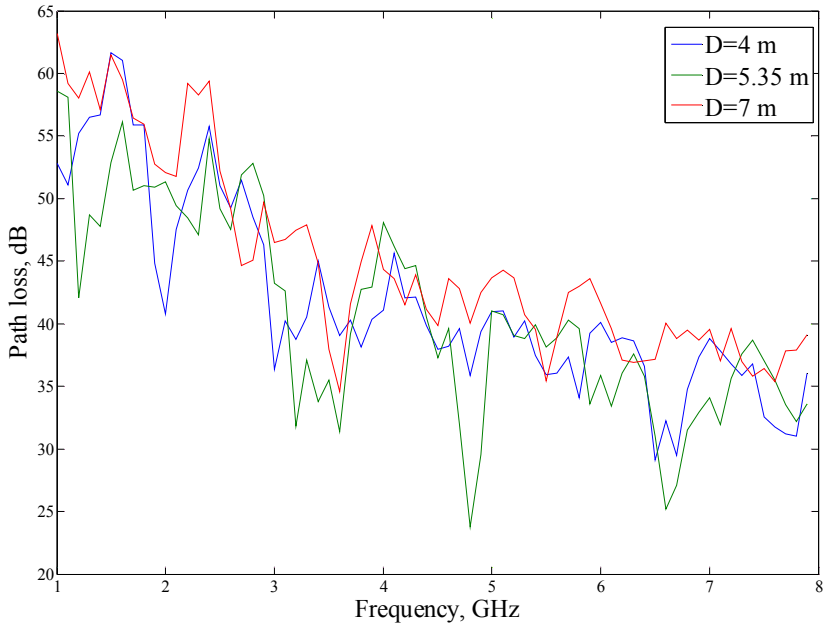

Fig. 42 Path loss measurement in corridor 3

In corridor 2, for 7m interval measurement the result was similar with a former circumstance. In contrast to, in 3.1 and 3.8 GHz frequency bands tend to have similar low path loss values. However, 5.35 m distance the lowest losses are measured in 5.4, 6.2 and 7.1 GHz occasions.

Throughout the measurement in the corridor 3, in the 4 m distance the lowest path losses are resulted in 2, 2.9, 6.6, and 6.8 GHz cases. For a 5.35m transmission distance, 1.2, 3.2-3.6, 4.7, and 6.6 GHz frequency bands resulted in a respectively low loss. Interesting situation is occurred for a 3.6 GHz transmission showed the same low values for 7 and 5.35m ranges. Mean path loss (five different power levels) evaluations for rooms are provided by **Appendixes, I** and **J**.

The latter Figures 43 and 44 illustrates measured path loss models for the rooms. For the time of the test in the rooms, in respectively short transmission range by means of 4 m 1.7 frequency bands resulted for a low loss value for the both rooms. However, for the rest of the measurement, the condition has departed.

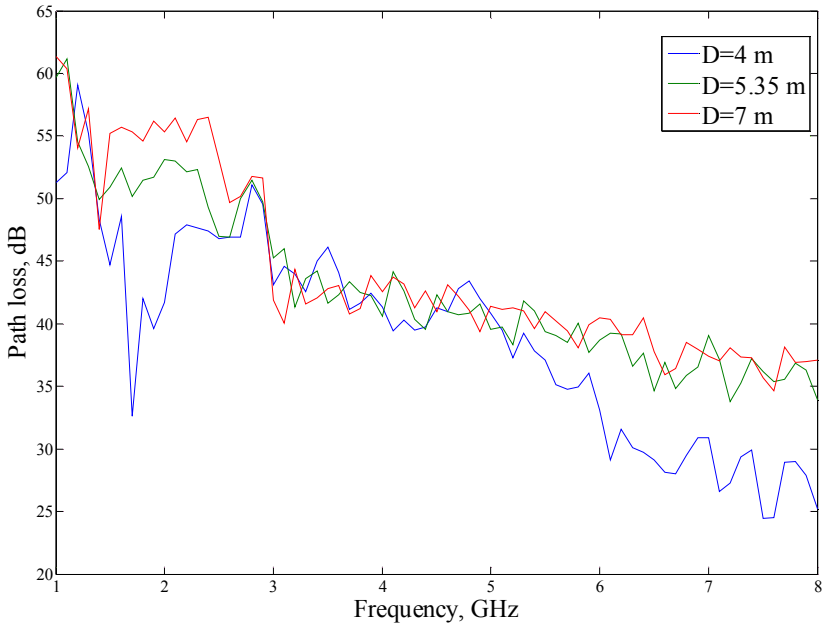

Fig. 43 Path loss measurement in room 309

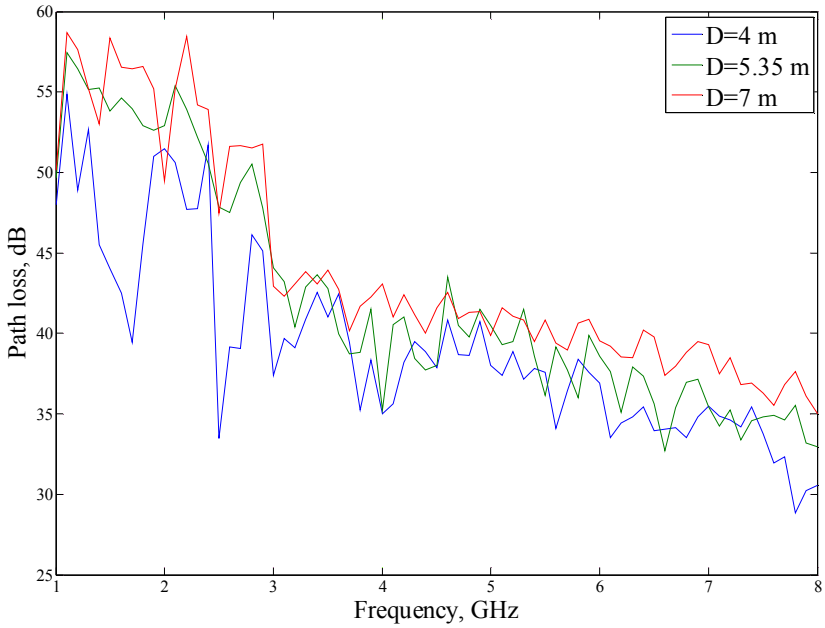

Fig. 44 Path loss measurement in room 306

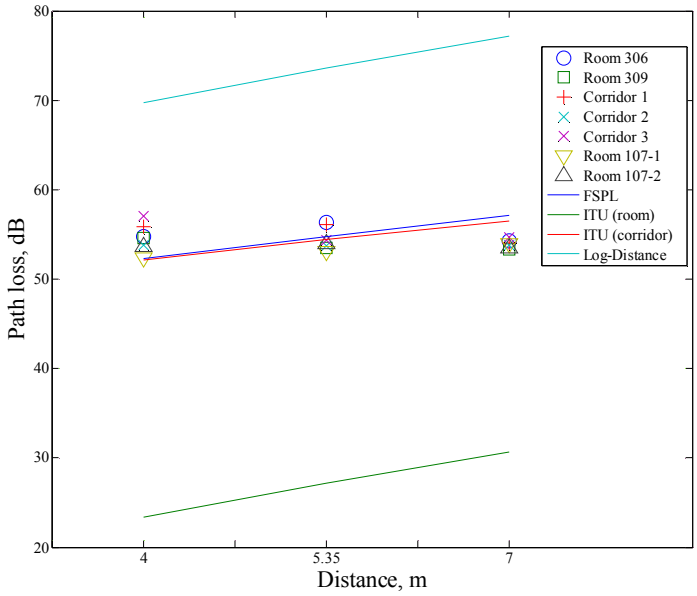

Fig. 45 Path loss measurement of zstar3 kit

In order to investigate a hypothesis of measurements with Zstar3 kit the measured results are given by Fig 45. From the measured result, the path loss models in the corridor 1and 3, room 309 tends to decrease with respect to the distance. In contrast to, the measured results in the industrial hall were increasing. It should be noted that during the measurement in the industrial hall, a drilling machine was in an operation randomly. From the compared result, it is clear that FSPL and ITU (with power decay index value of 18) models were merely suit to the outcome. It should be notable that, the measured values of Zstar3 kit can fluctuate by ±3 dB, due to changing detector of the analyzer.

Above all comparative estimates are possible to be clarified by contrasting the result to each other as well as with propagation models. Fig 46 compares the measured results in the corridors. As is often the case, the tendencies of path loss values were merely similar; a small difference may can be explained by the indoor architecture and sudden external influence, which means the reflection, refraction and the multipath. However, a noticeable remark lies in corridor1 especially in 4 m transmission distance; the loss values are measured to be relatively low in some frequency bands.

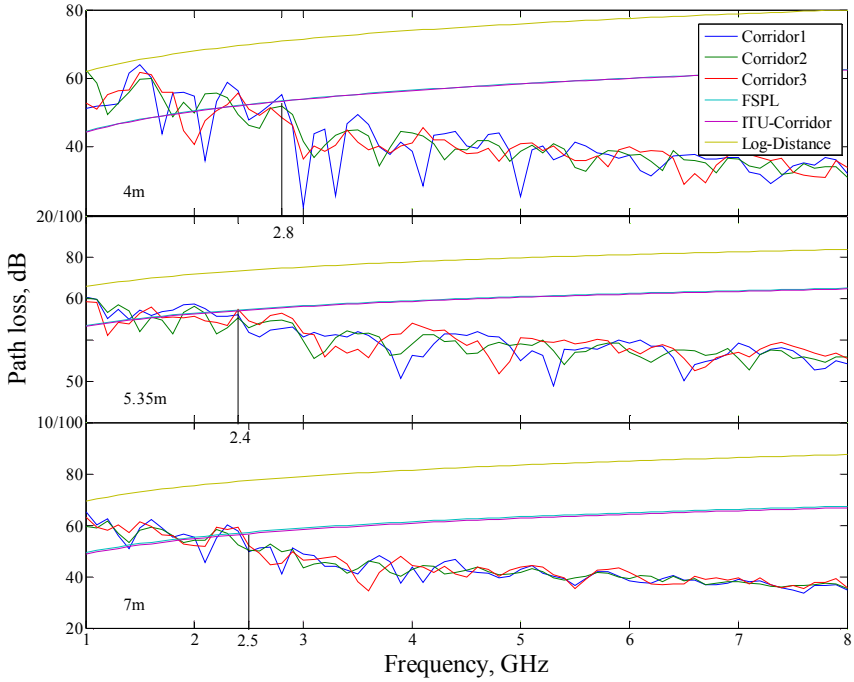

Fig. 46 Path loss comparisons in corridors

With comparison to the empirical propagation models, previous contributions [60, and 62] have revealed that ECC-33 model has much differed from the measured result and COST231-Hata model is designed for 1.5 to 2 GHz frequency bands. As can be seen in Fig 45, there is very probable to predict the path loss by Log – distance model for a maximum loss, by neither FSPL nor ITU (corridor) for the 1 to 2.8 GHz frequency bands in the corridors scenario for 4 m distance. For 5.35m transmission distance the former assumptions are predicted up to 2.4 GHz and for 2.5 GHz for 7 m range. With comparability to the COST231-Hata model is predicted to be higher loss values than that Log-Distance model.

Table 15 computes the partial correlation analysis for the measured results in the corridors. As demonstrated by detailed analyses there are a quite strong positive correlation between for various indoor scenarios and different power levels with a control variable of the frequency from 1 to 8 GHz bands. During the test of propagation in -10 dBm power, there was a null hypothesis. However, with a comparison to others, it appears that it would have been affected by the external unsought influence.

Table 15 Partial correlation analysis for Corridors **Corridor 1**

	4 m						5.35 m						7 m				
	-10	-20	-30	-40	-50		-10	-20	-30	-40	-50		-10	-20	-30	-40	-50
-10		1.000	0.998	0.998	0.960	-10		0.999	0.997	0.994	0.925	-10		1.000	0.998	0.996	0.993
-20	1.000		0.998	0.998	0.960	-20	0.999		0.999	0.992	0.920	-20	1.000		0.998	0.996	0.994
-30	0.998	0.998		0.997	0.962	-30	0.997	0.999		0.989	0.912	-30	0.998	0.998		0.999	0.996
-40	0.998	0.998	0.997		0.973	-40	0.994	0.992	0.989		0.955	-40	0.996	0.996	0.999		0.996
-50	0.960	0.960	0.962	0.973		-50	0.925	0.920	0.912	0.955		-50	0.993	0.994	0.996	0.996	
	Corridor 2																
	-10	-20	-30	-40	-50		-10	-20	-30	-40	-50		-10	-20	-30	-40	-50
-10		0.553	1.000	0.999	0.991	-10		1.000	1.000	0.998	0.982	-10		1.000	0.999	0.998	0.983
-20	0.553		0.557	0.557	0.550	-20	1.000		1.000	0.998	0.983	-20	1.000		1.000	0.998	0.984
-30	1.000	0.557		0.999	0.992	-30	1.000	1.000		0.999	0.983	-30	0.999	1.000		0.999	0.986
-40	0.999	0.557	0.999		0.995	-40	0.998	0.998	0.999		0.985	-40	0.998	0.998	0.999		0.991
-50	0.991	0.550	0.992	0.995		-50	0.982	0.983	0.983	0.985		-50	0.983	0.984	0.986	0.991	
	Corridor 3																
	-10	-20	-30	-40	-50		-10	-20	-30	-40	-50		-10	-20	-30	-40	-50
-10		0.999	0.999	0.999	0.992	-10		1.000	0.999	0.997	0.962	-10		0.200	0.203	0.197	0.201
-20	0.999		1.000	0.999	0.993	-20	1.000		1.000	0.997	0.964	-20	0.200		1.000	0.999	0.994
-30	0.999	1.000		1.000	0.994	-30	0.999	1.000		0.998	0.967	-30	0.203	1.000		0.999	0.995
-40	0.999	0.999	1.000		0.996	-40	0.997	0.997	0.998		0.975	-40	0.197	0.999	0.999		0.997
-50	0.992	0.993	0.994	0.996		-50	0.962	0.964	0.967	0.975		-50	0.201	0.994	0.995	0.997	

Control variable: frequency (1÷8 GHz), Significance: (2-tailed)<0.0001, >0.05, Degree of freedom 68

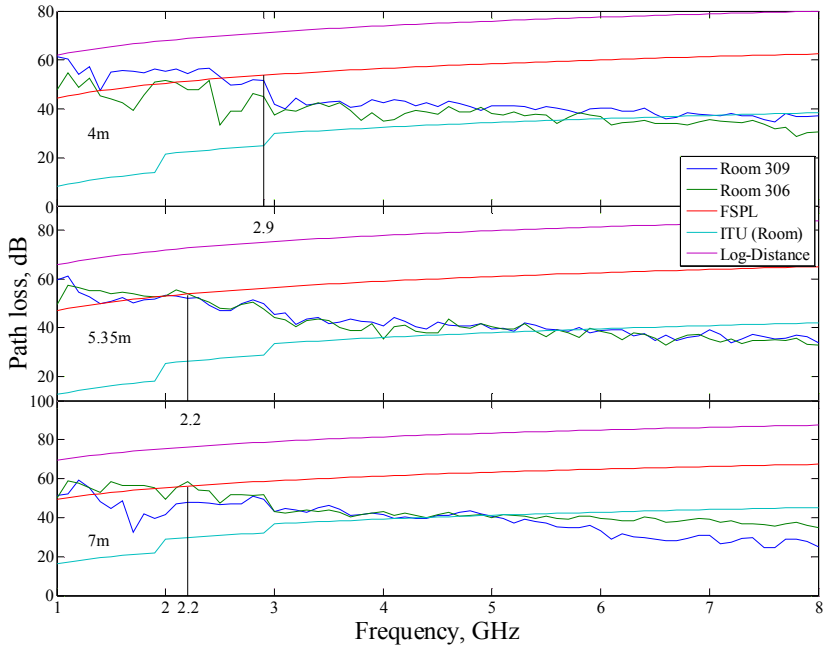

Fig. 47 Path loss comparisons in rooms

Fig 47 depicts the compared results of the measurement in the rooms. A similar tendency repeated in the range between 1 to 2.9 frequencies bands for the 4 m range. In the rest of the transmission distance, the hypotheses are predicted up to 2.2 GHz frequency bands. Controversially, ITU model which has the distance power decay value of 28 tends to predict close path loss values with the measurement from 4 GHz to 8 GHz frequency bands. Nonetheless, it has a trend to predict a higher value with respect to an increase of the transmission distance. The correlation analyses of the measurement result in the rooms are displayed in Table 16. The results of the analyses state that there are robust positive relations for different power levels in varying indoor schemes. In all occasions of diagnosis of the significance levels were lower than 0.0001. Therefore, from all former issues it possibly can be concluded that with respect to the change of transmission distance the path loss tends to be undistinguishable from each other in indoor scenario. Log-Distance, FSPL models apparently potential to predict a path loss evaluation as boundary conditions for the sensor communication system up to the 3 GHz frequency bands. In heavily furnished indoor scenario the ITU (N=28÷33) model appears to be convenient.

Table 16 Partial correlation analysis for Rooms **Room 309**

	4 m						5.35 m						7 m				
	-10	-20	-30	-40	-50		-10	-20	-30	-40	-50		-10	-20	-30	-40	-50
-10		0.996	0.997	0.994	0.882	-10		1.000	0.999	0.998	0.409	-10		0.995	0.995	0.991	0.700
-20	0.996		0.996	0.996	0.892	-20	1.000		1.000	0.998	0.409	-20	0.995		0.999	0.994	0.680
-30	0.997	0.996		0.996	0.885	-30	0.999	1.000		0.999	0.412	-30	0.995	0.999		0.996	0.680
-40	0.994	0.996	0.996		0.889	-40	0.998	0.998	0.999		0.413	-40	0.991	0.994	0.996		0.690
-50	0.882	0.892	0.885	0.889		-50	0.409	0.409	0.412	0.413		-50	0.699	0.680	0.678	0.687	

Room 306

	4 m						5.35 m						7 m				
	-10	-20	-30	-40	-50		-10	-20	-30	-40	-50		-10	-20	-30	-40	-50
-10		0.999	0.999	0.999	0.995	-10		0.999	0.996	0.970	0.837	-10		1.000	0.998	0.993	0.957
-20	0.999		1.000	0.999	0.995	-20	0.999		0.998	0.974	0.845	-20	1.000		0.998	0.994	0.959
-30	0.999	1.000		0.999	0.996	-30	0.996	0.998		0.984	0.871	-30	0.998	0.998		0.997	0.967
-40	0.999	0.999	0.999		0.997	-40	0.970	0.974	0.984		0.939	-40	0.993	0.994	0.997		0.980
-50	0.995	0.995	0.996	0.997		-50	0.837	0.845	0.871	0.939		-50	0.957	0.959	0.967	0.980	

Control variable: frequency (1÷8 GHz), Significance: (2-tailed)<0.0001, Degree of freedom 68

As stated in Table 17, the correlation coefficients tend to decrease with -50dBm transmitted power. With comparison to the evaluation in the corridors the significance level was lower than 0.0001 for all cases.

The uncertainties of high precision measurement techniques such as the SMR20 signal generator and FSP40 spectrum analyzer from Rohde&Schwarz were evaluated from the manufacturer company is applicable and used to estimate the uncertainty of these measurements. In addition, the normal distribution is chosen.

Attenuation or uncertainty of the LMR – 195 coaxial cable for 100m is given by Equation (5.2.4).

$$U_{LMR195} = F_W\left((1.17086)\sqrt{f} + (0.00154)f\right) \tag{5.2.4}$$

Where: the frequency f is in (MHz). In our case 6.5 m cable, and the weighting factor $F_W = 1/\sqrt{2}$ for U distribution is used [32].

Maximum cable assembly attenuation for the UFA147B cable can be calculated by using the following equation:

$$U_{UFA147B} = F_W\left(L \times (0.148\sqrt{f} + 0.004f) + C_1\sqrt{f} + C_2\sqrt{f}\right) \tag{5.2.5}$$

Where: L is the length (f) (1.5), C_1 and C_2 are the connector constants (0.03 for straight connector), and the frequency is in (GHz).

The uncertainties diverge for the HF906 antennas can be evaluated by using Voltage Standing Wave Ratio (VSWR) of the antenna as follows:

$$\begin{aligned} U_{(A+)} &= F_W\left(20\log_{10}\left(1 + \Gamma_1\Gamma_2\right)\right) \\ U_{(A-)} &= F_W\left(20\log_{10}\left(1 - \Gamma_1\Gamma_2\right)\right) \end{aligned} \tag{5.2.6}$$

Where: Γ_1 and Γ_2 are the reflection coefficients of the receiving and transmitting antennas respectively. When considering the same antennas $\Gamma_1 = \Gamma_2$,and the expression relative to the VSWR is:

$$\Gamma = \frac{VSWR - 1}{VSWR + 1} \tag{5.2.7}$$

Where: $VSWR = 3$ is used from 1 to 1.5 GHz range, and $VSWR = 2$ for the rest of the frequency bands as provided by the manufacturer company.

A half width of the uncertainty interval of the antenna is regarded as the measure of the uncertainty:

$$\Delta U_A = \frac{U_{(A+)} - U_{(A-)}}{2} \tag{5.2.8}$$

The uncertainty values such as the analyzer and signal generator were given for 95% confidence level as follows:

$$U_1 = \sqrt{U_{SMR}^2 + U_{FSP}^2} \tag{5.2.9}$$

Where: $U_{SMR} = 1$ is uncertainty of the signal generator (dB), $U_{FSP} = 0.259$ is the uncertainty of the spectrum analyzer.

The rest of the system units supposed to be computed for the same level of the confidence level which is 95%, the system units are calculated by using Equation (5.2.10).

$$U_2 = t\sqrt{U^2 + U_{LMR195}^2 + U_{UFA147B}^2 + \Delta U_A^2} \tag{5.2.10}$$

Where: $t = 1.671$ is the Student's t distribution value for the degree of freedom 68 for the confidence interval of 95%. U is the uncertainty of the measured result or mean error. This error is chosen to be a maximum value of error along with the same distribution conditions from **Appendixes F** to **H** for corridors $U_{Cor} = \sigma_{C,\max}$, and **Appendixes I** and **J** for rooms $U_R = \sigma_{R,\max}$.

Then the total expanded system uncertainties are estimated for the Room (U_{SR}) based uncertainty of corridors (U_{2R}), and for Corridors (U_{SC}) based on a (U_{Cor}) is:

$$U_S = \sqrt{U_1^2 + U_2^2} \tag{5.2.11}$$

For the estimation of uncertainty with ZStar3 kit measurement the following expression is proposed:

$$U_{SZ} = t\sqrt{U_{UFA}^2 + U_{FSP}^2} \tag{5.2.12}$$

It should be noted that, the uncertainty of the antenna is not included in this calculation due to a license of the product.

As has been demonstrated by an uncertainty budget in **Appendix K**, the uncertainties of the measurement were ranging from 6.104 to 9.719 dB in the corridors with respect to the frequency. During the measurement in the rooms, the statements were almost lower by 1dB, which is 5.303 to 9.702 regarding the frequency ranges. A maximum uncertainty of ZStar3 kit found to 1.708 dB. However, as mentioned former the antennas are left behind the estimation.

5.3 Measurement of RF signal penetration

5.3.1 Introduction

In recent years, bringing a reliable communication and transmission in an indoor scenario via wirelessly due to its advantages, which is the elimination of the electric wire as well as a conveyance with a moving object is emerging. Considering that the electromagnetic radiation trough a commercial construction material has been drawing particular attention. From the sensor communication system point of view a wide frequency range for an ultra-low power transmission level consideration would be useful for a further development. Moreover, the fires, accidents, and other unforeseen incidents are just another day in the life of firefighters; hence the same frequency ranges were tested with 10 dBm transmission power.

5.3.2 Material and site description

A. Descriptions of the tested material

In order to achieve a reliable connection of the RF measurement system, a property of the electromagnetic radiation trough a construction material such as concrete, brick, and glass are paid a special attention here. Mechanical characteristics of the material under the test are drawn in Fig 48.

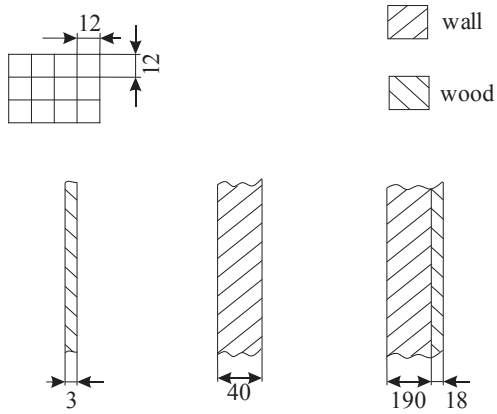

Fig. 48 Tested material and their mechanical dimensions

As can be seen, the wooden door was a fire resistance specific application door, and a glass door contains 12x12mm metal wire set. The wall is constructed by blocks, bricks and wooden attachment for the clothes hanger. The relative parameters are in Table 17 [13, 39, 56, 66, 71, and 103].

Table 17 Relative parameters of the materials

	Concrete	Brick	Glass	Wood
Permeability	0.97	0.99	0.99	0.81
Permittivity	6.14	3.58-4.44	5.98	2-4
Conductivity	0.1-0.41	0.12	0.35	0.07-0.87
Loss tangent	0.32	0.07	0.01	0.14

One of a most interesting measurement is carried out with a protective fir – fighting garment from DEVA F-M. s.r.o. according to EN 469: 2005 standard.

A photograph of the suit and the materials are illustrated in Fig 49, as can be seen that NOMEX Diamond Ultra fabric is considered to be a composition of the three materials.

a) a Photograph of the suite *b) a Photograph of the materials*

Fig. 49 TIGER Plus – fire fighting garment from [17]

The approximate thickness of the fabrics can be expected from their densities. However, the necessarily of the accuracy might have a low reliability. The parameters of the materials are tested in Faculty of Technology for different frequency bands, and the average value is used. A material composition and their relative characteristics are provided by Table 18.

Table 18 Material composition and relative parameters of the suit

Material composition	Content	ε (Re)	ε (Im)	Loss Tan	Thickness, mm
NOMEX Diamond Ultra (orange, red, dark blue)	210	1.600	0.010	0.005	0.234
GORE-TEX Fiberblocker N	140	1.382	0.020	0.014	0.183
NOMEX Comfort/Aramid Gird	200	1.588	0.009	0.005	0.229

B. Description of the site for fireman suit measurement

The measurement of the penetration trough firemen garment is tested at the gym rooms of the university. A reason to select these environments was, in order to avoid from

undesired multipath reflections. The main dimensions of the gym room are: width is 8.35m, and length is17.60 m.

5.3.3 Measurement setup

During the measurement of the penetration trough the construction material is assumed to be relatively no multipath propagation as shown in Fig 50. The antennas were located in 250mm from the materials. The rest of the system units is remained the same with the measurement of the propagation, including the software and measurement constant as shown in Table 14.

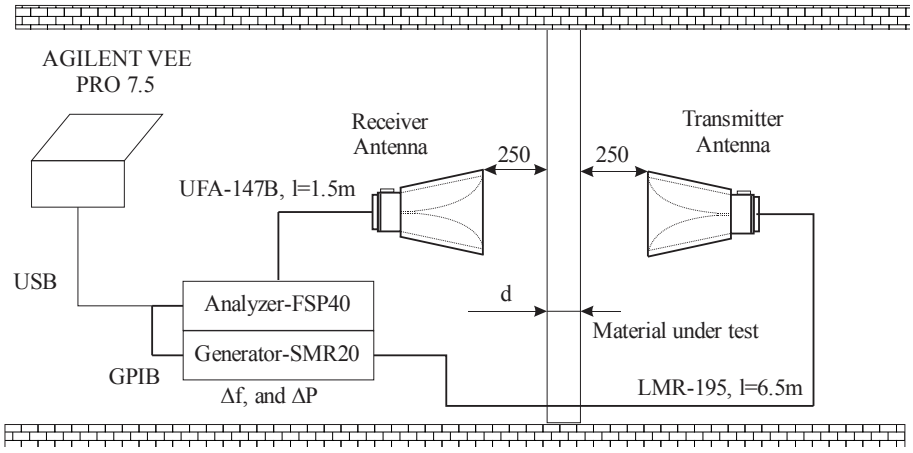

Fig. 50 Penetration measurement setup

However, for the firemen garment penetration measurement, 10m long UFA-147B cable, and 6cm a rod type probe from HZ11 set is used as a sensor. A diagram of the measurement setup is shown below.

The sensor is attached in the chest of the man (Fig 50) by using a polypropylene material in order to avoid from absorption of the signal into the body. The same setup is used including the software, and constants. First, the measurement is carried out without the garment from 1 to 10 m range. Then, the measurement is repeated with the garment. The loss due to the garment is considered to be:

$$P = P_1 - P_2 = \left(P_t - G_A - G_P - P_{1N}\right) - \left(P_t - G_A - G_P - P_{2N}\right) \qquad (5.2.13)$$

Where: P_1 and P_2 are the received powers with the garment and without the garment respectively. G_A and G_P are the gains of the antenna and probe. P_{1N} and P_{2N} are the noise floor level (with and without garment).

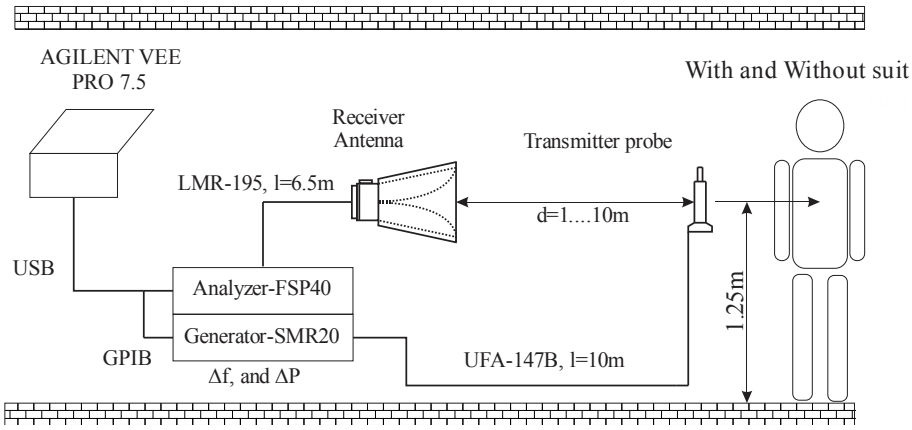

Fig. 51 Firemen garment measurement setup

5.3.4 Result and Discussion

The Fig 52 displays a result of the penetration measurement trough the construction materials. The loss tendency of the wall and wooden door were solely similar with respect to the frequency.

However, they were differing by 10 dB in most cases. The penetration losses, up to 3 GHz frequency band were increasing with regard to the frequency in the glass door. In the rest of the ranges, the tendency of the loss in two doors was found to be closely related. A minimum loss is culminated in the wall penetration measurement. The same tendency occurred with the measurement of the ZStar3 kit. However, there are differed by from 2.239 dB to 5.434dB. The difference could be derived by misalignment error and the gain of the antenna of the sensor board.

The correlation analysis of the result in a Table 19 indicates that the lowest coefficients incline to be found with the transmission of -50dBm power. In the majority situations, the coefficient if found to be 1.000. The minimum coefficients performed during transmission of – 50 dBm power level.

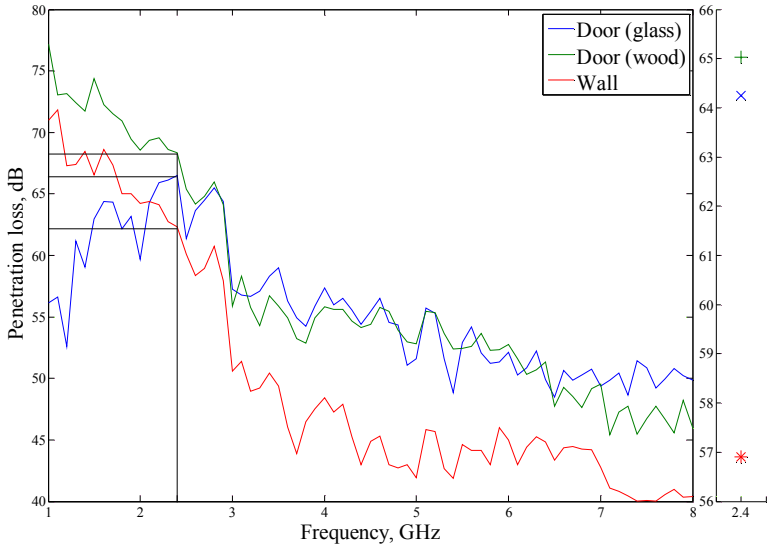

Fig. 52 Result of penetration measurement

Table 19 Partial correlation analysis for penetration

Glass door					
	-10	-20	-30	-40	-50
-10		1.000	1.000	1.000	0.890
-20	1.000		1.000	1.000	0.889
-30	1.000	1.000		1.000	0.889
-40	1.000	1.000	1.000		0.889
-50	0.890	0.889	0.889	0.889	
Wooden door					
	-10	-20	-30	-40	-50
-10		1.000	1.000	0.998	0.966
-20	1.000		1.000	0.998	0.966
-30	1.000	1.000		0.998	0.965
-40	0.998	0.998	0.998		0.966
-50	0.966	0.966	0.965	0.966	
Wall					
	-10	-20	-30	-40	-50
-10		1.000	1.000	1.000	0.532
-20	1.000		1.000	1.000	0.534
-30	1.000	1.000		1.000	0.533
-40	1.000	1.000	1.000		0.533
-50	0.532	0.534	0.533	0.533	
Control variable: frequency (1÷8 GHz),Significance:(2-tailed)<0.0001,Degree of freedom 68					

The measured result is not only insertion loss but also includes free space loss by means of penetration loss with respect to the transmitted power. The insertion loss of the materials can be modeled by using a data in Table 17 and 18.

The uncertainty values for analyzer and signal generator are the same with the previous analysis according to Equation (5.2.9).

A derivation of Equation (5.2.10) (for uncertainty analysis of penetration) is based on a standard sample error for the glass door ($U_{GD} = \sigma_{GD}$), for the wooden door ($U_{WD} = \sigma_{WD}$), and for the wall ($U_W = \sigma_W$). And the resulting expanded uncertainties (U_{2GD} for glass door, U_{2WD} for wooden door, and for wall U_{2W}) are used to determine the system uncertainties by using Equation (5.2.11).

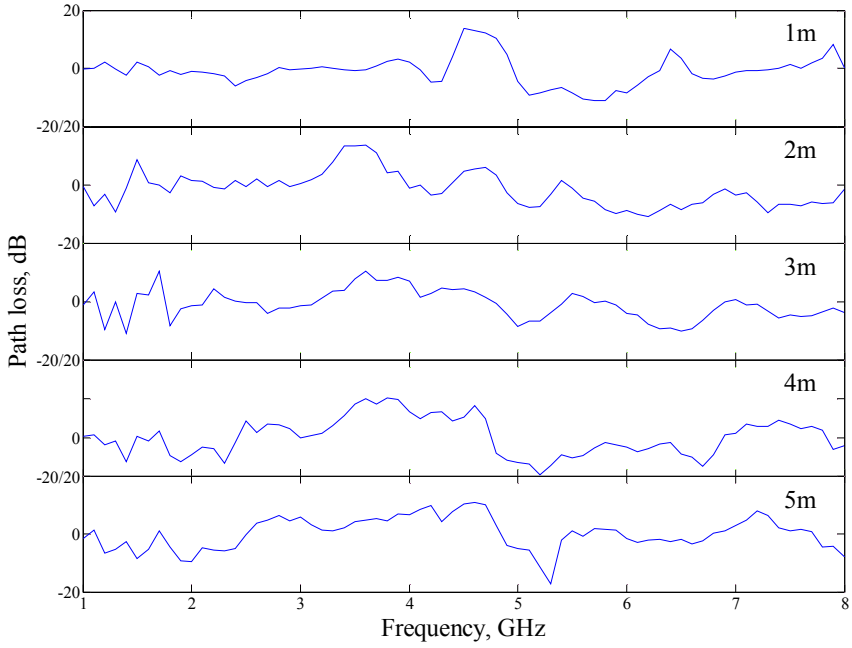

Fig. 53 Result of garment measurement

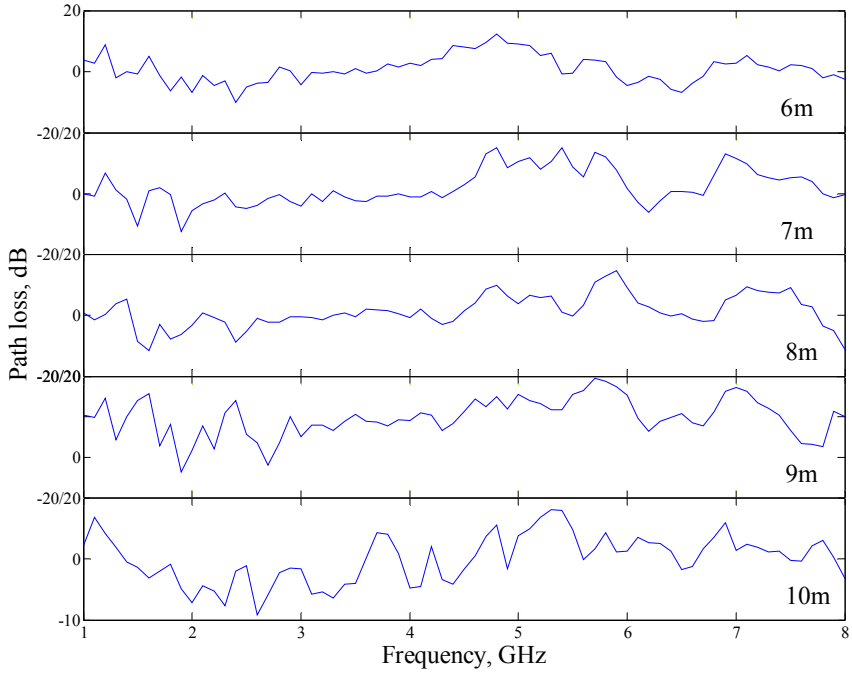

Fig. 54 Result of garment measurement

The Figures 53 and 54 reveals the measured result of the garment. The loss due to garment was randomly varying with consideration to the frequency bands and distances. A minus loss is the gain, and it could have been affected by a gap which was produced by a cable connection to the probe. In addition, it should be noted that the trousers of the suit is not used during the measurement, hence may perhaps be another effect. Uncertainty evaluation for the garment measurement can be estimated including signal generator, spectrum analyzer, and 2 cables. Moreover, the uncertainty diverge of the antennas should have considered.

6 DISCUSSION OF THE RESULT

6.1 Contribution to science and practice

The thesis contributes to some theoretical approach of a measurement system as well as to modeling of experimental setup for a laboratory measurement system.

A real laboratory model, including all necessarily subfield and the analysis of a measurement system which has been studied by this thesis is applicable both for the research and pedagogical purposes.

The next experiments of electromagnetic propagation in an indoor scenario and penetration through a construction medium describe a contemporary state of a reliable wireless communication system for sensors, in a range from 1 to 8 GHz frequency bands, and for ultra-low power transmission up to 0.1 mW.

From practical point of view, it is applicable to characterize and predict a reliable wireless communication system for sensors by estimating the signal loss from the result of propagation and penetration, for former frequency range of signals.

Moreover, the thesis reports a preliminary result of a penetration measurement throughout a firemen garment for a development of a further smart suit. However, the result indicates that a supplementary development and more proper measurements are necessary.

6.2 Conclusion

Increasing demand of a reliable measurement system with an innovation of the wireless communication system as a field of growing importance, require a comprehensive optimization of a measurement system.

In order to meet the supra specified aims, this thesis first studies a modern measurement system. Particular attention is paid on sensor system covering the sensor technology, material, sensing principles, and characteristics. The work also overviews the primary and secondary signal processing as well as a communication system for sensors.

Moreover, an example of a laboratory measurement system is constructed in order to experiment and characterize the important parameters of the measurement system including signal conditioning both analogue and digital, as well as wireless communication system. The model is based on the strain gauge bridge circuit, and for the analogue signal conditioning the difference, non-inverting operational, and instrumentation amplifiers are tested. Digital signal processing and 2.4 GHz wireless communication system is accomplished with the ZStar3 kit. Evaluations of the statistical analysis specially, uncertainty estimations for the constructed laboratory measurement system have rated.

The experiment of propagation and penetration are carried out between 1 to 8 GHz frequency ranges for -50 dBm, -40 dBm, -30 dBm, -20 dBm and -10 dBm power levels. The propagation measurement in an indoor scenario is conducted in four different environments, and for the transmission distances of 4m, 5.35m and 7m. The penetration of the electromagnetic signal has tested for three various construction materials, due to its predominant existent.

Resulting path loss models have evaluated and compared with well known empirical models. Corresponding statistical analysis has compromised partial correlation analysis and uncertainty estimation for both measurement cases, to reveal satisfactorily confidence of the result.

Due to limited time of period, modeling and simulation of insertion loss of the construction material, and firemen garment is under the process, which requires a more collaboration with other professionals. The results of the modeling and simulation of the sensor signal conditioning and the insertion loss are expected to report at the defense date of the dissertation work.

The author’s knowledge acquired at TBU will be shared at home country as a monograph, and the result of the study will be translated (into Mongolian), and published in corresponding journals or magazines.

Furthermore, the modeling and simulation of the sensor loops in Matlab/Simulink, ANSYS, COMSOL, and CST may include sensors, appropriate signal conditioning moreover, wireless communication system is achievable for a development of the field.

7 AUTHOR PUBLICATION ACTIVITY

HRUŠKA, F., LKHAGVATSEREN, T. 2009. Aspects of signal condition from DC bridge circuits. In 17th International Conference on Process Control 2009. Hotel Baník, Slovakia: Štrbské Pleso, 2009, pp. 609-612. ISBN 978-80-227-3081-5

HRUŠKA, F., LKHAGVATSEREN, T. 2009. Signal condition of DC bridges. In 10th Int. Carpathian Control Conference 2009 – ICCC 2009. Poland: Zakopane, 2009, pp. 285-288. ISBN 8389772-51-5.

LKHAGVATSEREN, T. , HRUŠKA, F. 2010. Measurement systems connection between sensors and Embedded system. In 35th proceeding of Seminar ASR '2010 "Instruments and Control". Czech Republic: Ostrava, 2010, pp. 243-249. ISBN 978-80-248-2191-7

LKHAGVATSEREN, T. , OTÁHAL, J., HRUŠKA, F. Dual – axis wireless force measurement study. 9th International Conference – Process Control 2010. Kouty nad Desnou, Czech Republic, 2010, pp. C011a-1. ISBN 978-80-7399-951-3

LKHAGVATSEREN, T. , HRUŠKA, F. 2010. Wireless communication for sensors. International Conference on Communication and Management in Technological Innovation and Academic Globalization (COMATIA '10). Puerto De La Cruz, Tenerife. pp. 72-78. ISBN: 978-960-474-254-7. ISSN: 1792-6823 (Electronic). ISSN: 1792-6718 (Print)

LKHAGVATSEREN, T., HRUŠKA, F. 2011Path loss aspects of a wireless communication system for sensors. International Journal of Computers and Communications. pp. 18-26. Issue 1, Volume 5. ISSN: 2074-1294.

LKHAGVATSEREN, T., HRUŠKA, F., GERLICH, V. Aspects of wireless communication of sensors. 12th International Carpathian Control Conference – ICCC 2011. Ostrava – Beskydy, Czech Republic, 25-28 May 2011 *(Accepted paper)*.

LKHAGVATSEREN, T. Sensors and Signal conditioning. Monograph in Mongolia (June 2011). *(Under process)*.

8 REFERENCES

[1] ABHAYAWARDHANA V.S., WASSELL, I.J., CROSBY, D., SELLARS, M.P., BROWN, M.G Comparison of Empirical Propagation Path Loss Models for Fixed Wireless Access Systems [Journal] // VTC, IEEE.. - Vehicular Technology Conference, 2005. VTC 2005-Spring. 2005 IEEE 61st: IEEE, Jun 2005. - pp. 73-77: Vol. 1. ISSN: 1550-2252

[2] AGILENT TECHNOLOGIES Spectrum Analysis Basics [Report]. - Printed in USA: Agilent Technologies, Inc., August 2, 2006.

[3] ANALOG DEVICES www.analog.com [Online]. - Feb 18, 2011. - http://www.analog.com/en/index.html.

[4] ANN WITVROUW CMOS – MEMS integration today and tomorrow. [Journal] // Scripta Materialia: Elsevier, Nov 2008. - pp. 945-949: Vol. 59. ISSN: 1359-6462

[5] BALTAG O., COSTANDACHE, D., SALCEANU, A Tilt measurement sensor [Journal] // Sensors and Actuators. - Sensors and Actuators A: Physical: Elsevier, Apr 2000. - pp. 336-339: Vol. 81. ISSN 0924-4247

[6] BARRY J. M., KAHN AND J. R Wireless infrared communications [Journal] // Proc.of the IEEE. - [s.l.]: Proceeding of the IEEE, Feb. 1997. - pp. 265-298: Vol. 85.

[7] BERTONI H.L., HONCHARENKO, W., MACEL, L.R., XIA, H.H UHF Propagation Prediction for Wireless Personal Communications [Journal] // PROCEEDINGS OF THE IEEE. - Proceedings of the IEEE: IEEE, Sep 1994. - pp. 1333-1359: Vol. 82. NO. 9. ISSN: 0018-9219

[8] BOBIER K., WELLS, J., DAPPER, M Enhanced unattended ground sensor system communications [Journal] // MILCOM 2002. Proceedings. - Proceedings of MILCOM 2002: IEEE, 2003. - pp. 282-289: Vol. 1. ISBN: 0-7803-7625-0

[9] CASTRO B.S.L., GOMES, I.R., RIBEIRO, F.C.J., CAVALCANTE, G.P.S COST231-Hata and SUI Models Performance Using a LMS Tuning Algorithm on 5.8GHz in Amazon Region Cities [Journal] // Proc of IEEE. EuCAP-2010. - Proc of IEEE. EuCAP-2010: INCTCSF, Jul 2010. - pp. 1-3 ISBN: 978-1-4244-6431-9. - pp. ISBN: 978-84-7653-472-4.

[10] CHANG-FA YANG BOAU-CHENG WU, CHUEN-JYIKO A Ray-Tracing Method for Modeling Indoor Wave Propagation and Penetration [Journal] // IEEE Transactions on ANTENNAS AND PROPAGATION. - IEEE Transactions on Antennas and Propagation: IEEE, Jun 1998. - pp. 907 - 919: Vol. 46. ISSN: 0018-926X

[11] CHEN L.F.,ONG, C.K., NEO, C.P., VARADANAND, V.V., VARADAN, V.K Microwave Electronics Measurement and Materials Characterization [Book]. - TheAtrium, SouthernGate, Chichester: JohnWiley&Sons Ltd, 2004. - pp. 175-205 ISBN0-470-84492-2.

[12] COLOGNE., MATHIAS SCHULENBURG Nanotechnology Innovation for Tomorrow's World [Journal] // European Commission, Research. - German: European Commission, Research DG, 2004. - pp. 1-60: EUR 21151EN. ISBN: 92-894-7498.

[13] CORREIA L. M., FRANCES, P. O Transmission and Isolation of Signals in Buildings at 60 GHz [Journal] // Personal, Indoor and Mobile Radio Communications, 1995. PIMRC'95. 'Wireless: Merging onto the Information Superhighway'. Sixth IEEE International Symposium on. - Sixth IEEE International Symposium on PIMRC 1995: IEEE, 1995. - pp. 1031-1034: Vol. 3. ISBN: 0-7803-3002-1

[14] DAG STRANNEBY., WILLIAM WALKER Digital Signal Processing and Applications [Book]. - Oxford, UK: Elsevier, 2004. - pp. 1-68, 241-275 ISBN 0750663448.

[15] DATAFORTH CORPORATION Industrial Signal Conditioning, A Tutorial [Report]. - pp. 1-26: Dataforth Corporation.

[16] DAVARSILVATHAM, D http://www.wirelesscommunication.nl/reference/chaptr03/indoor.htm [Online]. - 2010. - http://www.wirelesscommunication.nl/reference/chaptr03/indoor.htm.

[17] DEVA F-M. S.R.O. http://www.deva-fm.cz/ [Online]. - March 2, 2010. - http://www.deva-fm.cz/sortiment.php.

[18] EATON W.P., SMITH, J.H., MONK, D.J., O`BRIEN, G., MILLER, T.F Comparison of Bulk- and Surface- Micromachined Pressure Sensors [Journal] //

Micromachined Devices and Components. - Proceedings of SPIE, Micromachined Devices and Components: [s.n.], Aug 1998. - pp. 431-438: Vol. 3514.

[19] EDMUND LAI Practical Digital Signal Processing for Engineers and Technicians [Book]. - Oxford OX2 8DP, UK: An imprint of Elsevier, 2003. - pp. 1-131 ISBN 07506 57987.

[20] EMMANUEL, O.O., OJAKOMINOR., TIAN F. LAI Statistical (Radio) Path Loss Modelling: For RF Propagations within localized Indoor and Outdoor Environments of the Academic Building of INTI University College (Laureate International Universities) [Journal]. - World Academy of Sceince, Engineering and Technology: WCSET 2008 PROGRAM Feb 2009. - pp. 660-682: Vol. 50. ISSN: 2070-3740

[21] FERRAN BAYES PWM circuit uses one op amp [Report]. - Barcelona, Spain pp. 136: Electronica Digital, Jul 2000.

[22] FREESCALE SEMICONDUCTOR INC DRM103 Designer Reference Manual [Report]. - USA, Canada, Europe: Freescale Semiconductor, Nov, 2009.

[23] FREESCALE SEMICONDUCTOR INC www.freescale.com [Online]. - Feb 22, 2011. - http://www.freescale.com/.

[24] FREESCALE SEMICONDUCTOR INC MC1321x 2.4 GHz “System in a Package” [Report]. - [s.l.]: www.freescale.com/zigbee, 2008.

[25] FREESCALE SEMICONDUCTOR INC Technical Data [Report]. - Document Number: MC13191: Freescale Semiconductor Inc, Aug, 2005.

[26] FREESCALE SEMICONDUCTOR INC Technical Data [Report]. - Document Number: MC1321x: Freescale Semiconductor LLC, Aug, 2009.

[27] FRENCH, P. J. , SARRO, P. M Surface versus bulk micromachining the contest for suitable applications [Journal] // Micromech.Microeng. - Journal of Micromechanics and Microengineering: Elsevier, Jun 1998. - pp. 45-53: Vol. 8. ISSN 1361-6439

[28] GARDNER J, W., VARADAN, K, V., AWADELKARIM, O, O Microsensors, MEMS, and Smart Devices [Book]. - New York: John Willey&Sons, 2001. -pp. 1-225 ISBN - 13: 9780471861096.

[29] GHODGAONKAR D.K., VARADAN, V.V., ANDVARADAN, V.K Free-space measurement of complex permittivity and complex permeability of magnetic

materials at microwave frequencies [Journal] // IEEE Transactions on Instrumentation and Measurement. - 1990. - pp. 789–793 Vol.38.

[30] HASHEMI H., GANG, Y., KAVEHRAD, M., BEHBAHANI, F., GALKO, P.A Indoor propagation measurements at infrared frequencies for wireless local area networks applications [Journal] // IEEE Trans. Vehicular Technology,. - IEEE Transactions on Vehicular Technology: IEEE, Aug 1994. - 3 pp. 562 - 576: Vol. 43. ISSN: 0018-9545

[31] HONCHARENKO, W., BERTONI, H.L., DAILING, J Mechanisms Governing Propagation Between Different Floors in Buildings [Journal] // IEEE Transactions on ANTENNAS AND PROPAGATION. - IEEE Transactions on Antennas and Propagation: IEEE, Jun 1993. - pp. 787-790: Vol. 41. ISSN: 0018-926X

[32] HOWARD CASTRUP Error Distribution Variances and Other Statistics [Report]. - http://www.isgmax.com/: ISG Technical Document, Jan, 2009. - pp. 1-18.

[33] HOWE, R.T., MULLER, R.S., GABRIEL, K.J., TRIMMER, W.S.N Silicon micromechanics: sensors and actuators on a chip [Journal] // Spectrum, IEEE. - IEEE on Spectrum: IEEE, Jul 1990. - pp. 29-35: Vol. 27. ISSN : 0018-9235

[34] HRUŠKA F., LKHAGVATSEREN, T Signal condition of DC bridges [Journal] // In 10th Int. Carpathian Control Conference 2009. - In 10th Int. Carpathian Control Conference 2009. Poland: Zakopane: [s.n.], 2009. - pp. 285-288 ISBN 8389772-51-5.

[35] HTTP://WWW.RADIO-ELECTRONICS.COM http://www.radio-electronics.com [Online]. - Feb 28, 2010. - http://www.radio-electronics.com/info/t_and_m/spectrum_analyser/rf-analyzer-basics-tutorial.php.

[36] HUNTER, M.T., KOURTELLIS, A.G., ZIOMEK, C.D., MIKHAEL, W.B Fundamentals of Modern Spectral Analysis [Journal] // IEEE. - IEEE Autotestcon: IEEE, Sep 2010. - pp. 1-5 ISSN: 1088-7725.

[37] HUNTER, M.T Efficient FFT-based spectral analysis using polynomial-based filters for next generation test systems [Journal] // IEEE in Autotestcon. - IEEE Autotestcon: IEEE, Sep 2007. - pp. 677-686 ISBN: 978-1-4244-1239-6 ISSN: 1088-7725.

[38] IIC BUS http://www.i2c-bus.org/ [Online]. - Feb 15, 2011. - http://www.i2c-bus.org/.

[39] IÑIGO CUIÑAS., MANUEL GARCÍA SÁNCHEZ Permittivity and Conductivity Measurements of Building Materials at 5.8 GHz and 41.5 GHz [Journal] // Wireless Personal Communications. - International Journal of Wireless Personal Communications: Kluwer Academic Publishers, Jan 2002. - 1 pp. 93-100: Vol. 20. ISSN 0929-6212

[40] INTERNATIONAL ORGANIZATION FOR STANDARDIZATION International Vocabulary of Basic and General Terms in Metrology [Case] : ISO DGUIDE 99999. - www.iso.org: ISO VIM, 2004.

[41] JACOB FRADEN Handbook of Modern Sensors: Physics, Designs, and Applications. 3th ed. [Book]. - New York: Springer - Verlag, 2004. - pp. 1-579 ISBN: 0-387-00750-4.

[42] JAE Y.PARK., GEUN H.KIM., KI W.CHUNG., JONG U.BU Monolithically Integrated Micromachined RF MEMS Capacitive Switches [Journal] // Sensors and Actuators. - Sensors and Actuators A: Physical: Elsevier, Mar 2001. - 1-2 pp. 88-94: Vol. 89. ISSN: 0924-4247

[43] JOHN S. SEYBOLD Introduction to RF propagation [Book]. - Hoboken,New Jersey : JOHN WILEY& SONS, INC. , 2005. - pp. 208-214 ISBN-13 978-0-471-65596-1.

[44] JOHN G.WEBSTER Electrical Measurement, Signal Processing, and Displays [Book]. - Florida: CRC Press, 2004. - pp. 23.1-23.15, 25.1-25.19 ISBN: 0849317339.

[45] JOHN G.WEBSTER The measurement, Instrumentation and Sensors Handbook [Book]. - USA: CRC Press LLC, 1999. - pp. S1-S5 ISBN: 0-8493-2145-X.

[46] JON S.WILSON Sensor Technology Handbook [Book]. - USA: Elsevier, Inc,, Oct 2004. - pp. 1-108 ISBN-13: 978-0-7506-7729-5.

[47] JOSE PERHI., LAWRENCE S. COHEN Design of Broad-Band Radar-Absorbing Materials for Large Angles of Incidence [Journal] // IEEE Transactions on ELECTROMAGNETIC COMPATIBILITY VOL.35 No. 2. - IEEE Transactions on Electromagnetic Compatibility: IEEE, May 1993. - pp. 223-230: Vol. 35..

[48] KAI CHANG RF and Microwave Wireless Systems [Book]. - New York: John Wiley&Sons, 2000. - pp. 243-248. ISBN: 0-471-22432-4.

[49] KALIYUGAVARADAN, S A simple resistance-to-time converter for signal conditioning of resistive transducers [Journal] // Measurement Science and Technology. - Measurement Science and Technology: IOP Science, May 2000. - pp. N73-N75: Vol. 11. ISSN: 1361-6501

[50] KE LIN DU., SWAMY, M. N. S. Wireless Communication System [Book]. - UK : Cambridge University Press. , 2009. ISBN: 978-0-521.

[51] KUNG J.T., LEE, H.S An Integrated Air-Gap-Capacitor Pressure Sensor and Digital Readout with Sub- 100 Attofarad Resolution [Journal] // JOURNAL OF MICROELECTROMECHANICAL SYSTEMS. - Journal of Microelectromechanical Systems: IEEE, Sep 1992. - pp. 121-129: Vol. 1. ISSN: 1057-7157

[52] KUNG J.T., MILLS, R.N., HAE-SEUNG LEE Digital cancellation of noise and offset for capacitive sensors [Journal] // Instrumentation and Measurement, IEEE Transactions on. - IEEE Transactions on Instrumentation and Measurement: IEEE, Oct 1993. - pp. 939 - 942: Vol. 42. ISSN: 0018-9456

[53] KWOK-SIONGTEH., LIWEI LIN MEMS sensor material based on polypyrrole-carbon nanotube nanocomposite: film deposition and characterization. [Journal] // Micromechanics and Microengineering.. - Journal of Micromechanics and Microengineering: Elsevier, Jul 2005. - pp. 2019-2027: Vol. 15.

[54] KYO – HO SH., CHANG RUOUL, M., TAE HEE, L., CHANG HYUN, L Flexible wireless pressure sensor module [Journal] // Sensors and Actuators.. - Sensors and Actuators A: Physical: Elsevier, Sep 2005. - pp. 30-35: Vols. 123-124. ISSN: 0924-4247

[55] LAN J., NAHAVANDI, S., YIN, Y., LAN, T Development of the low cost motion sensing system [Journal] // Measurement. - Measurement: Elsevier, May 2007. - pp. 2789-2794: Vol. 40. ISSN: 0263-2241

[56] LANDRON O., FEUERSTEIN M.J. AND RAPPAPORT T.S A Comparison of Theoretical and Empirical Reflection Coefficients for Typical Exterior Wall Surfaces in a Mobile Radio Environment [Journal] // IEEE TRANSACTIONS ON

ANTENNAS AND PROPAGATION. - IEEE Transactions on Antennas and Propagation: IEEE, Mar 1996. - pp. 341-351: Vol. 44. ISSN: 0018-926X

[57] LEE D, S Thermal accelerometer based predictive drop sensor. [Journal] // Sensors and Actuators.. - Sensors and Actuators A: Physical: Elsevier, Apr 2007. - pp. 889-894: Vol. 135. ISSN: 0924-4247

[58] LIN X., KOSUGI, K., ITOH, H Indoor information support system using optical wireless communication technique [Journal] // WSEAS Trans. Communication. - WSEAS Transactions on COMMUNICATIONS: WSEAS, Apr 2008. - pp. 42-45: Vol. 7. ISSN: 1109-2742

[59] LIYONG JIANG., XIANGYIN LI Design High performance Microwave Absorbers Using Adaptive Genetic Algorithm (AGA) [Journal] // Electromagnetic Compatibility and 19th International Zurich Symposium on Electromagnetic Compatibility, 2008. APEMC 2008. Asia-Pacific Symposium on. - Symposium on APEMC 2008: IEEE, May 2008. - pp. 758-761 ISBN: 978-981-08-0629-3.

[60] LKHAGVATSEREN, T. , HRUŠKA, F. Wireless communication for sensors [Journal] // Wireless communication for sensors. International Conference on Communication and Management in Technological Innovation and Academic Globalization (COMATIA '10).. - Proceedings of COMATIA '10 Puerto De La Cruz, Tenerife: [s.n.], 2010. - pp. 72-78 ISBN: 978-960-474-254-7. ISSN: 1792-6823 (Electronic). ISSN: 1792-6718 (Print)

[61] LKHAGVATSEREN, T. , JIŘÍ, O., HRUŠKA, F Dual – axis wireless force measurement study [Journal] // 9th International Conference – Process Control 2010. - 9th International Conference – Process Control 2010. Kouty nad Desnou Czech Republic: [s.n.], 2010. - pp. C011a-1ISBN 978-80-7399-951-3. - pp. C011a-1. ISBN 978-80-7399-951-3.

[62] LKHAGVATSEREN, T., HRUŠKA, F Path loss aspects of a wireless communication system for sensors [Journal] // International Journal of Computers and Communications. - International Journal of Computers and Communications: NAUN Press, 2011. - pp. 18-26: Vol. 5. ISSN: 2074-1294

[63] LOWDERMILK W., HARRIS, F Cost effective, versatile, high performance, spectral analysis in a synthetic instrument [Journal] // IEEE in Autotestcon. - IEEE Autotestcon: IEEE, Sep 2008. - pp. 148-153 ISSN: 1088-7725.

[64] MAILADIL T.SEBASTIAN Dielectric Materials for Wireless Communication [Book]. - [s.l.]: Elsevier Ltd., 2008. - pp. 1-670 ISBN -13: 978-0-08-045220-9.

[65] MICROCHIP TECHNOLOGY INC UNI/O Bus Specification [Case]: DS22076B. - ISO/TS-16949:2002: Microchip Technology Inc, 2008.

[66] MIKKO HAVIMO A literature-based study on the loss tangent of wood in connection with mechanical pulping [Journal] // Wood Science and Technology. - Wood Science and Technology: Springer, Jul 2009. - 7-8 pp. 627-642: Vol. 43.

[67] MIYAMOTO, S., MORINAGA, N A study on performance improvement of indoor optical wireless communication system [Journal] // IEICE Tech. Rep. MWP98-5. - IEICE Tech. Rep. MWP98-5: [s.n.], 1998. - pp. 25-32.

[68] MITSUBISHI ELECTRIC CORPORATION POWER DEVICE DIV. MITSUBISHI Acceleration Sensor. - pp. 1-10. www.mitsubishichips.com/Global/files/manuals/AccelerationSensor.pdf

[69] MOOJIN KIM., WONKYU MOON., EUISUNG YOON., KWANG-RYEOL LEE A new capacitive displacement sensor with high accuracy and long range [Journal] // Sensors and Actuators.. - Sensors and Actuators A: Physical: Elsevier, Aug 2006. - pp. 135-141: Vols. 130-131. ISSN: 0924-4247

[70] MOTOROLA SEMICONDUCTORS www.motorola.com [Online]. - Feb 23, 2011. - http://www.motorola.com/semiconductors/dsp/support.

[71] MUQAIBEL, A., SAFAAI-JAZI, A., BAYRAM, A., ATTIYA, A.M., RIAD, S.M Ultrawideband through-the-wall propagation [Journal] // Microwaves, Antennas and Propagation, IEE Proceedings -. - IEE Proceedings of Microwaves, Antennas and Propagation: IEEE, Dec, 2005. - pp. 581-588 ISSN: 1350-2417.

[72] NATIONAL INSTRUMENTS CORPORATION Data Acquisition and Signal Conditioning Course Manual [Report]. - pp. 5.2-5.64, 6.2-6.62: National Instruments Corporation, Aug, 2003.

[73] PARASKEVOPOLOUS, P.N Modern Control Engineering [Book]. - NewYork, NY10016: Marcel Dekker Inc, 2002. - pp. 1-147 ISBN: 0-8247-8981-4.

[74] PARSONS, J.D The mobile radio Propagation Channel, Second Ed [Book]. - NY: Lohn Wiley & Sons, 2000. - pp. 15-22, 190-215 ISBN: 0-471-98857-x.

[75] PATRICK GAYDECKI Digital Signal Processing [Book]. - United Kingdom: University of Manchester, 2006. - pp. 30- 130 ISBN-13: 9780852964316.

[76] PAUL, P.L., REGTIEN, G. LINSS Journal: Measurement [Journal] // Measurement. - Measurement science and education in the Internet era: [s.n.], Feb 2007. - pp. 107-108: Vol. 40. ISSN 0263-2241

[77] PAVEL RIPKA., ALOIS TIPEK Modern Sensors Handbook [Book]. - UK, USA: ISTE Ltd,, 2007. - pp. 477-510 ISBN 978-1-905209-66-8.

[78] RAMÓN PALLÁS-ARENY., JOHN G. WEBSTER Sensors and Signal Conditioning, Second Ed [Book]. - USA: Wiley&Sons, 2001. - pp. 1-498 ISBN: 0-471-33232-1.

[79] RANDY FRANK Understanding Smart Sensors, Second Ed [Book]. - Norwood: Artech house, Inc,, 2000. - pp. 17-223 ISBN 1-58053-398-1.

[80] RAPPAPORT, T.S Wireless Communications Principles and Practice, Second Ed [Book]. - Upper Saddle River,NJ: Prentice-Hall , 2002. - pp. 161–166. ISBN: 0130422320.

[81] REZAZADEH, G., LOTFIANI, A., KHALILARYA, SH On the modeling of a MEMS based capacitive wall shear stress sensor. [Journal] // Measurement. - Measurement: Elsevier, Feb 2009. - pp. 202-207: Vol. 42. ISSN: 0263-2241

[82] RICHARD C.DORF The Electrical Engineering Handbook, Second Ed [Book]. - Boca Raton: CRC Press LLC, 2000. - pp. 3.1, 14-21, 35-41 ISBN: 978-1-4200-4976-3.

[83] ROBERT B. ANGUS., THOMAS E. HULBERT VEE Pro: Practical Graphical Programming [Book]. - Baston MA: Springer, Dec 2004. - pp. 1-448 ISBN 978-1852338701.

[84] ROLAND S.BURNS Advanced control engineering, First Ed [Book]. - Weburn: Butterworth-Heinemann, Nov 2001. - pp. 13-60 ISBN-13: 978-0750651004.

[85] SALIM AHMED., BIAO HUANG., SIRISH L SHAN Novel identification method from step response [Journal]. - Control Engineering Practice: Elsevier, May 2007. - pp. 545-556: Vol. 15. ISSN: 0967-0661

[86] SAMMARCO, J. J, PADOCK, R., FRIES, E. F., KARRA, V. K NOISH [Online] // A Technology review of Smart Sensors with Wireless Networks for Application in hazardous Work Environments. 2009. - http://www.cdc.gov/niosh/mining/pubs/pubreference/outputid2307.htm.

[87] SARKAR, T.K., ZHONG JI., KYUNGJUNG KIM., MEDOURI, A. SALAZAR-PALMA, M A Survey of Various Propagation Models for Mobile Communication [Journal] // Antennas and Propagations Magazine, IEEE. - IEEE Antennas and Propagation Magazine: IEEE, Jun 2003. - pp. 51-82: Vol. 45. ISSN: 1045-9243

[88] SEICULESCU, C., LIE, I., GONTEAN, A Wireless communication techniques for home automation sensors [Journal] // WSEAS. CIMMACS-6. [s.l.]: WSEAS. CIMMACS.6, Dec. 2007. - pp. 151-155 ISSN: 1790-5117 ISBN: 978-960-6766-25-1.

[89] SENSORS POLLS AND SURVEYS 2006/2007 HTTP://WWW.SENSORSPORTAL.COM/HTML/POLLS.HTM

[90] SHAO LICHUN., MOORTHI PALANIAPAN., TAN WOEI WAN A continuous-time capacitance to voltage converter for micro-capacitive pressure sensors [Journal] // Journal of Physics: Conference Series 34. - Journal of Physics: Conference Series: IOP Publishing Ltd May 2006. - pp. 1014-1019: Vol. 34. ISSN 1742-6596

[91] SHU-PARK CHAN The Electrical Engineering Handbook, Second Ed [Book]. - Boca Raton: CRC Press LLC, Sep 1997. - pp. 1-150 ISBN: 978-1-4200-4976-3.

[92] STAMPFER, C., GÜTTINGER, J., ROMAN, C., JUNGEN, A., HELBLING, T., HIEROLD, C Electron Shuttle Instability for Nano Electro Mechanical Mass Sensins [Journal] // Nano letters. - Nano Letters: [s.n.], Aug 2007. - pp. 2747-2752: Vol. 7. ISSN:1530-6984

[93] STEVEN W.SMITH www.dspguide.com [Online]. - Feb 20, 2011. - http://www.dspguide.com/.

[94] SUZANNE CASTRUP Comparison of Methods for Establishing Confidence Limits and Expanded Uncertainties [Journal] // Measurement Science Conference. - Proc. of 2010 Measurement Science Conference: Pasadena, CA, Mar 2010. - pp. 1-23.

[95] TEXAS INSTRUMENTS www.ti.com [Online]. - Feb 25, 2011. - http://www.ti.com/.

[96] TOPOLNICKI, J., SKOCZYLAS, N Low cost dislocation sensor with differential capacitor. [Journal] // Sensors and Actuators.. - Sensors and Actuators A: Physical: Elsevier, Nov 2007. - pp. 139-144: Vol. 140. ISSN: 0924-4247

[97] TUMANSKI, S Principle of Electrical Measurement, Sensors Series [Book]. - USA: CRC Press. Taylor&Francis Group, 2006. - pp. 13-40, 73-431 ISBN: 0-7503-1038-3.

[98] VIRENDRA KUMAR Digital electronics Theory and Experiment [Book]. - New Delhi: New Age International, 2006. - pp. 1-230 ISBN: 81-224-1346-3.

[99] WEEKS MICHAEL Digital Signal Processing Using MATLAB and Wavelets [Book]. - Hingham, Massachusetts: Infinity Science Press LLC, 2007. - pp. 1-130 ISBN 0-9778582-0-0.

[100] WILLIAM C.DUNN Fundamentals of Industrial Instrumentation and Process Control [Book]. - USA: McGraw-Hill Companies, Inc, 2005. - pp. 1-250 ISBN: 0-07-145735-6.

[101] WILLIAM C.STONE Non Line of Sight (NLS) Construction Metrology [Report]. - Gaithersburg: NIST Construction Automation Program Report No.1, Feb. 1996.

[102] WILLIAM C. STONE Electromagnetic Signal Attenuation in Construction Materials [Report]. - Gaithersburg: NIST Construction Automation Program Report No. 3, October 1997.

[103] YIZHU SHEN., CHOI LOOK LAW., WENBIN DOU Ultra-Wideband Measurement of the Dielectric Constant and Loss Tangent of Concrete Slabs [Journal] // Microwave Conference, 2008 China-Japan Joint. - China-Japan Joint Microwave Conference: IEEE, Sep 2008. - pp. 537-540 ISBN: 978-1-4244-3821-1.

[104] ZUZULKA, F., VRBA, R., BRADAC, Z Wireless networked single sensors [Journal] // WSEAS Trans.on Electronics. - WSEAS Trans.on Electronics: WSEAS, 2004. - pp. 151-155: Vol. 2. ISSN: 1109- 9445.

CURRICULUM VITAE

Personal information	
First name(s) / Surname(s)	**Tumenbayar Lkhagvatseren**
Address	Nam. T.G.M-3050, 00420 Zlin (Czech Republic)
Telephone(s)	576035125: 722784040
E-mail(s)	lkhagvatseren@fai.utb.cz
Nationality	Mongolian
Date of birth, Gender, Marital	19 Oct 82, Male, Married
Work experience	
Dates	1 Feb 05 - 25 Jan 06
Occupation or position held	Electrical technician
Main activities and responsibilities	Troubleshoot the mechanical, hydraulic, especially electrical problems and fix for Caterpillar techniques
Name and address of employer	Wagner Asia Equipment LLC Bayangol District, Dund Gol – 46, Wagner Asia Bldg, P.O.Box – 26, 00976 Ulaanbaatar - 211121 (Mongolia)
Type of business or sector	Mining equipment Service, Sell, and Rental
Education and training	
Dates	01/09/1990 - 30/07/1999
Title of qualification awarded	Secondary education
Principal subjects / occupational skills covered	Comprehensive learning in preparation for higher education or vocational schooling
Name and type of organization providing education and training	Tuv Province 1st school (Secondary school) 00976-01272 Tuv (Mongolian)
Dates	01/09/1999 - 25/07/2003
Title of qualification awarded	Mining Electrical Engineering
Principal subjects / occupational skills covered	Transmission and distribution, substations, transformers, and mining machinery.
Dates	01/09/2003 - 25/07/2005
Title of qualification awarded	Mining Electrical Engineering Master of Engineering
Principal subjects / occupational skills covered	Open pit mines, prospecting and site analysis equipment, environmental and safety systems, mine equipment, facilities and logistics.

Name and type of organization providing education and training	Mongolian University of Science and Technology Baga toiruu, Sukhbaatar district, 00976-46520 Ulaanbaatar Mongolia
Dates	17/09/2007 →
Title of qualification awarded	PhD Student
Name and type of organization providing education and training	Tomas Bata University Nad Stráněmi 4511, 760 05 Zlin (Czech Republic)
Level in international classification	ISCED 5

Personal skills and competences

Mother tongue(s) **Mongolian**

Other language(s)

Self-assessment	**Understanding**		**Speaking**		**Writing**
European level (*)	Listening	Reading	Interaction	Production	
English	C1	C1	C1	C1	C1
Russian	B1	B1	B1	B1	B1
Czech	A2	A2	A1	A1	A1

(*) Common European Framework of Reference (CEF) level

Social skills and competences	Fine with multicultural environments; Pleasant experience with team management and sports activity; gained through my study experience abroad
Technical skills and competences	Good ability of troubleshooting typical mechanical, hydraulic, as well as electrical problems of mining equipment and machinery. Studied Measurement system
Computer skills and competences	Good command of Microsoft office, CorelDraw Partly Matlab, Labview, SPSS
Annexes	Assoc. Prof. Ing.František Hruška, Ph.D. Fakulta aplikované informatiky Univerzita Tomáše Bati ve Zlíně Nad Stráněmi 4511,760 05 Zlín Tel. 00420 576 035 246 email: hruska@fai.utb.cz

APPENDIX A

F_x Model Summary				
Model	R	R^2	Adjusted R^2	SD Error of the Estimate
F_x vs Raw value $F_y = 0$	0.981	0.961	0.952	2.100
F_x vs Raw value $F_y = 3.96$	0.979	0.959	0.949	2.169
F_x vs Raw value $F_y = 9.25$	0.981	0.962	0.953	2.074
F_x vs Raw value $F_y = 14.54$	0.981	0.962	0.953	2.080
F_x vs Raw value $F_y = 19.83$	0.981	0.963	0.953	2066
F_x vs Raw value $F_y = 25.13$	0.981	0.963	0.953	2.066
F_y Model Summary				
F_y vs Raw value $F_x = 0$	0.999	0.997	0.996	0.579
F_y vs Raw value $F_x = 3.72$	0.999	0.997	0.996	0.579
F_y vs Raw value $F_x = 8.37$	0.998	0.996	0.995	0.664
F_y vs Raw value $F_x = 13.95$	0.998	0.996	0.995	0.656
F_y vs Raw value $F_y = 19.53$	0.998	0.996	0.995	0.671
F_y vs Raw value $F_y = 25.11$	0.998	0.996	0.995	0.664

APPENDIX B

Floor plan of room 306

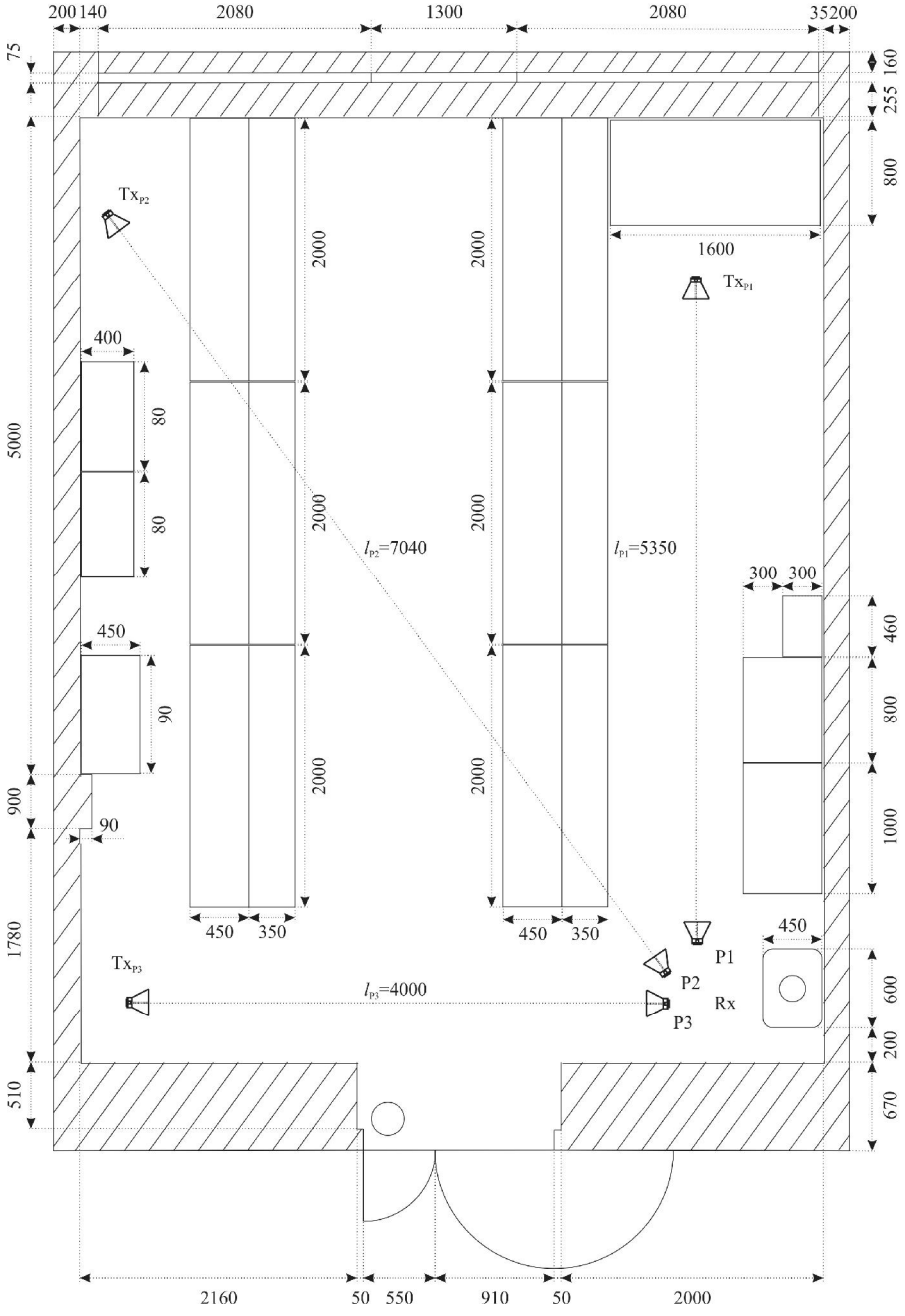

APPENDIX C

Floor plan of room 309

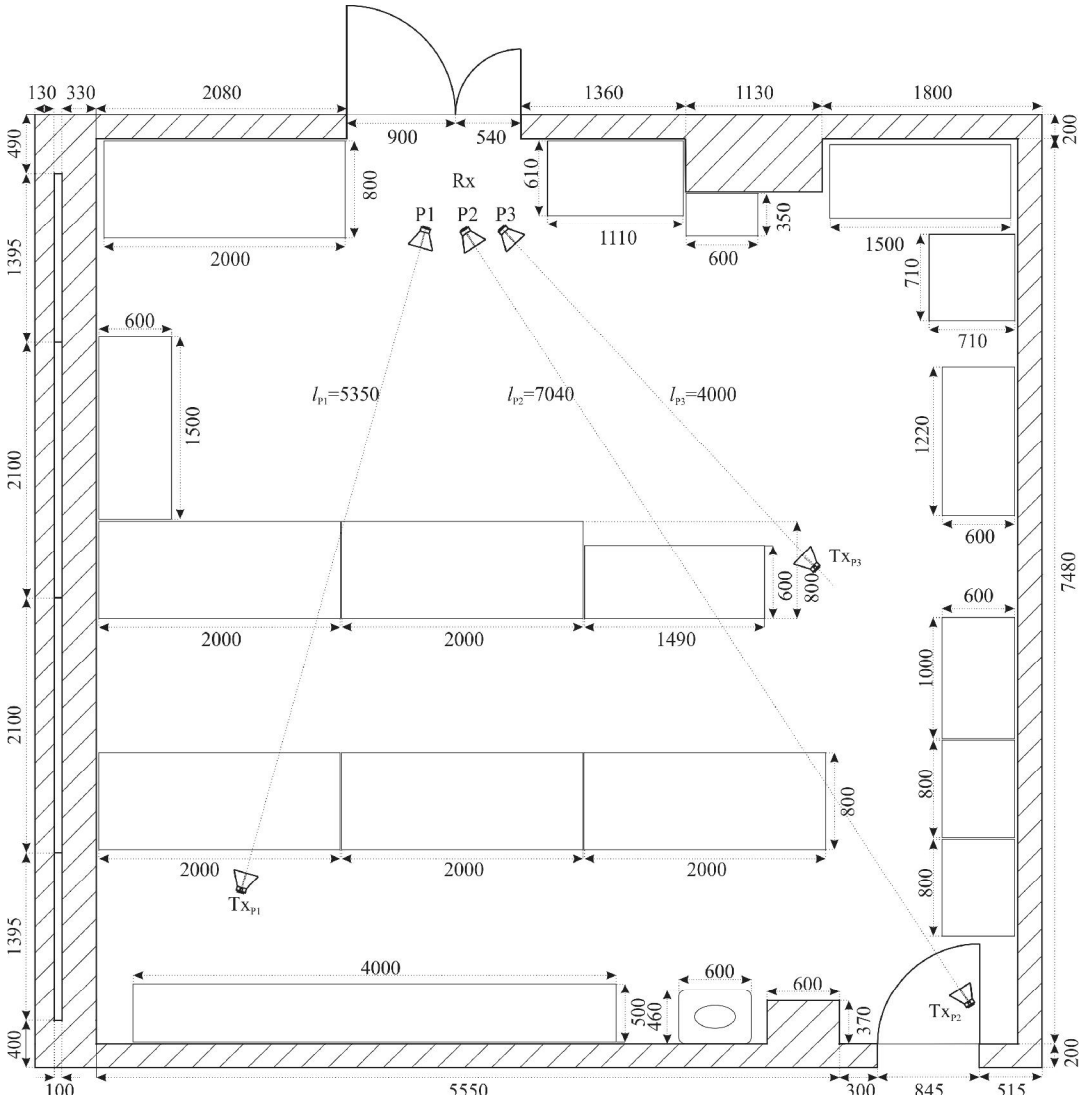

APPENDIX D

Floor plan of Industrial hall 107

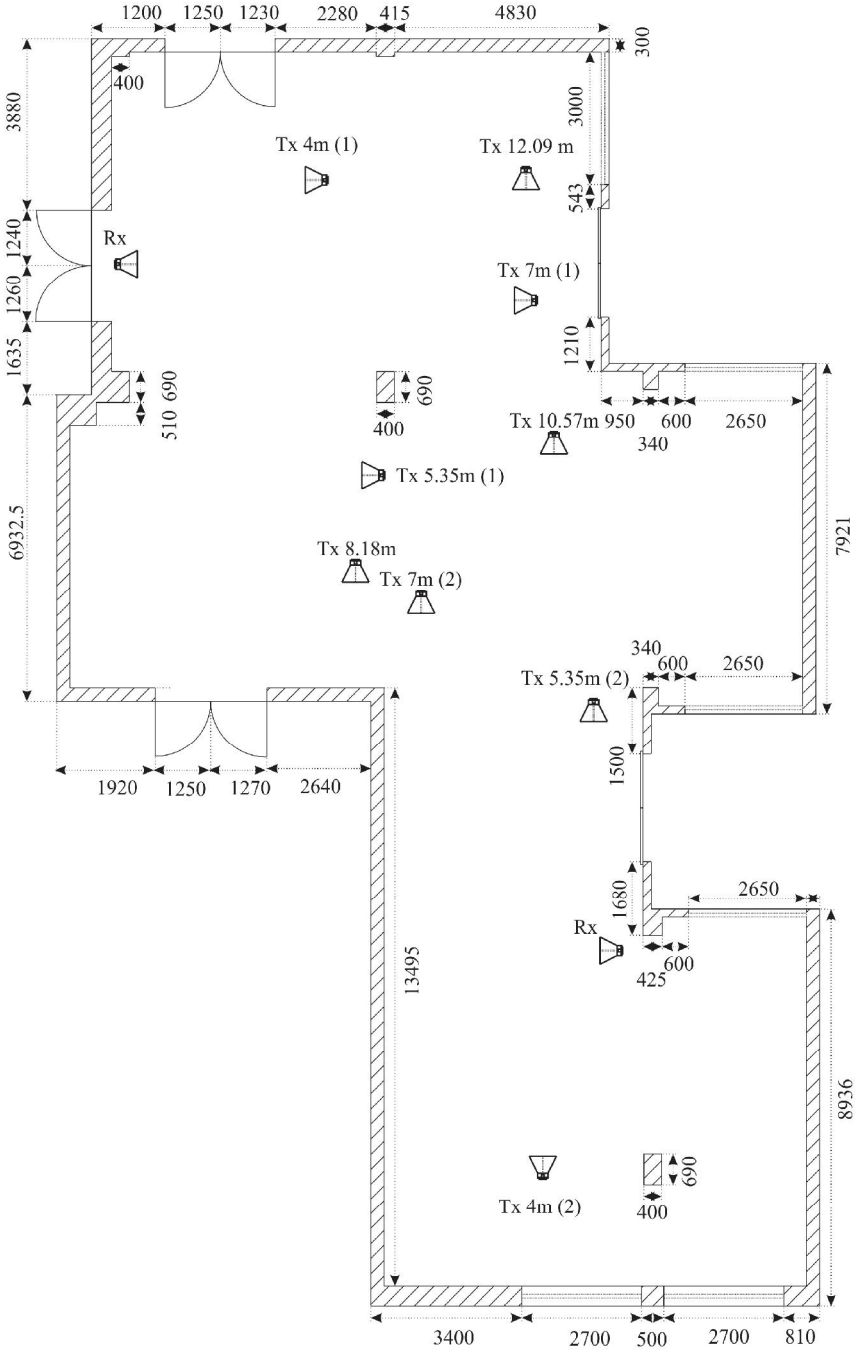

APPENDIX E

Floor plan of Corridors

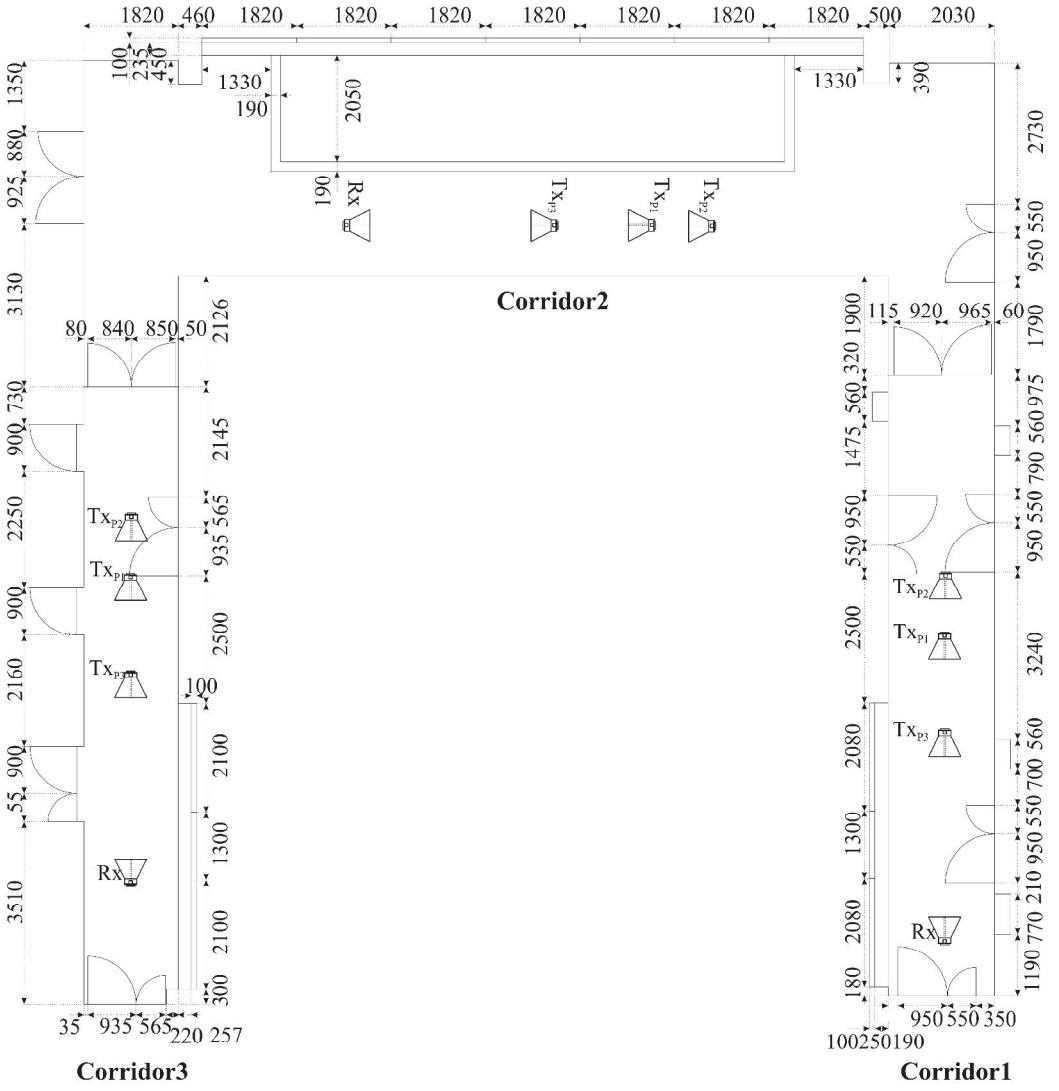

APPENDIX F

Corridor 1 Path loss evaluation, dB									
	4 m			5.35 m			7 m		
F, GHz	Mean	SD	Mean ε	Mean	SD	Mean ε	Mean	SD	Mean ε
1.0	51.126	0.474	0.212	60.848	0.062	0.028	65.320	0.030	0.020
1.1	51.882	0.122	0.054	59.600	0.079	0.035	60.070	0.160	0.070
1.2	52.222	0.179	0.080	50.292	0.158	0.071	62.410	0.210	0.100
1.3	52.598	0.095	0.042	54.652	0.085	0.038	55.890	0.120	0.050
1.4	61.480	0.028	0.013	49.852	0.174	0.078	50.900	0.380	0.170
1.5	63.938	0.026	0.012	54.620	0.203	0.091	58.900	0.070	0.030
1.6	60.132	0.019	0.009	51.896	0.154	0.069	62.220	0.040	0.020
1.7	43.954	0.176	0.079	53.880	0.156	0.070	59.070	0.110	0.050
1.8	55.722	0.133	0.060	54.536	0.113	0.050	55.250	0.170	0.080
1.9	55.992	0.124	0.055	56.984	0.056	0.025	56.690	0.130	0.060
2.0	54.828	0.238	0.107	57.508	0.064	0.029	55.350	0.260	0.120
2.1	35.908	0.444	0.198	55.248	0.059	0.026	45.500	0.180	0.080
2.2	53.300	0.365	0.163	51.414	0.149	0.067	54.970	0.200	0.090
2.3	58.872	0.147	0.066	51.552	0.259	0.116	60.240	0.050	0.020
2.4	56.410	0.048	0.022	52.136	0.092	0.041	57.710	0.120	0.050
2.5	47.892	0.099	0.044	43.612	0.107	0.048	49.840	0.150	0.070
2.6	49.952	0.026	0.012	41.458	0.285	0.127	51.320	0.210	0.090
2.7	52.330	0.064	0.028	44.682	0.370	0.166	51.540	0.160	0.070
2.8	55.370	0.074	0.033	45.632	0.130	0.058	40.970	0.220	0.100
2.9	45.990	0.060	0.027	46.268	0.084	0.038	51.310	0.220	0.100
3.0	22.236	5.364	2.399	41.432	0.106	0.047	48.790	0.210	0.090
3.1	43.860	0.064	0.029	43.622	0.128	0.057	48.120	0.120	0.050
3.2	45.100	0.074	0.033	41.852	0.194	0.087	44.060	0.250	0.110
3.3	25.748	2.839	1.269	42.436	0.215	0.096	44.170	0.180	0.080
3.4	46.786	0.072	0.032	41.340	0.162	0.072	42.540	0.230	0.100
3.5	49.404	0.075	0.034	43.936	0.194	0.087	41.100	0.530	0.240
3.6	46.520	0.111	0.050	42.144	0.143	0.064	45.800	0.210	0.100
3.7	39.978	0.209	0.094	38.652	0.143	0.064	48.310	0.070	0.030
3.8	37.888	0.338	0.151	34.648	0.229	0.103	45.680	0.080	0.030
3.9	41.348	0.343	0.153	21.554	4.987	2.230	37.360	0.480	0.220
4.0	38.760	0.473	0.211	32.674	1.533	0.686	43.590	0.110	0.050
4.1	28.728	0.967	0.433	31.652	0.448	0.200	37.740	0.580	0.260
4.2	43.448	0.329	0.147	37.944	0.072	0.032	43.400	0.310	0.140

4.3	43.790	0.225	0.101	43.062	0.173	0.077	45.800	0.070	0.030
4.4	44.490	0.307	0.137	42.808	0.215	0.096	46.830	0.210	0.090
4.5	40.250	0.316	0.141	42.366	0.151	0.068	42.130	0.190	0.080
4.6	39.598	0.254	0.113	44.050	0.096	0.043	41.630	0.170	0.080
4.7	43.642	0.300	0.134	41.766	0.042	0.019	41.360	0.240	0.110
4.8	44.088	0.329	0.147	41.440	0.173	0.077	39.470	0.330	0.150
4.9	38.630	0.394	0.176	36.898	0.162	0.072	40.110	0.200	0.090
5.0	25.454	2.094	0.937	29.990	0.222	0.099	42.840	0.170	0.080
5.1	39.026	0.264	0.118	34.776	0.404	0.181	44.300	0.110	0.050
5.2	40.192	0.359	0.161	32.568	0.465	0.208	41.380	0.050	0.020
5.3	36.304	0.313	0.140	17.646	6.773	3.029	40.290	0.070	0.030
5.4	37.504	0.257	0.115	35.598	0.539	0.241	39.110	0.060	0.030
5.5	41.380	0.553	0.247	35.072	0.166	0.074	36.540	0.310	0.140
5.6	40.242	0.521	0.233	36.100	0.164	0.073	39.380	0.340	0.150
5.7	38.284	0.410	0.184	35.576	0.279	0.125	42.060	0.060	0.020
5.8	37.782	0.569	0.255	37.734	0.244	0.109	41.820	0.240	0.110
5.9	36.702	0.397	0.178	39.982	0.258	0.116	40.060	0.150	0.070
6.0	37.480	0.537	0.240	38.360	0.234	0.105	38.340	0.320	0.140
6.1	33.170	0.716	0.320	39.978	0.588	0.263	37.830	0.370	0.170
6.2	31.498	0.795	0.355	36.828	0.144	0.065	37.440	0.100	0.050
6.3	34.492	1.303	0.583	37.072	1.213	0.543	39.220	0.100	0.050
6.4	37.462	0.541	0.242	31.410	0.311	0.139	40.340	0.110	0.050
6.5	37.636	0.481	0.215	20.392	3.230	1.445	38.700	0.080	0.040
6.6	37.868	0.367	0.164	28.038	0.153	0.068	38.540	0.150	0.070
6.7	36.458	0.509	0.228	29.652	1.406	0.629	36.740	0.290	0.130
6.8	36.378	0.172	0.077	30.624	0.382	0.171	36.930	0.210	0.090
6.9	37.012	0.331	0.148	33.110	0.733	0.328	37.360	0.180	0.080
7.0	36.870	0.290	0.130	38.384	0.468	0.209	39.010	0.290	0.130
7.1	32.550	0.302	0.135	36.542	0.924	0.413	38.160	0.060	0.030
7.2	32.044	0.668	0.299	33.038	0.741	0.331	38.220	0.190	0.090
7.3	29.312	0.174	0.078	35.364	0.218	0.098	36.990	0.170	0.080
7.4	31.586	1.863	0.833	36.278	0.182	0.082	35.550	0.230	0.100
7.5	34.486	1.272	0.569	34.752	1.380	0.617	34.710	0.480	0.220
7.6	35.328	0.669	0.299	31.092	0.982	0.439	33.490	0.520	0.230
7.7	34.722	0.529	0.236	25.626	1.566	0.700	36.570	0.180	0.080
7.8	36.978	0.841	0.376	26.342	0.875	0.391	36.460	0.090	0.040
7.9	36.168	0.484	0.216	30.078	0.806	0.361	36.980	0.320	0.140
8.0	32.096	0.343	0.154	28.506	0.208	0.093	34.690	0.370	0.160

APPENDIX G

Corridor 2 Path loss evaluation, dB									
	4 m			5.35 m			7 m		
F, GHz	Mean	SD	Mean ε	Mean	SD	Mean ε	Mean	SD	Mean ε
1.0	59.441	2.924	1.307	60.311	0.122	0.055	62.428	0.087	0.039
1.1	58.932	0.713	0.319	59.850	0.029	0.013	58.548	0.055	0.025
1.2	61.584	0.676	0.302	53.344	0.083	0.037	49.527	0.362	0.162
1.3	56.938	1.348	0.603	56.960	0.090	0.040	52.860	0.102	0.045
1.4	53.404	1.725	0.771	53.951	0.023	0.010	55.997	0.064	0.029
1.5	58.188	0.351	0.157	44.232	0.750	0.335	59.668	0.064	0.029
1.6	59.295	1.691	0.756	51.267	0.092	0.041	59.930	0.022	0.010
1.7	58.395	0.357	0.160	49.593	0.178	0.079	54.553	0.137	0.061
1.8	56.064	0.315	0.141	42.845	0.114	0.051	48.763	0.129	0.058
1.9	53.227	1.715	0.767	53.225	0.035	0.016	53.025	0.096	0.043
2.0	54.278	0.523	0.234	56.448	0.137	0.061	49.786	0.301	0.134
2.1	54.087	4.767	2.132	52.930	0.052	0.023	55.529	0.035	0.015
2.2	58.448	1.231	0.550	43.114	0.627	0.281	55.706	0.104	0.046
2.3	56.933	1.854	0.829	45.984	0.216	0.096	54.306	0.017	0.007
2.4	52.351	3.332	1.490	50.843	0.082	0.037	49.439	0.091	0.041
2.5	50.433	0.133	0.059	45.754	0.046	0.020	46.308	0.124	0.055
2.6	50.050	0.499	0.223	48.170	0.078	0.035	45.464	0.104	0.046
2.7	52.552	0.462	0.207	49.129	0.140	0.063	51.329	0.100	0.045
2.8	49.851	5.028	2.248	49.607	0.160	0.071	51.852	0.066	0.030
2.9	50.515	0.457	0.205	48.063	0.143	0.064	49.537	0.081	0.036
3.0	43.361	2.980	1.333	39.487	0.144	0.064	41.614	0.101	0.045
3.1	44.868	1.583	0.708	31.054	0.572	0.256	36.855	0.427	0.191
3.2	45.489	0.569	0.255	34.402	0.337	0.151	40.406	0.089	0.040
3.3	44.939	0.811	0.363	41.235	0.144	0.065	43.355	0.063	0.028
3.4	41.239	0.833	0.372	44.379	0.094	0.042	44.648	0.125	0.056
3.5	43.052	1.662	0.743	42.994	0.157	0.070	44.964	0.076	0.034
3.6	46.068	0.277	0.124	43.188	0.133	0.060	43.203	0.155	0.069
3.7	45.370	1.684	0.753	41.621	0.061	0.027	34.502	0.073	0.033
3.8	41.580	2.573	1.151	32.421	0.209	0.093	39.737	0.186	0.083
3.9	40.059	1.321	0.591	33.367	0.181	0.081	44.452	0.033	0.015
4.0	42.919	0.218	0.097	38.248	0.087	0.039	43.978	0.045	0.020
4.1	44.210	4.395	1.966	42.445	0.032	0.014	43.135	0.220	0.098
4.2	43.997	0.495	0.221	42.463	0.173	0.077	40.999	0.128	0.057

4.3	41.182	2.800	1.252	39.404	0.061	0.027	36.308	0.136	0.061
4.4	41.768	2.590	1.158	39.548	0.085	0.038	39.416	0.155	0.069
4.5	42.679	0.151	0.068	33.425	0.408	0.183	39.220	0.205	0.092
4.6	43.626	0.815	0.364	33.741	0.251	0.112	41.789	0.133	0.059
4.7	41.840	0.468	0.209	37.280	0.146	0.065	41.812	0.114	0.051
4.8	40.643	0.988	0.442	38.907	0.048	0.021	40.236	0.169	0.075
4.9	41.082	0.293	0.131	37.280	0.171	0.077	35.809	0.103	0.046
5.0	41.664	0.819	0.366	37.952	0.107	0.048	38.744	0.158	0.071
5.1	43.259	0.339	0.152	37.270	0.094	0.042	40.415	0.128	0.057
5.2	41.839	0.103	0.046	40.117	0.090	0.040	38.324	0.060	0.027
5.3	39.430	0.214	0.096	34.773	0.414	0.185	40.865	0.040	0.018
5.4	38.775	0.275	0.123	28.213	0.984	0.440	39.438	0.022	0.010
5.5	39.603	2.016	0.901	34.104	0.200	0.089	34.102	0.046	0.021
5.6	40.209	0.138	0.062	34.499	0.398	0.178	32.954	0.659	0.295
5.7	41.576	0.776	0.347	37.181	0.241	0.108	37.114	0.326	0.146
5.8	41.348	0.891	0.399	38.307	0.286	0.128	38.904	0.171	0.076
5.9	39.795	0.460	0.206	38.416	0.253	0.113	38.656	0.624	0.279
6.0	39.155	0.417	0.186	33.989	0.197	0.088	37.482	0.126	0.056
6.1	40.523	1.109	0.496	31.816	0.446	0.200	37.850	0.471	0.211
6.2	40.285	0.974	0.435	29.068	0.238	0.106	35.779	0.684	0.306
6.3	38.190	1.021	0.457	32.678	0.200	0.090	33.139	1.144	0.511
6.4	40.031	0.529	0.236	35.197	0.463	0.207	38.839	0.205	0.092
6.5	38.288	0.197	0.088	35.081	0.052	0.023	36.326	0.148	0.066
6.6	39.240	0.424	0.190	34.923	0.128	0.057	36.005	0.233	0.104
6.7	36.927	0.259	0.116	32.695	0.206	0.092	35.278	0.130	0.058
6.8	37.512	0.397	0.178	33.398	0.082	0.037	32.469	0.390	0.174
6.9	38.152	0.446	0.200	35.867	0.314	0.140	36.639	0.550	0.246
7.0	38.155	0.429	0.192	30.958	0.170	0.076	36.455	0.075	0.034
7.1	37.584	0.660	0.295	25.329	1.858	0.831	34.499	0.804	0.359
7.2	37.216	0.510	0.228	32.956	0.359	0.160	33.796	0.059	0.027
7.3	36.277	0.698	0.312	35.025	0.398	0.178	35.785	0.272	0.122
7.4	36.023	0.459	0.205	34.694	0.356	0.159	32.041	0.389	0.174
7.5	36.620	0.897	0.401	30.858	0.276	0.123	32.534	0.946	0.423
7.6	36.585	1.198	0.536	31.701	1.214	0.543	35.108	0.224	0.100
7.7	36.840	0.211	0.094	30.827	0.553	0.247	33.872	0.202	0.091
7.8	37.549	0.363	0.162	29.297	0.184	0.082	34.207	0.346	0.155
7.9	37.172	0.621	0.278	31.719	0.164	0.074	34.317	0.144	0.064
8.0	35.252	0.288	0.129	31.905	0.410	0.183	30.993	0.054	0.024

APPENDIX H

Corridor 3 Path loss evaluation, dB									
	4 m			5.35 m			7 m		
F, GHz	Mean	SD	Mean ε	Mean	SD	Mean ε	Mean	SD	Mean ε
1.0	52.815	4.780	2.138	58.611	0.143	0.064	63.159	0.043	0.019
1.1	51.113	4.323	1.933	58.098	0.133	0.059	59.211	0.126	0.057
1.2	55.226	6.384	2.855	42.097	0.424	0.190	58.030	0.093	0.042
1.3	56.465	4.166	1.863	48.666	0.304	0.136	60.109	0.045	0.020
1.4	56.666	4.767	2.132	47.800	0.564	0.252	57.105	0.025	0.011
1.5	61.681	5.231	2.339	52.848	0.188	0.084	61.463	0.118	0.053
1.6	61.075	2.298	1.028	56.108	0.145	0.065	59.490	0.075	0.033
1.7	55.913	2.626	1.175	50.682	0.089	0.040	56.409	0.055	0.025
1.8	55.863	2.697	1.206	51.042	0.410	0.183	55.935	0.079	0.035
1.9	44.813	3.815	1.706	50.919	0.100	0.045	52.776	0.058	0.026
2.0	40.809	5.776	2.583	51.369	0.129	0.058	52.087	0.066	0.029
2.1	47.553	0.760	0.340	49.438	0.172	0.077	51.771	0.014	0.006
2.2	50.652	0.844	0.378	48.472	0.280	0.125	59.181	0.017	0.007
2.3	52.452	3.518	1.573	47.075	0.354	0.158	58.295	0.071	0.032
2.4	55.787	0.820	0.367	54.797	0.049	0.022	59.359	0.035	0.016
2.5	51.060	1.400	0.626	49.208	0.034	0.015	52.212	0.067	0.030
2.6	49.242	0.624	0.279	47.540	0.082	0.037	49.211	0.035	0.016
2.7	51.472	0.357	0.160	51.872	0.018	0.008	44.620	0.085	0.038
2.8	48.490	2.002	0.895	52.806	0.007	0.003	45.104	0.212	0.095
2.9	46.310	2.054	0.919	50.256	0.078	0.035	49.666	0.036	0.016
3.0	36.366	4.080	1.825	43.258	0.091	0.041	46.511	0.056	0.025
3.1	40.207	1.373	0.614	42.614	0.077	0.034	46.721	0.118	0.053
3.2	38.760	4.635	2.073	31.800	0.321	0.144	47.457	0.410	0.183
3.3	40.543	2.523	1.128	37.102	0.373	0.167	47.878	0.247	0.110
3.4	45.033	6.340	2.835	33.799	0.214	0.096	44.817	0.352	0.157
3.5	41.324	3.547	1.586	35.534	0.229	0.102	37.932	0.230	0.103
3.6	39.062	4.572	2.045	31.386	0.436	0.195	34.597	0.202	0.090
3.7	40.301	0.620	0.277	39.184	0.229	0.103	41.576	0.082	0.037
3.8	38.162	2.495	1.116	42.728	0.030	0.013	44.941	0.085	0.038
3.9	40.354	1.573	0.703	42.946	0.178	0.080	47.818	0.059	0.027
4.0	41.071	4.099	1.833	48.089	0.057	0.025	44.349	0.128	0.057
4.1	45.662	0.492	0.220	46.205	0.059	0.026	43.606	0.155	0.069
4.2	42.043	1.344	0.601	44.395	0.034	0.015	41.525	0.136	0.061

4.3	42.114	1.490	0.666	44.652	0.133	0.060	43.894	0.120	0.054
4.4	39.881	0.847	0.379	40.525	0.090	0.040	41.148	0.076	0.034
4.5	37.976	0.558	0.249	37.287	0.159	0.071	39.872	0.153	0.069
4.6	38.229	0.887	0.397	39.606	0.150	0.067	43.600	0.107	0.048
4.7	39.599	4.386	1.961	31.979	0.298	0.133	42.785	0.122	0.054
4.8	35.873	8.154	3.647	23.758	3.365	1.505	40.049	0.100	0.045
4.9	39.371	4.726	2.114	29.534	0.361	0.161	42.495	0.095	0.042
5.0	40.984	0.274	0.123	41.016	0.065	0.029	43.683	0.068	0.030
5.1	41.051	0.344	0.154	40.719	0.072	0.032	44.305	0.087	0.039
5.2	38.961	0.185	0.083	39.075	0.070	0.031	43.660	0.135	0.060
5.3	40.228	0.921	0.412	38.833	0.072	0.032	40.728	0.122	0.055
5.4	37.475	1.001	0.448	39.930	0.163	0.073	39.579	0.171	0.076
5.5	35.921	1.427	0.638	38.126	0.065	0.029	35.416	0.253	0.113
5.6	36.043	1.980	0.886	38.888	0.321	0.144	38.910	0.175	0.078
5.7	37.363	1.116	0.499	40.280	0.078	0.035	42.533	0.062	0.028
5.8	34.122	3.296	1.474	39.637	0.190	0.085	42.983	0.077	0.034
5.9	39.232	2.229	0.997	33.574	0.578	0.258	43.584	0.027	0.012
6.0	40.099	2.357	1.054	35.872	0.466	0.209	41.667	0.525	0.235
6.1	38.486	2.699	1.207	33.403	0.683	0.305	39.623	0.217	0.097
6.2	38.866	1.908	0.853	36.058	0.747	0.334	37.083	0.227	0.101
6.3	38.662	1.382	0.618	37.580	1.416	0.633	36.894	0.513	0.229
6.4	36.591	0.678	0.303	35.802	0.136	0.061	37.038	0.075	0.033
6.5	29.142	0.976	0.436	31.029	0.490	0.219	37.171	0.512	0.229
6.6	32.234	4.736	2.118	25.204	2.322	1.038	40.030	0.306	0.137
6.7	29.470	0.799	0.357	27.116	0.241	0.108	38.833	0.045	0.020
6.8	34.745	1.251	0.560	31.496	1.128	0.504	39.509	0.050	0.022
6.9	37.325	1.606	0.718	32.912	1.004	0.449	38.672	0.374	0.167
7.0	38.839	2.728	1.220	34.118	0.315	0.141	39.548	0.625	0.279
7.1	37.812	2.536	1.134	31.948	0.123	0.055	37.026	0.646	0.289
7.2	36.814	0.388	0.173	35.637	0.237	0.106	39.633	0.048	0.022
7.3	35.898	0.832	0.372	37.580	0.388	0.174	36.955	0.121	0.054
7.4	36.766	1.210	0.541	38.677	0.079	0.035	35.789	0.207	0.093
7.5	32.551	2.523	1.128	37.037	0.116	0.052	36.417	0.136	0.061
7.6	31.758	2.137	0.956	35.523	0.761	0.340	35.373	0.300	0.134
7.7	31.219	1.297	0.580	33.543	0.516	0.231	37.822	0.431	0.193
7.8	31.030	0.814	0.364	32.195	1.131	0.506	37.885	0.167	0.075
7.9	36.043	0.758	0.339	33.571	0.913	0.408	39.112	0.074	0.033
8.0	33.952	1.895	0.848	30.947	0.423	0.189	35.668	0.390	0.175

APPENDIX I

Room 309 Path loss evaluation, dB									
	4 m			5.35 m			7 m		
F, GHz	Mean	SD	Mean ε	Mean	SD	Mean ε	Mean	SD	Mean ε
1.0	51.258	2.548	1.139	59.700	1.191	0.533	61.338	1.692	0.757
1.1	52.068	0.737	0.330	61.138	0.877	0.392	60.344	1.138	0.509
1.2	59.092	2.160	0.966	54.528	2.005	0.897	54.026	0.380	0.170
1.3	55.184	0.377	0.168	52.584	0.541	0.242	57.202	0.423	0.189
1.4	48.344	2.162	0.967	49.954	0.942	0.421	47.558	1.472	0.658
1.5	44.720	0.619	0.277	50.910	2.404	1.075	55.210	1.264	0.565
1.6	48.604	1.675	0.749	52.446	2.190	0.980	55.716	0.377	0.169
1.7	32.616	5.878	2.629	50.180	2.964	1.326	55.338	0.962	0.430
1.8	42.020	0.536	0.240	51.452	0.751	0.336	54.616	0.805	0.360
1.9	39.592	1.730	0.774	51.682	1.928	0.862	56.156	0.084	0.037
2.0	41.708	1.208	0.540	53.152	1.520	0.680	55.314	1.247	0.558
2.1	47.188	2.466	1.103	53.020	0.235	0.105	56.462	0.379	0.170
2.2	47.934	0.909	0.406	52.152	1.486	0.665	54.540	0.352	0.158
2.3	47.650	0.736	0.329	52.346	1.011	0.452	56.304	0.601	0.269
2.4	47.400	0.281	0.126	49.286	2.853	1.276	56.480	0.263	0.117
2.5	46.792	0.810	0.362	46.968	2.992	1.338	53.128	0.379	0.169
2.6	46.912	0.948	0.424	46.924	2.772	1.240	49.668	0.457	0.204
2.7	46.946	0.626	0.280	49.968	1.186	0.530	50.166	0.744	0.333
2.8	51.112	0.509	0.228	51.462	1.003	0.449	51.768	0.731	0.327
2.9	49.542	0.336	0.150	49.720	1.411	0.631	51.620	0.541	0.242
3.0	43.108	1.085	0.485	45.286	0.221	0.099	41.874	0.398	0.178
3.1	44.610	0.623	0.279	45.990	0.211	0.094	40.022	1.758	0.786
3.2	43.950	0.486	0.217	41.310	0.677	0.303	44.356	0.212	0.095
3.3	42.570	0.600	0.268	43.578	1.059	0.474	41.580	1.193	0.534
3.4	45.022	0.559	0.250	44.212	1.442	0.645	42.052	0.917	0.410
3.5	46.144	0.227	0.102	41.664	0.665	0.297	42.828	0.491	0.220
3.6	44.110	0.541	0.242	42.300	1.084	0.485	43.030	3.015	1.348
3.7	41.182	0.287	0.128	43.388	1.561	0.698	40.762	0.516	0.231
3.8	41.662	0.058	0.026	42.522	3.401	1.521	41.186	1.164	0.521
3.9	42.438	0.815	0.365	42.238	3.085	1.380	43.876	0.804	0.360
4.0	41.346	0.265	0.119	40.592	2.539	1.136	42.538	1.147	0.513
4.1	39.416	0.447	0.200	44.144	2.129	0.952	43.724	0.293	0.131
4.2	40.256	1.194	0.534	42.652	3.903	1.746	43.152	0.578	0.259

4.3	39.518	0.699	0.313	40.336	2.839	1.270	41.298	1.528	0.683
4.4	39.734	0.096	0.043	39.552	5.375	2.404	42.632	0.825	0.369
4.5	41.256	0.621	0.278	42.306	4.481	2.004	40.974	0.502	0.224
4.6	40.994	0.283	0.127	40.994	3.855	1.724	43.110	0.224	0.100
4.7	42.812	0.579	0.259	40.690	2.695	1.205	42.200	0.263	0.118
4.8	43.408	1.078	0.482	40.842	2.786	1.246	41.074	0.583	0.261
4.9	42.000	0.776	0.347	41.554	3.318	1.484	39.392	0.338	0.151
5.0	40.816	0.823	0.368	39.584	3.369	1.507	41.394	0.572	0.256
5.1	39.494	0.296	0.132	39.744	3.407	1.524	41.164	0.224	0.100
5.2	37.274	0.584	0.261	38.348	3.443	1.540	41.252	0.169	0.076
5.3	39.270	0.773	0.346	41.830	2.443	1.093	41.002	0.897	0.401
5.4	37.862	0.358	0.160	41.032	1.729	0.773	39.624	0.907	0.406
5.5	37.088	0.506	0.226	39.376	3.174	1.420	40.994	0.158	0.070
5.6	35.164	0.290	0.130	39.048	1.117	0.500	40.200	0.182	0.081
5.7	34.772	0.550	0.246	38.498	0.695	0.311	39.404	0.522	0.233
5.8	34.958	1.263	0.565	40.042	0.399	0.178	38.092	1.180	0.528
5.9	36.042	0.458	0.205	37.722	0.653	0.292	39.904	0.598	0.268
6.0	33.114	0.731	0.327	38.692	0.038	0.017	40.448	1.241	0.555
6.1	29.100	3.041	1.360	39.230	0.056	0.025	40.382	0.427	0.191
6.2	31.576	0.976	0.437	39.214	0.234	0.105	39.138	0.173	0.077
6.3	30.082	1.836	0.821	36.592	0.125	0.056	39.118	0.496	0.222
6.4	29.718	0.774	0.346	37.622	0.774	0.346	40.448	0.183	0.082
6.5	29.116	0.774	0.346	34.634	1.021	0.457	37.758	0.558	0.250
6.6	28.130	2.369	1.060	36.888	0.349	0.156	35.934	0.416	0.186
6.7	28.028	0.873	0.391	34.802	0.212	0.095	36.416	0.453	0.203
6.8	29.466	1.173	0.525	35.858	0.132	0.059	38.522	0.160	0.072
6.9	30.906	1.769	0.791	36.544	0.242	0.108	37.938	0.097	0.044
7.0	30.872	1.061	0.474	39.056	1.217	0.544	37.408	0.922	0.412
7.1	26.592	0.887	0.397	37.170	0.677	0.303	37.060	0.296	0.133
7.2	27.278	0.349	0.156	33.770	0.783	0.350	38.104	0.094	0.042
7.3	29.380	0.854	0.382	35.232	0.311	0.139	37.330	0.270	0.121
7.4	29.916	1.338	0.598	37.238	1.022	0.457	37.284	0.488	0.218
7.5	24.476	1.764	0.789	36.204	0.100	0.045	35.698	0.360	0.161
7.6	24.500	1.839	0.822	35.356	0.754	0.337	34.658	0.285	0.127
7.7	28.942	0.207	0.093	35.586	0.083	0.037	38.134	0.624	0.279
7.8	29.018	1.161	0.519	36.850	0.263	0.118	36.896	0.726	0.324
7.9	27.910	0.379	0.170	36.276	1.659	0.742	36.952	0.266	0.119
8.0	25.172	1.686	0.754	33.898	1.734	0.776	37.076	0.105	0.047

APPENDIX J

Room 306 Path loss evaluation, dB									
	4 m			5.35 m			7 m		
F, GHz	Mean	SD	Mean ε	Mean	SD	Mean ε	Mean	SD	Mean ε
1.0	47.995	0.054	0.024	49.640	0.179	0.080	50.138	0.036	0.016
1.1	54.881	0.062	0.028	57.455	0.135	0.061	58.668	0.058	0.026
1.2	48.905	0.055	0.025	56.444	0.110	0.049	57.644	0.014	0.006
1.3	52.674	0.042	0.019	55.165	0.058	0.026	55.218	0.029	0.013
1.4	45.486	0.335	0.150	55.268	0.240	0.108	53.001	0.045	0.020
1.5	44.018	0.837	0.374	53.819	0.119	0.053	58.368	0.032	0.014
1.6	42.492	0.525	0.235	54.611	0.247	0.110	56.518	0.023	0.010
1.7	39.448	0.558	0.249	53.967	0.196	0.088	56.433	0.072	0.032
1.8	45.548	0.332	0.149	52.886	0.240	0.107	56.566	0.015	0.007
1.9	51.000	0.110	0.049	52.608	0.164	0.073	55.208	0.077	0.034
2.0	51.462	0.060	0.027	52.923	0.104	0.046	49.487	0.040	0.018
2.1	50.619	0.091	0.041	55.396	0.114	0.051	55.179	0.123	0.055
2.2	47.722	0.160	0.072	53.923	0.381	0.170	58.428	0.067	0.030
2.3	47.762	0.251	0.112	52.186	0.337	0.151	54.210	0.033	0.015
2.4	51.734	0.096	0.043	50.575	0.312	0.140	53.896	0.052	0.023
2.5	33.482	0.466	0.209	47.842	0.331	0.148	47.458	0.019	0.008
2.6	39.145	0.050	0.022	47.503	0.181	0.081	51.625	0.048	0.022
2.7	39.050	0.324	0.145	49.375	0.266	0.119	51.680	0.045	0.020
2.8	46.117	0.194	0.087	50.516	0.184	0.082	51.541	0.047	0.021
2.9	45.117	0.057	0.025	47.783	0.326	0.146	51.743	0.046	0.020
3.0	37.393	0.195	0.087	44.069	0.364	0.163	42.944	0.088	0.040
3.1	39.680	0.196	0.087	43.228	0.437	0.195	42.285	0.048	0.022
3.2	39.129	0.085	0.038	40.424	0.778	0.348	43.093	0.100	0.045
3.3	40.864	0.102	0.046	42.901	0.664	0.297	43.852	0.280	0.125
3.4	42.565	0.059	0.026	43.664	0.136	0.061	43.052	0.106	0.047
3.5	41.009	0.159	0.071	42.768	0.168	0.075	43.927	0.174	0.078
3.6	42.442	0.079	0.036	39.966	0.228	0.102	42.722	0.182	0.081
3.7	39.449	0.091	0.041	38.723	0.462	0.207	40.176	0.061	0.027
3.8	35.259	0.252	0.113	38.843	0.557	0.249	41.669	0.322	0.144
3.9	38.352	0.066	0.030	41.513	0.395	0.177	42.250	0.111	0.050
4.0	34.983	0.709	0.317	35.224	0.181	0.081	43.054	0.154	0.069
4.1	35.624	0.246	0.110	40.539	0.195	0.087	41.006	0.040	0.018
4.2	38.203	0.234	0.105	41.019	0.856	0.383	42.421	0.147	0.066

4.3	39.508	0.045	0.020	38.449	0.425	0.190	41.149	0.209	0.093
4.4	38.855	0.401	0.180	37.715	0.082	0.037	40.015	0.134	0.060
4.5	37.881	0.741	0.331	38.027	0.509	0.228	41.599	0.048	0.021
4.6	40.847	0.112	0.050	43.477	0.224	0.100	42.574	0.032	0.014
4.7	38.695	0.331	0.148	40.496	1.026	0.459	40.922	0.077	0.035
4.8	38.640	0.242	0.108	39.780	0.084	0.037	41.305	0.052	0.023
4.9	40.732	0.208	0.093	41.519	0.136	0.061	41.354	0.131	0.059
5.0	38.002	0.146	0.065	40.482	0.135	0.061	39.852	0.084	0.038
5.1	37.408	0.429	0.192	39.316	0.319	0.143	41.592	0.199	0.089
5.2	38.871	0.227	0.102	39.467	0.849	0.380	41.088	0.235	0.105
5.3	37.146	0.098	0.044	41.507	0.173	0.078	40.848	0.136	0.061
5.4	37.826	0.192	0.086	38.599	0.455	0.203	39.472	0.140	0.062
5.5	37.571	0.222	0.099	36.148	1.310	0.586	40.815	0.051	0.023
5.6	34.102	0.249	0.112	39.153	0.524	0.234	39.421	0.161	0.072
5.7	36.447	0.093	0.042	37.744	0.569	0.254	38.976	0.133	0.059
5.8	38.386	0.249	0.112	36.022	0.154	0.069	40.664	0.054	0.024
5.9	37.603	0.524	0.234	39.887	0.391	0.175	40.891	0.211	0.094
6.0	36.914	0.807	0.361	38.566	0.952	0.426	39.520	0.123	0.055
6.1	33.496	0.931	0.417	37.643	0.371	0.166	39.224	0.095	0.042
6.2	34.411	0.421	0.188	35.113	0.371	0.166	38.546	0.100	0.045
6.3	34.788	0.852	0.381	37.931	1.268	0.567	38.514	0.206	0.092
6.4	35.439	0.142	0.063	37.338	0.395	0.177	40.195	0.049	0.022
6.5	33.940	0.744	0.333	35.622	0.519	0.232	39.763	0.131	0.058
6.6	34.046	0.636	0.285	32.715	3.054	1.366	37.409	0.434	0.194
6.7	34.162	1.299	0.581	35.371	1.497	0.669	37.943	0.050	0.022
6.8	33.512	0.645	0.289	36.982	2.109	0.943	38.798	0.233	0.104
6.9	34.802	0.150	0.067	37.139	1.494	0.668	39.484	0.203	0.091
7.0	35.485	0.708	0.317	35.421	0.860	0.385	39.303	0.052	0.023
7.1	34.884	0.240	0.107	34.254	1.692	0.757	37.487	0.359	0.161
7.2	34.607	0.303	0.136	35.232	0.143	0.064	38.507	0.116	0.052
7.3	34.211	0.105	0.047	33.367	0.516	0.231	36.839	0.091	0.041
7.4	35.454	0.368	0.165	34.571	0.137	0.061	36.925	0.229	0.102
7.5	33.780	0.493	0.221	34.805	2.145	0.959	36.312	0.175	0.078
7.6	31.937	0.760	0.340	34.916	1.517	0.678	35.543	0.128	0.057
7.7	32.322	0.067	0.030	34.609	2.097	0.938	36.837	0.033	0.015
7.8	28.819	0.262	0.117	35.546	1.771	0.792	37.654	0.334	0.150
7.9	30.250	0.797	0.356	33.201	0.078	0.035	36.097	0.142	0.063
8.0	30.562	0.410	0.184	32.930	0.344	0.154	34.991	0.104	0.046

APPENDIX K

Uncertainty budgets for the measurement of the propagations

	Type A		Type B					U_1	U_2		Uncertainty, dB (95%)		
f, GHz	U_{Cor}	U_R	U_{LMR}	U_{UFA}	ΔU_A	U_{SMR}	U_{FSP}	U_1	U_{2C}	U_{2R}	U_{SC}	U_{SR}	U_{SZATR}
1.0	2.138	1.139	1.773	0.571	2.219	1.000	0.259	1.033	6.016	5.201	6.104	5.303	0.627
1.1	1.933	0.509	1.863	0.600	2.219	1.000	0.259	1.033	5.905	5.016	5.995	5.121	0.653
1.2	2.855	0.966	1.949	0.627	2.219	1.000	0.259	1.033	6.943	5.297	7.020	5.397	0.679
1.3	1.863	0.242	2.032	0.654	2.219	1.000	0.259	1.033	6.013	5.161	6.101	5.263	0.703
1.4	2.132	0.967	2.113	0.679	2.219	1.000	0.259	1.033	6.339	5.487	6.423	5.583	0.727
1.5	2.339	1.075	2.190	0.704	2.219	1.000	0.259	1.033	6.618	5.635	6.698	5.729	0.750
1.6	1.028	0.980	2.266	0.727	0.968	1.000	0.259	1.033	4.624	4.595	4.738	4.709	0.772
1.7	1.175	2.629	2.339	0.750	0.968	1.000	0.259	1.033	4.829	6.226	4.938	6.311	0.794
1.8	1.206	0.360	2.411	0.773	0.968	1.000	0.259	1.033	4.957	4.568	5.063	4.684	0.815
1.9	1.706	0.862	2.480	0.795	0.968	1.000	0.259	1.033	5.448	4.861	5.545	4.970	0.836
2.0	2.583	0.680	2.548	0.816	0.968	1.000	0.259	1.033	6.422	4.889	6.504	4.996	0.856
2.1	2.132	1.103	2.615	0.837	0.968	1.000	0.259	1.033	6.029	5.202	6.117	5.303	0.876
2.2	0.550	0.665	2.680	0.857	0.968	1.000	0.259	1.033	5.056	5.095	5.161	5.198	0.896
2.3	1.573	0.452	2.744	0.877	0.968	1.000	0.259	1.033	5.718	5.134	5.810	5.237	0.915
2.4	1.490	1.276	2.806	0.897	0.968	1.000	0.259	1.033	5.749	5.603	5.841	5.698	0.934
2.5	0.626	1.338	2.868	0.916	0.968	1.000	0.259	1.033	5.387	5.738	5.485	5.830	0.952
2.6	0.279	1.240	2.928	0.935	0.968	1.000	0.259	1.033	5.405	5.770	5.503	5.861	0.970
2.7	0.207	0.530	2.987	0.954	0.968	1.000	0.259	1.033	5.495	5.555	5.591	5.650	0.988
2.8	2.248	0.449	3.046	0.972	0.968	1.000	0.259	1.033	6.728	5.632	6.807	5.726	1.006
2.9	0.919	0.631	3.103	0.990	0.968	1.000	0.259	1.033	5.882	5.775	5.972	5.867	1.023

3.0	2.399	0.485	3.160	1.007	0.968	1.000	0.259	1.033	7.028	5.830	7.104	5.921	1.040
3.1	0.708	0.786	3.216	1.025	0.968	1.000	0.259	1.033	5.985	6.012	6.073	6.100	1.057
3.2	2.073	0.348	3.271	1.042	0.968	1.000	0.259	1.033	6.893	5.988	6.970	6.076	1.073
3.3	1.269	0.534	3.325	1.059	0.968	1.000	0.259	1.033	6.412	6.116	6.494	6.203	1.090
3.4	2.835	0.645	3.379	1.075	0.968	1.000	0.259	1.033	7.756	6.235	7.825	6.320	1.106
3.5	1.586	0.297	3.431	1.092	0.968	1.000	0.259	1.033	6.771	6.250	6.849	6.335	1.122
3.6	2.045	1.348	3.484	1.108	0.968	1.000	0.259	1.033	7.184	6.708	7.258	6.787	1.138
3.7	0.753	0.698	3.535	1.124	0.968	1.000	0.259	1.033	6.529	6.512	6.610	6.593	1.153
3.8	1.151	1.521	3.586	1.140	0.968	1.000	0.259	1.033	6.772	6.972	6.850	7.048	1.169
3.9	2.230	1.380	3.637	1.155	0.968	1.000	0.259	1.033	7.560	6.971	7.630	7.047	1.184
4.0	1.833	1.136	3.687	1.171	0.968	1.000	0.259	1.033	7.333	6.928	7.405	7.004	1.199
4.1	1.966	0.952	3.736	1.186	0.968	1.000	0.259	1.033	7.504	6.932	7.575	7.008	1.214
4.2	0.601	1.746	3.785	1.201	0.968	1.000	0.259	1.033	6.903	7.427	6.980	7.498	1.228
4.3	1.252	1.270	3.833	1.216	0.968	1.000	0.259	1.033	7.221	7.230	7.295	7.304	1.243
4.4	1.158	2.404	3.881	1.231	0.968	1.000	0.259	1.033	7.256	8.065	7.329	8.131	1.258
4.5	0.249	2.004	3.929	1.245	0.968	1.000	0.259	1.033	7.086	7.826	7.161	7.894	1.272
4.6	0.397	1.724	3.976	1.260	0.968	1.000	0.259	1.033	7.184	7.712	7.258	7.781	1.286
4.7	1.961	1.205	4.022	1.274	0.968	1.000	0.259	1.033	7.941	7.508	8.008	7.579	1.300
4.8	3.647	1.246	4.068	1.288	0.968	1.000	0.259	1.033	9.518	7.602	9.574	7.672	1.314
4.9	2.114	1.484	4.114	1.302	0.968	1.000	0.259	1.033	8.190	7.795	8.255	7.863	1.328
5.0	0.937	1.507	4.159	1.316	0.968	1.000	0.259	1.033	7.629	7.880	7.699	7.947	1.341
5.1	0.181	1.524	4.204	1.330	0.968	1.000	0.259	1.033	7.550	7.962	7.620	8.029	1.355
5.2	0.208	1.540	4.249	1.344	0.968	1.000	0.259	1.033	7.628	8.043	7.697	8.109	1.368
5.3	3.029	1.093	4.293	1.357	0.968	1.000	0.259	1.033	9.211	7.909	9.268	7.976	1.382
5.4	0.448	0.773	4.337	1.371	0.968	1.000	0.259	1.033	7.806	7.877	7.874	7.944	1.395

5.5	0.901	1.420	4.380	1.384	0.968	1.000	0.259	1.033	7.988	8.196	8.054	8.260	1.408
5.6	0.886	0.500	4.424	1.397	0.968	1.000	0.259	1.033	8.056	7.962	8.122	8.029	1.421
5.7	0.499	0.311	4.466	1.410	0.968	1.000	0.259	1.033	8.035	8.009	8.101	8.075	1.434
5.8	1.474	0.565	4.509	1.423	0.968	1.000	0.259	1.033	8.432	8.120	8.495	8.185	1.447
5.9	0.997	0.292	4.551	1.436	0.968	1.000	0.259	1.033	8.306	8.152	8.370	8.217	1.459
6.0	1.054	0.555	4.593	1.449	0.968	1.000	0.259	1.033	8.396	8.261	8.459	8.325	1.472
6.1	1.207	1.360	4.635	1.462	0.968	1.000	0.259	1.033	8.522	8.586	8.585	8.648	1.484
6.2	0.853	0.437	4.676	1.474	0.968	1.000	0.259	1.033	8.472	8.383	8.535	8.446	1.497
6.3	0.633	0.821	4.717	1.487	0.968	1.000	0.259	1.033	8.488	8.533	8.550	8.595	1.509
6.4	0.303	0.346	4.758	1.499	0.968	1.000	0.259	1.033	8.507	8.511	8.569	8.574	1.522
6.5	1.445	0.457	4.799	1.512	0.968	1.000	0.259	1.033	8.895	8.595	8.955	8.657	1.534
6.6	2.118	1.366	4.839	1.524	0.968	1.000	0.259	1.033	9.328	8.927	9.385	8.987	1.546
6.7	0.629	0.669	4.879	1.536	0.968	1.000	0.259	1.033	8.763	8.771	8.823	8.831	1.558
6.8	0.560	0.943	4.919	1.548	0.968	1.000	0.259	1.033	8.817	8.908	8.878	8.968	1.570
6.9	0.718	0.791	4.959	1.560	0.968	1.000	0.259	1.033	8.917	8.934	8.976	8.993	1.582
7.0	1.220	0.544	4.998	1.572	0.968	1.000	0.259	1.033	9.134	8.949	9.192	9.009	1.593
7.1	1.134	0.757	5.037	1.584	0.968	1.000	0.259	1.033	9.168	9.059	9.226	9.118	1.605
7.2	0.331	0.350	5.076	1.596	0.968	1.000	0.259	1.033	9.054	9.056	9.113	9.115	1.617
7.3	0.372	0.382	5.115	1.608	0.968	1.000	0.259	1.033	9.125	9.126	9.183	9.184	1.628
7.4	0.833	0.598	5.153	1.619	0.968	1.000	0.259	1.033	9.275	9.224	9.332	9.282	1.640
7.5	1.128	0.959	5.191	1.631	0.968	1.000	0.259	1.033	9.426	9.374	9.482	9.430	1.651
7.6	0.956	0.822	5.229	1.643	0.968	1.000	0.259	1.033	9.437	9.402	9.493	9.458	1.663
7.7	0.700	0.938	5.267	1.654	0.968	1.000	0.259	1.033	9.439	9.496	9.495	9.552	1.674
7.8	0.506	0.792	5.305	1.665	0.968	1.000	0.259	1.033	9.469	9.523	9.525	9.579	1.685
7.9	0.408	0.742	5.342	1.677	0.968	1.000	0.259	1.033	9.520	9.576	9.575	9.631	1.697
8.0	0.848	0.776	5.380	1.688	0.968	1.000	0.259	1.033	9.664	9.647	9.719	9.702	1.708

APPENDIX L

Penetration loss evaluation, dB									
	Glass door			Wooden door			Wall		
F, GHz	Mean	SD	Mean ε	Mean	SD	Mean ε	Mean	SD	Mean ε
1.0	56.117	2.383	1.066	77.146	1.044	0.467	70.998	0.765	0.342
1.1	56.631	0.076	0.034	73.070	0.408	0.183	71.852	0.065	0.029
1.2	52.621	0.749	0.335	73.136	0.088	0.040	67.308	0.188	0.084
1.3	61.153	0.831	0.372	72.436	0.287	0.128	67.408	0.458	0.205
1.4	59.066	2.291	1.025	71.742	0.083	0.037	68.480	0.392	0.175
1.5	62.981	0.342	0.153	74.348	0.776	0.347	66.546	0.254	0.114
1.6	64.372	0.098	0.044	72.238	1.531	0.685	68.618	0.438	0.196
1.7	64.323	0.977	0.437	71.540	0.962	0.430	67.370	0.326	0.146
1.8	62.150	0.437	0.196	70.930	0.225	0.101	65.044	0.468	0.210
1.9	63.183	0.048	0.021	69.442	0.139	0.062	65.028	0.219	0.098
2.0	59.692	1.718	0.768	68.580	0.789	0.353	64.236	0.998	0.446
2.1	64.293	0.374	0.167	69.350	0.304	0.136	64.360	0.805	0.360
2.2	65.942	0.085	0.038	69.586	0.181	0.081	64.102	0.570	0.255
2.3	66.117	0.102	0.046	68.626	0.119	0.053	62.768	0.745	0.333
2.4	66.489	1.127	0.504	68.350	0.204	0.091	62.334	1.015	0.454
2.5	61.372	0.539	0.241	65.382	0.138	0.062	60.114	0.490	0.219
2.6	63.662	0.416	0.186	64.180	0.170	0.076	58.360	0.433	0.194
2.7	64.485	0.543	0.243	64.818	0.194	0.087	58.952	0.116	0.052
2.8	65.510	0.306	0.137	65.980	0.212	0.095	60.720	0.565	0.253
2.9	64.363	0.567	0.254	64.106	0.155	0.069	57.944	0.494	0.221
3.0	57.231	0.089	0.040	55.880	0.098	0.044	50.590	0.049	0.022
3.1	56.775	0.348	0.155	58.320	0.399	0.178	51.374	0.328	0.147
3.2	56.669	0.105	0.047	55.750	0.269	0.120	48.978	0.944	0.422
3.3	57.086	0.498	0.223	54.288	0.185	0.083	49.196	0.272	0.122
3.4	58.319	0.171	0.077	56.742	0.123	0.055	50.434	0.232	0.104
3.5	58.976	0.125	0.056	55.900	0.120	0.054	49.376	0.447	0.200
3.6	56.309	0.064	0.028	54.938	0.104	0.046	46.054	1.682	0.752
3.7	54.926	0.115	0.051	53.220	0.554	0.248	43.904	2.414	1.080
3.8	54.241	0.051	0.023	52.894	0.352	0.158	46.494	1.353	0.605
3.9	55.873	0.189	0.085	54.930	0.474	0.212	47.552	0.905	0.405
4.0	57.377	0.145	0.065	55.848	0.449	0.201	48.438	1.284	0.574
4.1	55.996	0.863	0.386	55.602	0.325	0.145	47.288	0.494	0.221
4.2	56.503	0.169	0.076	55.618	0.074	0.033	47.888	0.105	0.047

4.3	55.560	0.354	0.158	54.652	0.263	0.118	45.246	0.466	0.208
4.4	54.418	0.540	0.242	54.112	0.137	0.061	43.002	0.909	0.407
4.5	55.436	0.035	0.016	54.408	0.114	0.051	44.870	0.509	0.228
4.6	56.517	0.659	0.295	55.752	0.093	0.041	45.320	0.109	0.049
4.7	54.580	0.954	0.427	55.474	0.273	0.122	42.988	0.302	0.135
4.8	54.322	0.075	0.034	53.922	0.213	0.095	42.736	0.232	0.104
4.9	51.046	0.618	0.276	52.958	0.170	0.076	42.962	1.969	0.881
5.0	51.618	0.559	0.250	52.824	0.056	0.025	41.930	6.026	2.695
5.1	55.722	0.192	0.086	55.436	0.203	0.091	45.840	8.698	3.890
5.2	55.310	0.157	0.070	55.328	0.122	0.055	45.686	6.745	3.017
5.3	51.578	0.858	0.384	53.668	0.065	0.029	42.680	7.424	3.320
5.4	48.870	0.968	0.433	52.366	0.323	0.144	41.884	5.906	2.641
5.5	52.931	0.181	0.081	52.440	0.519	0.232	44.634	7.040	3.149
5.6	54.212	0.068	0.030	52.612	0.370	0.166	44.138	7.467	3.340
5.7	52.087	0.126	0.056	53.660	0.158	0.071	44.172	4.625	2.068
5.8	51.223	0.272	0.122	52.282	0.440	0.197	42.986	5.437	2.432
5.9	51.328	0.493	0.220	52.360	0.372	0.166	46.020	4.092	1.830
6.0	52.112	0.060	0.027	52.774	0.400	0.179	44.974	4.230	1.892
6.1	50.267	0.799	0.357	51.580	0.226	0.101	42.992	4.614	2.063
6.2	50.835	0.555	0.248	50.306	0.444	0.199	44.398	4.734	2.117
6.3	52.233	0.050	0.022	50.698	0.390	0.175	45.264	3.027	1.354
6.4	49.918	0.789	0.353	51.336	0.156	0.070	44.832	2.752	1.231
6.5	48.487	0.083	0.037	47.718	0.375	0.168	43.382	2.785	1.246
6.6	50.633	0.135	0.060	49.294	0.110	0.049	44.338	2.135	0.955
6.7	49.858	0.300	0.134	48.532	0.282	0.126	44.462	1.757	0.786
6.8	50.303	0.305	0.136	47.640	0.389	0.174	44.232	1.483	0.663
6.9	50.727	0.057	0.026	49.172	0.205	0.092	44.194	0.998	0.446
7.0	49.398	0.752	0.336	49.534	0.457	0.204	42.748	0.025	0.011
7.1	49.853	0.317	0.142	45.388	0.426	0.190	41.074	0.423	0.189
7.2	50.441	0.241	0.108	47.290	0.405	0.181	40.806	0.715	0.320
7.3	48.656	0.199	0.089	47.728	0.457	0.205	40.442	1.415	0.633
7.4	51.449	0.248	0.111	45.488	0.154	0.069	40.026	1.570	0.702
7.5	50.864	0.385	0.172	46.748	0.377	0.169	40.102	1.487	0.665
7.6	49.197	0.192	0.086	47.736	0.562	0.252	40.018	0.740	0.331
7.7	49.942	0.280	0.125	46.664	0.566	0.253	40.584	0.300	0.134
7.8	50.834	0.395	0.177	45.586	0.655	0.293	41.000	0.409	0.183
7.9	50.223	0.093	0.042	48.238	0.206	0.092	40.326	0.158	0.070
8.0	49.873	0.340	0.152	45.928	0.061	0.027	40.414	0.416	0.186

APPENDIX M

Uncertainty budgets for the measurement of the penetrations

Type A				Type B					U1	U2			Uncertainty, dB (95%)		
f, GHz	U_{GD}	U_{WD}	U_{W}	U_{LMR}	U_{UFA}	ΔU_{A}	U_{SMR}	U_{FSP}	U_{1}	U_{2GD}	U_{2WD}	U_{2W}	U_{SGD}	U_{SWD}	U_{SW}
1.0	1.066	0.467	0.342	1.773	0.571	2.219	1.000	0.259	1.033	5.158	4.903	4.874	5.260	5.010	4.982
1.1	0.034	0.183	0.029	1.863	0.600	2.219	1.000	0.259	1.033	4.944	4.953	4.944	5.050	5.059	5.050
1.2	0.335	0.040	0.084	1.949	0.627	2.219	1.000	0.259	1.033	5.076	5.045	5.047	5.180	5.150	5.151
1.3	0.372	0.128	0.205	2.032	0.654	2.219	1.000	0.259	1.033	5.182	5.149	5.156	5.284	5.252	5.259
1.4	1.025	0.037	0.175	2.113	0.679	2.219	1.000	0.259	1.033	5.516	5.244	5.252	5.612	5.345	5.352
1.5	0.153	0.347	0.114	2.190	0.704	2.219	1.000	0.259	1.033	5.347	5.372	5.344	5.446	5.470	5.443
1.6	0.044	0.685	0.196	2.266	0.727	0.968	1.000	0.259	1.033	4.293	4.443	4.305	4.416	4.561	4.427
1.7	0.437	0.430	0.146	2.339	0.750	0.968	1.000	0.259	1.033	4.472	4.470	4.419	4.590	4.588	4.538
1.8	0.196	0.101	0.210	2.411	0.773	0.968	1.000	0.259	1.033	4.540	4.532	4.542	4.657	4.648	4.658
1.9	0.021	0.062	0.098	2.480	0.795	0.968	1.000	0.259	1.033	4.643	4.644	4.646	4.756	4.757	4.759
2.0	0.768	0.353	0.446	2.548	0.816	0.968	1.000	0.259	1.033	4.925	4.791	4.813	5.032	4.901	4.922
2.1	0.167	0.136	0.360	2.615	0.837	0.968	1.000	0.259	1.033	4.872	4.870	4.901	4.981	4.978	5.009
2.2	0.038	0.081	0.255	2.680	0.857	0.968	1.000	0.259	1.033	4.972	4.974	4.990	5.079	5.080	5.096
2.3	0.046	0.053	0.333	2.744	0.877	0.968	1.000	0.259	1.033	5.078	5.079	5.108	5.182	5.183	5.212
2.4	0.504	0.091	0.454	2.806	0.897	0.968	1.000	0.259	1.033	5.250	5.184	5.237	5.350	5.286	5.338
2.5	0.241	0.062	0.219	2.868	0.916	0.968	1.000	0.259	1.033	5.299	5.285	5.297	5.399	5.385	5.397
2.6	0.186	0.076	0.194	2.928	0.935	0.968	1.000	0.259	1.033	5.394	5.386	5.395	5.492	5.484	5.493
2.7	0.243	0.087	0.052	2.987	0.954	0.968	1.000	0.259	1.033	5.499	5.486	5.485	5.595	5.582	5.581
2.8	0.137	0.095	0.253	3.046	0.972	0.968	1.000	0.259	1.033	5.586	5.584	5.598	5.681	5.679	5.692
2.9	0.254	0.069	0.221	3.103	0.990	0.968	1.000	0.259	1.033	5.694	5.679	5.690	5.787	5.772	5.783

3.0	0.040	0.044	0.022	3.160	1.007	0.968	1.000	0.259	1.033	5.773	5.774	5.773	5.865	5.865	5.865
3.1	0.155	0.178	0.147	3.216	1.025	0.968	1.000	0.259	1.033	5.873	5.874	5.872	5.963	5.965	5.962
3.2	0.047	0.120	0.422	3.271	1.042	0.968	1.000	0.259	1.033	5.960	5.963	6.001	6.049	6.052	6.089
3.3	0.223	0.083	0.122	3.325	1.059	0.968	1.000	0.259	1.033	6.062	6.053	6.054	6.150	6.140	6.142
3.4	0.077	0.055	0.104	3.379	1.075	0.968	1.000	0.259	1.033	6.143	6.142	6.144	6.229	6.228	6.230
3.5	0.056	0.054	0.200	3.431	1.092	0.968	1.000	0.259	1.033	6.231	6.231	6.240	6.316	6.316	6.325
3.6	0.028	0.046	0.752	3.484	1.108	0.968	1.000	0.259	1.033	6.319	6.319	6.443	6.403	6.403	6.525
3.7	0.051	0.248	1.080	3.535	1.124	0.968	1.000	0.259	1.033	6.407	6.420	6.656	6.490	6.502	6.735
3.8	0.023	0.158	0.605	3.586	1.140	0.968	1.000	0.259	1.033	6.493	6.498	6.571	6.574	6.580	6.652
3.9	0.085	0.212	0.405	3.637	1.155	0.968	1.000	0.259	1.033	6.580	6.588	6.613	6.660	6.668	6.693
4.0	0.065	0.201	0.574	3.687	1.171	0.968	1.000	0.259	1.033	6.664	6.671	6.731	6.743	6.751	6.810
4.1	0.386	0.145	0.221	3.736	1.186	0.968	1.000	0.259	1.033	6.777	6.751	6.757	6.856	6.829	6.835
4.2	0.076	0.033	0.047	3.785	1.201	0.968	1.000	0.259	1.033	6.831	6.830	6.830	6.908	6.907	6.908
4.3	0.158	0.118	0.208	3.833	1.216	0.968	1.000	0.259	1.033	6.917	6.914	6.920	6.993	6.991	6.997
4.4	0.242	0.061	0.407	3.881	1.231	0.968	1.000	0.259	1.033	7.005	6.994	7.026	7.081	7.070	7.102
4.5	0.016	0.051	0.228	3.929	1.245	0.968	1.000	0.259	1.033	7.074	7.074	7.084	7.149	7.149	7.159
4.6	0.295	0.041	0.049	3.976	1.260	0.968	1.000	0.259	1.033	7.171	7.154	7.154	7.245	7.228	7.228
4.7	0.427	0.122	0.135	4.022	1.274	0.968	1.000	0.259	1.033	7.268	7.236	7.237	7.341	7.309	7.310
4.8	0.034	0.095	0.104	4.068	1.288	0.968	1.000	0.259	1.033	7.312	7.313	7.314	7.384	7.386	7.386
4.9	0.276	0.076	0.881	4.114	1.302	0.968	1.000	0.259	1.033	7.404	7.391	7.535	7.476	7.462	7.605
5.0	0.250	0.025	2.695	4.159	1.316	0.968	1.000	0.259	1.033	7.479	7.467	8.720	7.550	7.538	8.781
5.1	0.086	0.091	3.890	4.204	1.330	0.968	1.000	0.259	1.033	7.545	7.545	9.958	7.615	7.616	10.011
5.2	0.070	0.055	3.017	4.249	1.344	0.968	1.000	0.259	1.033	7.621	7.620	9.136	7.690	7.690	9.195
5.3	0.384	0.029	3.320	4.293	1.357	0.968	1.000	0.259	1.033	7.722	7.695	9.487	7.791	7.764	9.543
5.4	0.433	0.144	2.641	4.337	1.371	0.968	1.000	0.259	1.033	7.804	7.774	8.936	7.872	7.842	8.995

5.5	0.081	0.232	3.149	4.380	1.384	0.968	1.000	0.259	1.033	7.846	7.854	9.446	7.913	7.922	9.502
5.6	0.030	0.166	3.340	4.424	1.397	0.968	1.000	0.259	1.033	7.919	7.923	9.688	7.986	7.990	9.743
5.7	0.056	0.071	2.068	4.466	1.410	0.968	1.000	0.259	1.033	7.992	7.993	8.707	8.059	8.059	8.768
5.8	0.122	0.197	2.432	4.509	1.423	0.968	1.000	0.259	1.033	8.067	8.071	9.031	8.133	8.137	9.090
5.9	0.220	0.166	1.830	4.551	1.436	0.968	1.000	0.259	1.033	8.145	8.142	8.693	8.211	8.207	8.754
6.0	0.027	0.179	1.892	4.593	1.449	0.968	1.000	0.259	1.033	8.209	8.214	8.797	8.274	8.279	8.857
6.1	0.357	0.101	2.063	4.635	1.462	0.968	1.000	0.259	1.033	8.302	8.282	8.969	8.366	8.346	9.029
6.2	0.248	0.199	2.117	4.676	1.474	0.968	1.000	0.259	1.033	8.362	8.358	9.070	8.425	8.421	9.128
6.3	0.022	0.175	1.354	4.717	1.487	0.968	1.000	0.259	1.033	8.422	8.427	8.720	8.485	8.490	8.781
6.4	0.353	0.070	1.231	4.758	1.499	0.968	1.000	0.259	1.033	8.512	8.493	8.737	8.575	8.555	8.798
6.5	0.037	0.168	1.246	4.799	1.512	0.968	1.000	0.259	1.033	8.562	8.566	8.811	8.624	8.628	8.871
6.6	0.060	0.049	0.955	4.839	1.524	0.968	1.000	0.259	1.033	8.631	8.631	8.777	8.693	8.693	8.837
6.7	0.134	0.126	0.786	4.879	1.536	0.968	1.000	0.259	1.033	8.702	8.702	8.798	8.763	8.763	8.858
6.8	0.136	0.174	0.663	4.919	1.548	0.968	1.000	0.259	1.033	8.771	8.772	8.837	8.831	8.833	8.898
6.9	0.026	0.092	0.446	4.959	1.560	0.968	1.000	0.259	1.033	8.836	8.837	8.867	8.896	8.897	8.927
7.0	0.336	0.204	0.011	4.998	1.572	0.968	1.000	0.259	1.033	8.921	8.910	8.903	8.980	8.969	8.963
7.1	0.142	0.190	0.189	5.037	1.584	0.968	1.000	0.259	1.033	8.974	8.976	8.976	9.033	9.035	9.035
7.2	0.108	0.181	0.320	5.076	1.596	0.968	1.000	0.259	1.033	9.039	9.042	9.053	9.098	9.101	9.112
7.3	0.089	0.205	0.633	5.115	1.608	0.968	1.000	0.259	1.033	9.105	9.110	9.165	9.163	9.168	9.223
7.4	0.111	0.069	0.702	5.153	1.619	0.968	1.000	0.259	1.033	9.172	9.170	9.245	9.230	9.228	9.302
7.5	0.172	0.169	0.665	5.191	1.631	0.968	1.000	0.259	1.033	9.240	9.240	9.302	9.298	9.297	9.359
7.6	0.086	0.252	0.331	5.229	1.643	0.968	1.000	0.259	1.033	9.302	9.310	9.317	9.359	9.368	9.374
7.7	0.125	0.253	0.134	5.267	1.654	0.968	1.000	0.259	1.033	9.368	9.376	9.369	9.425	9.432	9.425
7.8	0.177	0.293	0.183	5.305	1.665	0.968	1.000	0.259	1.033	9.435	9.443	9.436	9.492	9.500	9.492
7.9	0.042	0.092	0.070	5.342	1.677	0.968	1.000	0.259	1.033	9.495	9.496	9.496	9.551	9.552	9.552
8.0	0.152	0.027	0.186	5.380	1.688	0.968	1.000	0.259	1.033	9.563	9.559	9.564	9.618	9.615	9.620

Tumenbayar Lkhagvatseren M.Eng

Measurement Systems – connection between Sensors and Embedded System

Měřicí Systémy – propojení mezi Senzory a Embedded Systémy

Doctoral Thesis

Published by Tomas Bata University in Zlin,

Nad Stráněmi 4511 760 05 Zlín

Printing: 8 copies

This publication has not been neither edited nor linguistically corrected.

Year of publishing: 2011